Characterisation of key elements involved in glutamate receptor assembly and functionality at the *Drosophila* neuromuscular junction

Von der Naturwissenschaftlichen Fakultät der
Gottfried Wilhelm Leibniz Universität Hannover
zur Erlangung des Grades
Doktor der Naturwissenschaften
Dr. rer. nat.
genehmigte Dissertation
von

Dipl.-Biochem. Tobias Schwarz

geboren am 28.04.1977 in Fulda

2007

Referent:	Prof. Dr. Walter Müller
Korreferent:	Prof. Dr. Bernd Otto
Tag der Promotion:	10.08.2007

Acknowledgements

First of all, I would like to thank my instructor Prof. Stephan Sigrist for giving me the opportunity to learn and work on a variety of different techniques in different places inside and outside of Göttingen. Stephan always found time to support me in my project with valuable discussions and good advice.

Furthermore, I am grateful for the assistance of PD Evgeni Ponimaskin, for fruitful discussions and steady assistance. Both Stephan and Evgeni encouraged me during my studies, to keep on going, since we all know that some results sometimes take a little longer…

I want to thank my doctor adviser Prof. Müller for giving me and so many other students that “somebody cares” feeling during my studies in Hannover as well as during my PHD thesis. I am very grateful to Prof. Bernd Otto for supporting my work as co-referee.

Furthermore I would like to thank Dr. Dietmar Hess, for teaching me patch clamp in his kind-hearted way, Prof. Manfred Heckmann for his assistance in the electrophysiology of *Drosophila* glutamate receptors and his confidence in me, Prof. Michael Hollmann and his laboratory in Bochum, especially Dr. Markus Werner, for providing me excellent support in my attempts to “sqeeze” significant currents out of *Xenopus* oocytes with TEVC.

Many thanks to all members of the ENI and the Ponimaskin laboratory, especially: Dr. Ute Renner, for her great kindness and steady attendance to support me and my work, Dr. Carolin Wichmann for her company in an almost deserted lab in Göttingen and her great assistance during the progress of this thesis, Christine Quentin for her great technical as well as personal helpfulness and her ability to manage the Sigrist lab, Dr. Andreas Schmid for his company, helpful conversations and his enjoyment of my “Beckenbauer imitations”, Fritz Kobe for great scientific and private communication, Franziska Zehe, Jasmin Held, Gabi Klaehn, Miriam Richter, Jens Hörl, Dagmar Crzan and Heiko Röhse for superb technical support, furthermore Robert Kittel for his consistent interest in my work, Gang Qin for his assistance in the glutamate receptor story, Andreas Frölich for his electrophysiological support concerning GluRIIF, Wernher Fouquet

for enliving the lab atmosphere with his singing to oldies in the radio, Sara Mertel and Dr. Manuela Schmidt for their kind support, furthermore Dr. Carola Sigrist, Dr. Carlos Merino, Rui Tian, David Owald, Frauke Christiansen, Dr. Elena Kvachnina, Dr. Ekaterina Papoucheva, Konstantin Glebov, Dr. Jakub Wlodarczyk, Andrew Woehler, Dr. Tobias Rasse, Wiebke Heinrich, Dagmar Thomiczek, Christiane Becker, Marina Ciottariello, Mika Ruonala, Juliane Gansert, Jan Hegermann, Katrin Hartwich, Katrin Schwarze, Christina Patzelt, Frank Kötting, Oliver Schade, Matthias Weyl, Andrea Möller, Magda Krause and Ulrike Borchardt. All of them contributed to an enjoyable atmosphere in the institutes and helped me feeling comfortable in Göttingen.

Special thanks to my friend Daniel Römermann for many enjoyable hours in which we were able to recover from scientific problems.

I am deeply thankful to my parents for their lifelong support, love and encouragement. Furthermore I want to thank my brother for his consistent belief in me.

Finally, I thank Ilonka from the bottom of my heart for her understanding, consistent support and all her love.

Summary

Ionotropic glutamate receptors are the most abundant excitatory neurotransmitter receptors in the vertebrate central nervous system (CNS). Glutamate receptors are thought to form tetrameric complexes consisting of different receptor subunits. The subunit composition can vary and defines the receptor functionality. Moreover, accessory proteins participate in the mediation of membrane trafficking and synaptic insertion and in the regulation of biophysical ion channel properties of glutamate receptor complexes. The neuromuscular junction (NMJ) of the fruit fly *Drosophila melanogaster* bears a resemblance with excitatory glutamatergic vertebrate CNS synapses. Both systems are glutamatergic, exhibit homologous glutamate receptors and display synaptic plasticity. The *Drosophila* NMJ offers a well accessible synaptic system to study glutamatergic synapses in vivo. Five non-*N*-methyl-D-aspartate (non-NMDA) glutamate receptor subunits, GluRIIA-E, have been identified at the *Drosophila* NMJ. The expression of subunits GluRIIC-E and either GluRIIA or GluRIIB is obligate for *in vivo* formation of functional synaptic glutamate receptors at the *Drosophila N*MJ. However, the precise stoichiometry of glutamate receptor complexes is still unknown.

In this thesis the importance of single glutamate receptor subunits and accessory proteins for glutamate receptor functionality and receptor trafficking was addressed by combining biochemical, electrophysiological and immunohistochemical analyses.

First of all, a rigorous genetic reduction of the expression levels of single receptor subunits, which results in the loss of synaptic receptor complexes as was previously shown, resulted in a concomitant reduction of receptor protein levels in somatic muscles. However, the detection of low receptor protein levels in the muscle indicates, that receptor complexes are not completely targeted for degradation but stabilised in internal pools. Furthermore, the first functional heterologously expressed glutamate receptor complex consisting of the four subunits GluRIIB-E was identified. However, the detection of glutamate-gated

currents for this receptor complex required the additional expression of an accessory protein, namely the *Drosophila* homologue of suppressor of lurcher (SOL-1). The combination of immunohistochemical and biochemical analyses demonstrated the involvement of the *Drosophila* homologue of stargazin in synaptic glutamate receptor assembly. *Drosophila* stargazin mutants displayed an increase in synaptic glutamate receptor complexes, indicating a regulatory role for stargazin on glutamate receptor ion channel functionality. GluRIIF, a sixth non-NMDA receptor subunit, was identified at the *Drosophila* NMJ. Synaptic colocalisation of GluRIIF with GluRIIA and GluRIIB containing receptor complexes was shown. Furthermore, decrease in GluRIIF levels resulted in a concomitant reduction of glutamatergic synaptic transmission at the *Drosophila* NMJ. These findings indicate a participation of GluRIIF in glutamatergic neurotransmission at the *Drosophila* NMJ.

In conclusion, interactions among the six different subunits as well as interactions between glutamate receptors and accessory proteins are required for glutamate receptor functionality.

Keywords: Glutamate receptor, *Drosophila melanogaster,* Neuromuscular junction

Zusammenfassung

Im zentralen Nervensystem (ZNS) der Wirbeltiere stellen Glutamatrezeptoren den vermutlich am meisten verbreiteten Typ exzitatorischer Neurotransmitter-rezeptoren dar.

Der vorherrschenden Meinung zufolge, handelt es sich bei Glutamatrezeptoren um tetramere Komplexe, die aus unterschiedlichen Untereinheiten bestehen. Die Untereinheitenkombination ist variabel und bestimmt die Rezeptoreigenschaften. Außerdem sind sog. akzessorische Proteine an Prozessen wie dem Membrantransport des Rezeptors und dem Einbau des Rezeptor-Komplexes in die Synapse sowie an der Regulation der biophysikalischen Eigenschaften des Rezeptor-Ionenkanals beteiligt. Das neuromuskuläre System der Fruchtfliege *Drosophila melanogaster* teilt mit den glutamatergen exzitatorischen Synapsen des ZNS der Vertebraten folgende Eigenschaften. Beide synaptischen Systeme sind glutamaterg, weisen homologe Glutamatrezeptoren auf und zeigen synaptische Plastizität. Das neuromuskuläre System von *Drosophila* ist experimentell sehr gut zugänglich und ermöglicht dadurch die *in vivo*-Untersu-chung glutamaterger Synapsen. Bisher konnten fünf verschiedene Nicht-*N*-Methyl-D-Aspartat (Nicht-NMDA) Rezeptor-Untereinheiten im neuromuskulären System von *Drosophila* identifiziert werden, die als GluRIIA-E bezeichnet werden. Die gemeinsame Expression von GluRIIC, GluRIID, GluRIIE und entweder GluRIIA oder GluRIIB ist die Voraussetzung dafür, dass funktionelle synaptische Glutamatrezeptoren *in vivo* ausgebildet werden. Die genaue Untereinheiten-Zusammensetzung eines Glutamatrezeptor-Komplexes des neuromuskulären Systems von *Drosophila* ist jedoch noch unbekannt.

Durch Kombination biochemischer, elektrophysiologischer und immunhistologi-scher Methoden wurde in der vorliegenden Arbeit gezeigt, wie wichtig einzelne Glutamatrezeptor-Untereinheiten und akzessorische Proteine für die Funktionalität des Rezeptorkomplexes sind.

Zunächst konnte über eine drastische Reduktion der Expressionsrate einzelner Rezeptoruntereinheiten, was nachweislich den Verlust synaptischer

Rezeptorkomplexe bewirkt, gezeigt werden, dass gleichzeitig die Proteinmengen des gesamten Glutamatrezeptor-Komplexes in der somatischen Muskulatur reduziert wurden, allerdings nicht gänzlich. Der Nachweis geringer Proteinmengen deutet allerdings darauf hin, dass der Komplex teilweise in internen Kompartimenten stabilisiert vorliegt und daher nicht vollständig abgebaut wird.
Desweiteren konnte zum ersten Mal erfolgreich ein funktioneller Glutamatrezeptor-Komplex des neuromuskulären Systems von *Drosophila*, bestehend aus den vier Rezeptoruntereinheiten GluRIIB-E, in einem heterologen Zellsystem rekonstruiert werden. Allerdings war die gleichzeitige Expression des akzessorischen Proteins suppressor of lurcher (SOL-1) erforderlich, um durch Glutamat evozierte Stromantworten dieses Rezeptor-Kanals zu erhalten. Durch Kombination immunhistologischer und biochemischer Analysen konnte gezeigt werden, dass das *Drosophila* stargazin-Homolog die Bildung von synaptischen Glutamatrezeptor-Komplexen beeinflusst. In *Drosophila* stargazin-Mutanten konnte eine erhöhte Anzahl synaptischer Glutamatrezeptoren festgestellt werden, was darauf hindeutet, dass stargazin an der Regulation des Rezeptor-Ionenkanals beteiligt ist. Weiterhin wurde mit GluRIIF eine sechste Nicht-NMDA Rezeptor-Untereinheit am neuromuskulären System von *Drosophila* identifiziert. GluRIIF kolokalisierte sowohl mit Rezeptor-Komplexen, die GluRIIA enthalten, als auch mit solchen, die GluRIIB enthalten. Außerdem führte die Verringerung der Expressionsrate von GluRIIF zur gleichzeitigen Reduktion der synaptischen glutamatergen Transmission im neuromuskulären System von *Drosophila*.
Zusammenfassend wurde festgestellt, dass die Funktionalität der Glutamatrezeptoren des neuromuskulären Systems von *Drosophila* sowohl von Interaktionen zwischen den einzelnen Untereinheiten als auch von Interaktionen zwischen dem Rezeptorkomplex und akzessorischen Proteinen abhängt.

Schlagwörter: Glutamatrezeptor, *Drosophila melanogaster,* Neuromuskuläres System

Table of Contents

1. Introduction

Ionotropic glutamate receptor channels are key elements for excitatory neurotransmission both in the central nervous system (CNS) and at the *Drosophila* neuromuscular junction (NMJ). In contrast to the vertebrate CNS the *Drosophila* NMJ provides a synaptic system which is well accessible, morphologically simple and physiologically well characterised. Moreover, *Drosophila* NMJ development is regulated by the levels of neuronal activity. A comparable activity dependant regulation of synaptic plasticity is crucial for processes involved in learning and memory in the vertebrate brain.

1.1 Synapses

The mammalian brain is a complex organised neuronal network consisting of about 10^{11} neurons connected by around 10^{14} specialised cell-cell junctions called synapses. Synapses mediate cell signalling between two neurons or between a neuron and a gland or muscle cell. Functionally, two subtypes of synapses can be distinguished: electrical and chemical synapses. At electrical synapses transmission is mediated directly via ion flow from one cell to another through tight gap junctions. Chemical synapses use chemical substances, so-called neurotransmitters, for transmission. They consist of a presynaptic part, a synaptic cleft and a postsynaptic part. At the presynaptic site action potentials activate voltage sensitive calcium channels. Calcium influx induces vesicle fusion at the presynaptic site. The vesicle content, the neurotransmitter, is released into the synaptic cleft and binds to ligand activated ion channels at the postsynaptic membrane causing channel opening and ion flux into the postsynaptic cell. Chemical synapses can be excitatory or inhibitory. Glutamate and acetylcholine are important excitatory neurotransmitters; γ-aminobutyric acid (GABA) and glycine are the most common inhibitory neurotransmitters.

1.2 Dendritic spines

Dendritic spines form the contact site for most excitatory synapses in the brain (Gray, 1959; Kirov and Harris, 1999). The human brain contains more than 10^{13} spines. Morphologically, a dendritic spine consists of a bulbous head connected to the dendritic shaft by a narrow neck (Matus, 2000). The spine exhibits a high actin microfilament concentration but in principle lacks microtubules (Fifkova and Delay, 1982; Matus et al., 1982; Capani et al., 2001). Most of the spines contain smooth endoplasmic reticulum (SER) (Spacek and Harris, 1997). Moreover, an organelle called spine apparatus, consisting of two or more SER discs which are separated by electron-dense material composed of microtubules or actin filaments, is found in pyramidal cell spines (Westrum et al., 1980; Capani et al., 2001). The microfilaments associate closely with this spine apparatus and the postsynaptic density (PSD) (compare Figure 1).

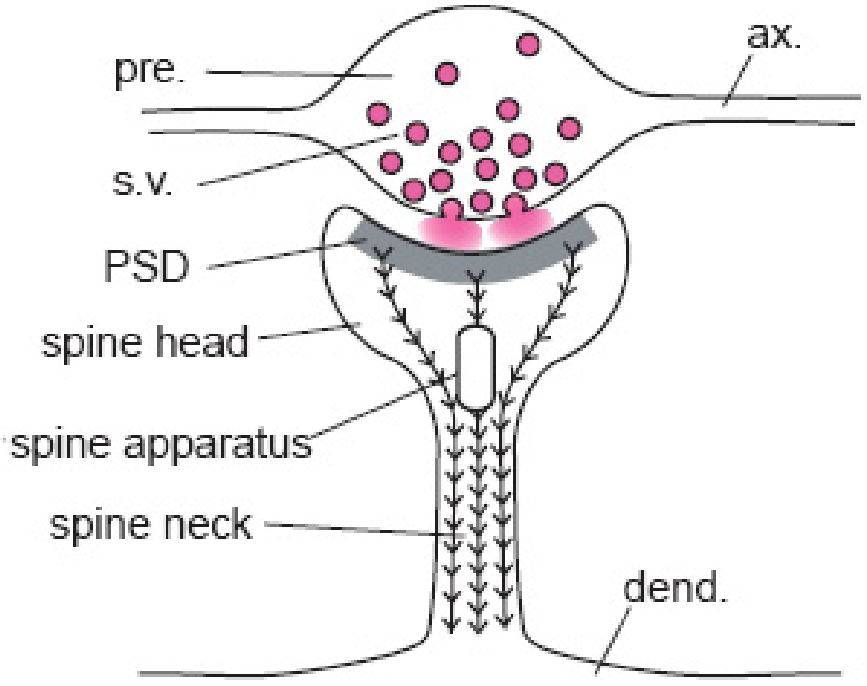

Figure 1 Spine structure scheme
Illustrated are a presynaptic bouton and a postsynaptic dendritic spine. The neurotransmitter glutamate (pink) stored in synaptic vesicles is released into the synaptic cleft. Consequently glutamate receptors located in the postsynaptic density (grey) are activated. Further characteristic spine features are the spine apparatus and the actin filaments (barbed lines) spanning both spine neck and spine head. ax.: axon, dend.: dendritic shaft, pre.: presynaptic bouton, s.v.: synaptic vesicle. Adapted from Matus (2000)

In spine development motile filopodia seek out active presynaptic partners in order to form synaptic contacts (Ziv and Smith, 1996; Jontes and Smith, 2000; Dunaevsky and Mason, 2003; Yuste and Bonhoeffer, 2004). During spine maturation synaptic vesicles accumulate presynaptically and glutamate receptors are inserted into the postsynaptic membrane (Matus, 2005). Three kinds of dendritic spines can be distinguished by their shape: mushroom spines, having a large head and a narrow neck, thin spines exhibiting a smaller head and a narrow neck and stubby spines exhibiting no obvious constriction between the head and the attachment to the shaft (Nimchinsky et al., 2002). Spine motility is inhibited by AMPA receptor activity. Low level stimulation of AMPA receptors is sufficient to maintain the stability of a mature spine (McKinney et al., 1999). This AMPA receptor mediated spine stabilisation requires Ca^{2+} influx through voltage-dependant calcium channels (Fischer et al., 2000).

1.3 Molecular organisation of the presynaptic site

Synaptic transmission requires both regulated neurotransmitter secretion at the presynaptic site as well as the presence of neurotransmitter specific receptors at the postsynaptic site. The presynaptic compartment includes up to thousands of neurotransmitter-filled vesicles which dock and fuse with the plasma membrane at so-called active zones, where they release the neurotransmitter into the synaptic cleft (Palay, 1956; Gray, 1963). An active zone comprises an electron-dense protein matrix forming a grid-like array termed the cytomatrix at the active zone (CAZ) (Zhai and Bellen, 2004) which is supposed to facilitate the delivery of synaptic vesicles to the active zone plasma membrane (Ziv and Garner, 2004).
After the contact between the pre- and postsynaptic site has been established at a newly formed synapse, scaffolding proteins and molecules of the vesicle release machinery are delivered by piccolo/bassoon transport vesicles (PTVs) (Ahmari et al., 2000). Either the formation of the active zone itself or of the CAZ is thought to be mediated via PTVs (Zhai and Bellen, 2004).
Neurotransmitter release is a process including different steps of vesicle

exocytosis and compensatory endocytosis, each of which is catalysed and regulated by a subset of specific molecules (see Figure 2). Within the presynaptic terminal a large vesicle pool, the so-called reserve pool, is present but fewer vesicles are docked to the active zone plasma membrane representing the readily releasable vesicle pool. After an action potential and vesicle release, synaptic vesicle membrane proteins re-enter the presynaptic site via clathrin mediated endocytosis. Endocytosed vesicles are then refilled with neurotransmitter and transported back to the reserve pool (Ziv and Garner, 2004).

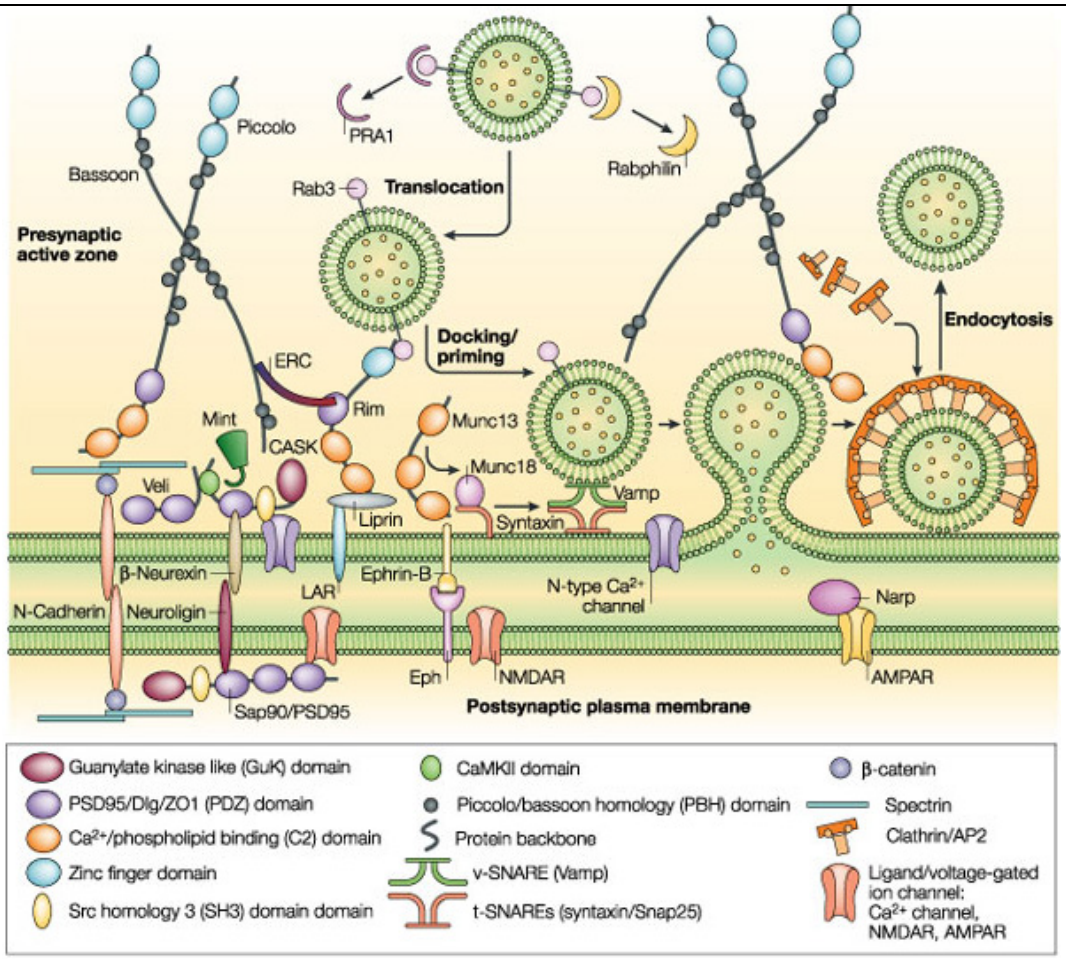

Figure 2 Molecular structures at the presynaptic site of glutamatergic synapses
At the presynaptic active zone vesicles from the reserve pool are translocated, docked and primed to the active zone plasma membrane. After vesicle fusion and neurotransmitter release, endocytosis of presynaptic membrane patches is necessary for the generation of new vesicles, which are refilled subsequently to maintain the vesicle pool. Modified from Ziv and Garner, (2004)

Three distinct types of complexes define the active zone. The first complex is

mainly structural, preserving the close orientation of the active zone to the PSD and clustering Ca^{2+} channels in the active zone plasma membrane. Members of this first complex are cell adhesion molecules (CAMs) like cadherins (Salinas and Price, 2005), neuroligin and neurexin (Dean and Dresbach, 2006), synaptic CAM and neuronal CAMS (SynCAMs and NCAMs), cytoskeleton proteins like piccolo, bassoon (Kim et al., 2003; Shapira et al., 2003) and ERC/Cast (Ohtsuka et al., 2002). In the second complex which mediates in synaptic vesicle docking and fusion, SNARE complex components like syntaxin and Snap25 are included as well as Rim and Munc 18 (Jahn and Sudhof, 1999; Shapira et al., 2003), which moderate the process preceding vesicle fusion termed vesicle priming. The third complex contains molecules involved in vesicle endocytosis like clathrin and dynamin (Ziv and Garner, 2004).

1.4 Molecular organisation of the postsynaptic site

In the central nervous system excitatory glutamatergic synapses exhibit a PSD, an electron-dense organisation underneath the postsynaptic membrane. The PSD includes several hundred proteins (Collins et al., 2006) which can be classified into membrane-bound receptors and channels, scaffolding and adaptor proteins, cell-adhesion proteins, G-proteins together with their modulators, signalling molecules and their phosphatases (Scott and Losowsky, 1976; Klauck and Scott, 1995; Ziff, 1997; Kennedy, 2000; Sheng and Sala, 2001).

The different glutamate receptors at excitatory synapses such as *N*-methyl-D-aspartate (NMDA), α-amino-3-hydroxy-5-methylisoxazole-4-propionic acid (AMPA), kainate as well as metabotropic glutamate receptors (compare chapter 1.6) are linked to the PSD via scaffolding proteins, many of which belong to the family of PSD95/DLG/ZO-1 (PDZ) domain proteins (see Figure 3). Those PDZ domains interact with short peptide motifs at the end of a protein's C-terminus (Hung and Sheng, 2002). Important PDZ proteins interacting with glutamate receptors are synapse associated protein 97kDa (SAP97), postsynaptic density protein 95 (PSD-95), GRIP/ABP, PICK1 and Homer. As an intensely studied member of PSD PDZ proteins, PSD-95 is reported to be directly linked to NMDA

receptors (Cho et al., 1992; Kistner et al., 1993; Kornau et al., 1995; Niethammer et al., 1996), kainate receptors (Garcia et al., 1998) and Shaker K^+ channels (Kim et al., 1995a; Kim et al., 1995b). AMPA receptors are linked to PSD-95 through stargazin (Chen et al., 2000b) (compare chapter 1.7).

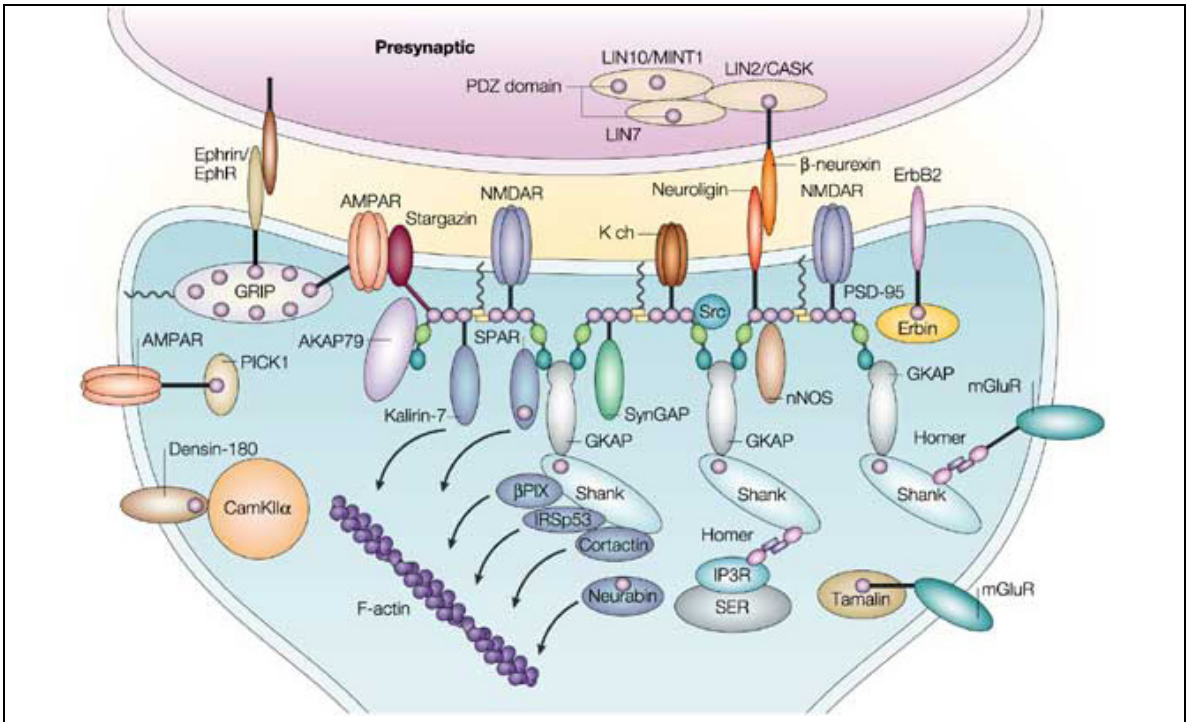

Figure 3 Proteins of the postsynaptic density (PSD)
Displayed are the main PSD PDZ-containing proteins and their interaction partners. PDZ domains are shown in purple circles. Cytoplasmic tails of membrane proteins are indicated by black lines. The overlap of proteins shows specific protein-protein interactions. Crooked lines indicate palmitoylation. This illustration shows a subset of selected proteins. Abbrevations: AKAP79, A-kinase anchor protein 79; AMPAR, AMPA (α-amino-3-hydroxy-5-methyl-4-isoxazole propionic acid) receptor; βPIX, PAAK-interactive exchange factor; CAMKII α, α-subunit of Ca^{2+}/calmodulin-dependent protein kinase II; GK, guanylate kinase-like domain; EphR, ephrin receptor; ErbB2, EGF-related peptide receptor; GKAP, guanylate kinase-associated protein; GRIP, glutamate-receptor-interacting protein; IP3R, IP3 receptor; IRSp53, insulin-receptor substrate p53; Kch, potassium channel; LIN7, lin7 homolog; LIN10, lin10 homolog; mGluR, metabotropic glutamate receptor; NMDAR, NMDA (N-methyl-D-aspartate) receptor; nNOS, neuronal nitric oxide synthase; PICK1, protein interacting with C kinase 1; PSD-95, postsynaptic density protein 95; SER, smooth endoplasmic reticulum; SH3, Src homology 3 domain; Shank, SH3 and ankyrin repeat-containing protein; SPAR, spine-associated RapGAP; SynGAP, synaptic Ras GTPase-activating protein. Modified from Kim and Sheng (2004)

1.5 The vertebrate neuromuscular junction

The neuromuscular junction in vertebrates is a specialised synapse which transmits electrical signals from the nerve terminal to the muscle. In contrast to the vertebrate CNS and the *Drosophila* NMJ, which are both glutamatergic, excitatory neurotransmission is mediated via the neurotransmitter acetylcholine

(ACh). Structurally, the vertebrate NMJ consists of a) the innervating axon terminal harbouring ACh-containing vesicles, b) Schwann cells covering the axon terminal except at the interface of pre- and postsynaptic membranes, c) the synaptic cleft consisting of a basal lamina whih contains acetylcholinesterase (AChE), d) the postsynaptic membrane in which acetylcholine receptors (AChR) are anchored and e) the junctional sarcoplasm supporting the endplate region structurally and metabolically (Wilson and Deschenes, 2005) (for an overview see Figure 4).

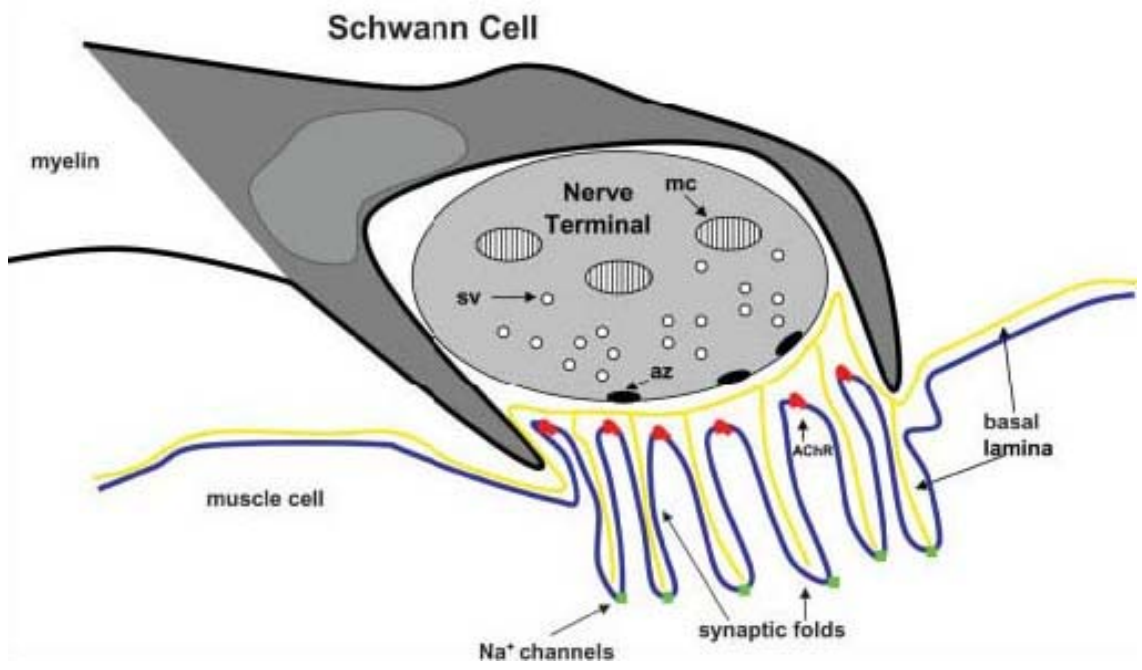

Figure 4 Assembly of the vertebrate neuromuscular junction
The vertebrate neuromuscular junction (NMJ) includes the presynaptic part namely the nerve terminal which is ensheathed by Schwann cells, the synaptic cleft containing a basal lamina and the postsynaptic part consisting of the infolded postsynaptic membrane in which acetylcholine receptors (AChR) and voltage gated sodium channels (Na^+ channels) are anchored. Mc: mitochondrium, sv: synaptic vesicle, az: active zone, adapted from Hughes et al. (2006)

AChR activation causes postsynaptic membrane depolarisation in the form of an endplate potential (EPP). If the depolarisation matches a certain threshold, an action potential arises, which spreads over the muscle fibre and through the T-tubular system stimulating Ca^{2+} release from the sarcoplasmic reticulum and causing muscle fibre contraction (Wood and Slater, 2001).

AchE is a homotetrameric enzyme composed of globular catalytic subunits

attached to a collagen tail (Krejci et al., 1991; Krejci et al., 1997). It is anchored in the basal lamina and catalyses ACh hydrolysis. Inhibition of AChE prolonges ACh's residence time in the synaptic cleft and consequently enhances AChR activation.

A characteristic of the vertebrate NMJ is illustrated by the postsynaptic membrane which exhibits deep infoldings of the sarcolemma, so-called secondary synaptic folds. AChRs are situated at their peaks (Wood and Slater, 1997, 2001) whereas their valleys contain voltage dependant sodium channels (Sanes and Lichtman, 1999).

Mature AChRs form pentameric receptors containing two α subunits and one β, δ and ε subunit respectively. A single subunit consists of an extracellular N-terminal tail followed by four transmembrane domains and an extracellular C-terminal tail. Receptor phosphorylation seems to modify channel properties and regulates receptor desensitisation (Hughes et al., 2006).

During NMJ formation innervation of the muscle fibre results in the formation of AChR containing clusters beneath the overlying nerve terminal. Several NMJ-proteins seem to be involved in AChR clustering. One of the most important proteins is agrin, a heparan sulphate proteoglycan, which is synthesised by the nerve, released into the synaptic cleft and is inserted into the basal lamina. Agrin is able to induce the formation of postsynaptic complexes including AChEs and AChRs even in the absence of a directly apposed nerve (Hughes et al., 2006). A knockout of the transmembrane muscle-specific kinase (MuSK), which colocalises with AChRs at the postsynaptic membrane, results in the failure of AChR clustering in mice. Furthermore, RNAi constructs directed against MuSK block NMJ formation (Kong et al., 2004; Madhavan et al., 2005). Agrin is supposed to signal through MuSK in the muscle. However, as there is no direct interaction between both molecules their linking proteins still have to be identified. A further important factor in AChR clustering is the cytoplasmic protein rapsyn. Rapsyn knockout mice show MuSK clustering but lack AChR clustering at synaptic sites (Gautam et al., 1995; Apel et al., 1997).

1.6 Glutamate receptors

Ionotropic glutamate receptors are ligand-gated ion channels mediating the majority of excitatory neurotransmission in the central nervous system (CNS). Besides ionotropic glutamate receptors which mediate fast synaptic transmission a second type of glutamate receptors, metabotropic glutamate receptors, exists.

Metabotropic glutamate receptors belong to the family of G-protein-coupled receptors and modulate slow synaptic transmission via intracellular second messenger pathways (Hollmann and Heinemann, 1994; Nakanishi et al., 1998; Dingledine et al., 1999; Hermans and Challiss, 2001; Madden, 2002).

Ionotropic glutamate receptors can be pharmacologically specified as NMDA receptors and non-NMDA receptors, the latter of which can be further subdivided into AMPA receptors and kainate receptors.

18 receptor subunits have been identified in rat. Seven subunits, termed NR1, NR2A-D, NR3A and NR3B, belong to the NMDA receptor class. Four other subunits (GluR1-4) belong to AMPA receptors, five subunits to kainate receptors (GluR5-7, KA1 and KA2).

The remaining two receptor subunits, δ1 and δ2, do not assemble in functional receptors and are referred to as orphan receptors.

1.6.1 Glutamate receptor structure and function

All ionotopic glutamate receptor subunits consist of three transmembrane domains and a pore-lining re-entrant membrane loop (Hughes, 1994) (compare Figure 5).

The N-terminal tail is extracellular, the C-terminal tail intracellular. A further classification of the N-terminal region results in two domains. The first roughly 400 amino acids form the N-terminal domain (NTD) sharing similarity with the bacterial periplasmic leucine-isoleucine-valine-binding protein (LIVBP) (O'Hara et al., 1993), the following approximately 150 amino acids, preceding the first transmembrane domain, form the S1 region, which is one part of the extracellular glutamate binding domain. The other part of this domain termed S2 region is situated between transmembrane domains three and four (Stern-Bach et al.,

1994; Kuusinen et al., 1995; Armstrong et al., 1998). The C-terminal part of the S2 region does not directly participate in ligand binding. Rather it contains the localisation for an alternative splicing site, whereby two different splice isoforms termed flip and flop that primarily control AMPA receptor desensitisation (Sommer et al., 1990; Mosbacher et al., 1994) are expressed. Finally, the receptor contains a C-terminal tail which mediates interactions with intracellular binding partners (Sheng and Pak, 2000).

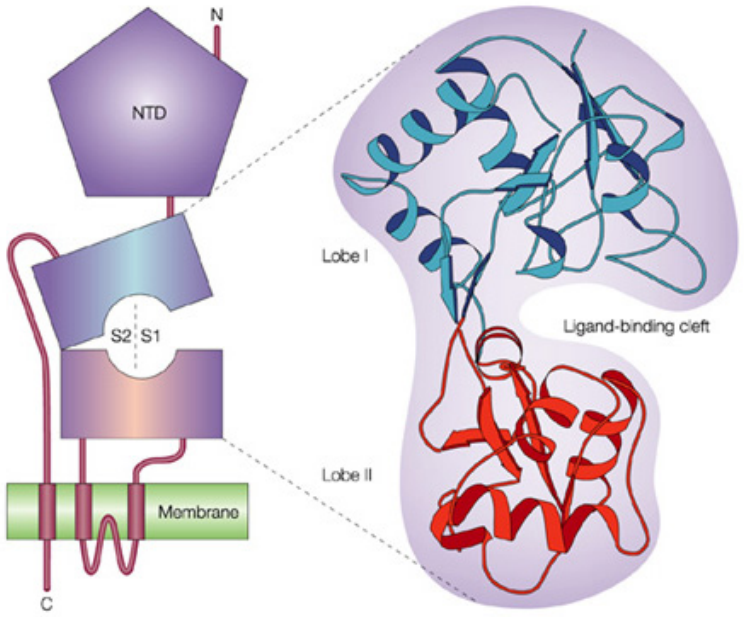

Figure 5 Domain structure of ionotropic glutamate receptor subunits
Ionotropic glutamate receptor subunits consist of an extracellular amino-terminal domain (NTD) followed by the S1 domain (the first part of the ligand binding domain), two transmembrane domains intercepted by a re-entrant loop, the S2 domain (the second part of the ligand binding domain), the third transmembrane domain and an intracellular carboxyl terminus. The S1S2 ligand binding domain forms two lobes (lobe I (blue) and lobe II (red)) separated by a ligand binding cleft. Adapted from Madden (2002)

The S1S2 domain structure resembles that of the glutamine binding protein QBP (Armstrong et al., 1998) where two lobes (lobe I and lobe II, both consisting of parts of the S1 and the S2 domain, compare Figure 5) form the ligand binding cleft. As long as no ligand is bound the ligand binding cleft remains open but ligand binding causes cleft closure. The structure of the ligand binding domain for NMDA, AMPA and kainate receptors is almost identical. The key amino acid side chains interacting with the agonist's α-amino and α-carboxy groups are the same, however the amino acid interacting with glutamate's γ-carboxygroup differs

(Mayer, 2005).

Based on electrophysiological, biochemical and hydrodynamic analyses ionotropic glutamate receptors are assumed to assemble as tetramers (Laube et al., 1998; Mano and Teichberg, 1998; Rosenmund et al., 1998; Kuusinen et al., 1999; Ayalon and Stern-Bach, 2001; Safferling et al., 2001). Functional assays for heteromer formation in AMPA and kainate receptors are compatible with a model where tetrameric glutamate receptors form in two sequential steps. In the first step two subunits interact via their N-terminal domains to form dimers. In the second step tetramers form a “dimer of dimers”. In this second step interactions via the NTD are not sufficient for tetramer stabilisation. In fact transmembrane domains as well as the C-terminal part of the S2 region are important for tetramer stabilisation (Ayalon and Stern-Bach, 2001) (see Figure 6).

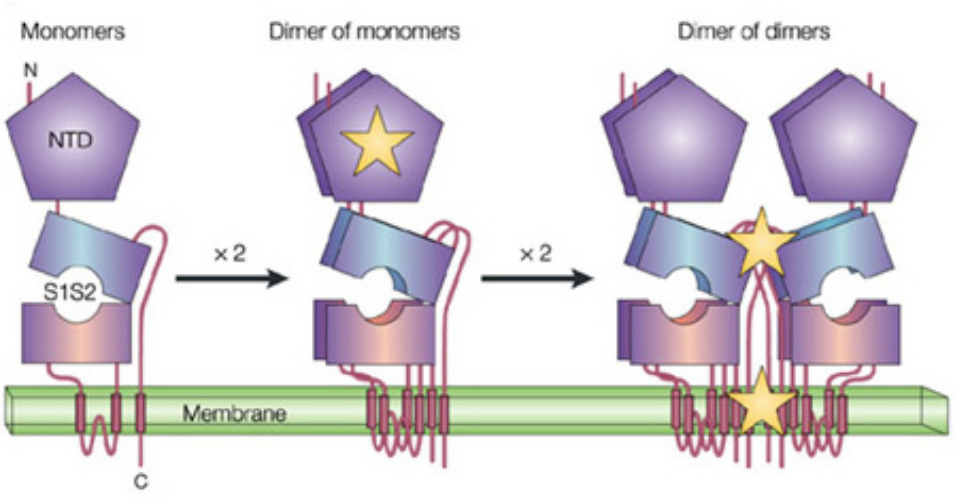

Figure 6 Ionotropic glutamate receptor assembly
Ionotropic glutamate receptors form as tetramers through two consecutive dimerisation steps. In the first step two monomers dimerise through interaction (displayed by a star in the middle figure) of their amino-terminal domains (NTD). In the second step dimers dimerise via interactions of the S2 domain and the transmembrane domains (displayed by stars in the right-hand figure). Adapted from Madden (2002)

The ligand-induced comformational change in the glutamate binding domain results in channel opening which can be followed by channel desensitisation. The exact mechanisms mediating these events remain unknown. However, it seems likely that cleft closure in the S1S2 domain of a given subunit pulls that subunit away from the pore axis resulting in channel opening. Subsequently, with the

ligand still bound the channel closes again assumably through a further interdomain conformational change (Armstrong et al., 1998; Mayer et al., 2001) (compare Figure 7).

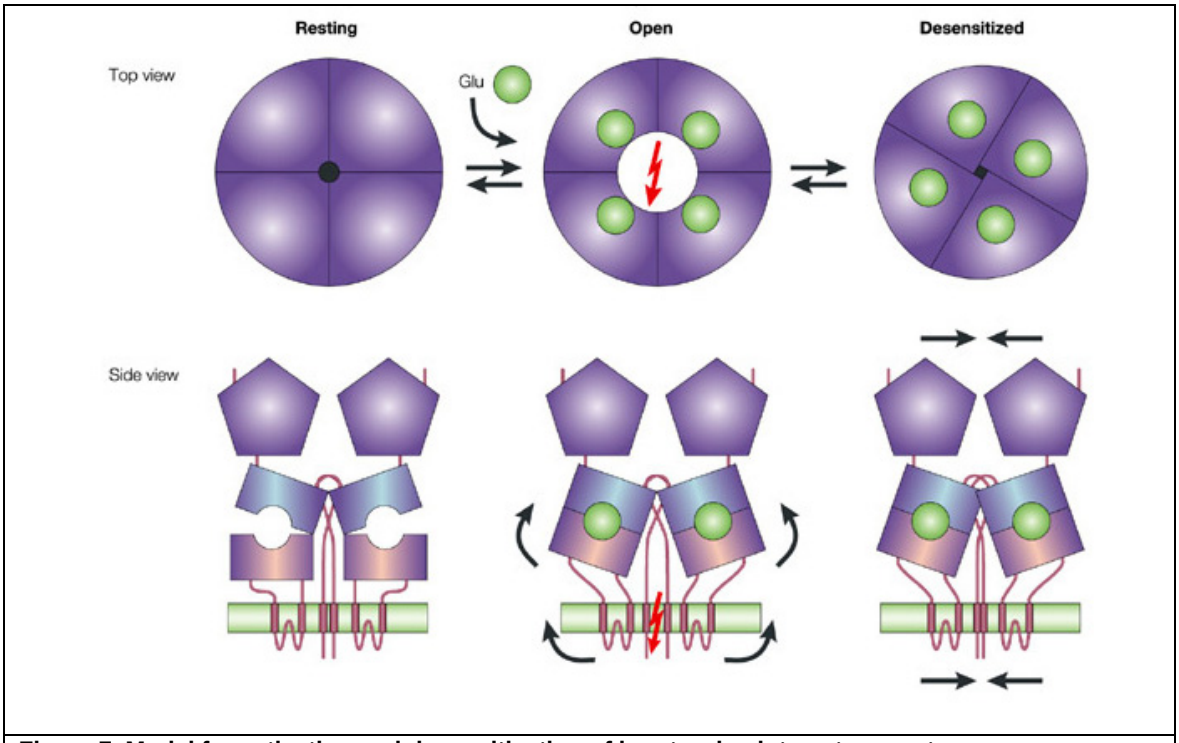

Figure 7 Model for activation and desensitisation of ionotropic glutamate receptors
Shown are the top view (upper row) and the side view (lower row) scheme of glutamate-induced channel opening and desensitisation of ionotropic glutamate receptors. In the absence of glutamate (Glu) the receptor remains in a resting state (left figures). Glutamate binding induces cleft closure in the ligand binding domain resulting in the opening of the channel pore through conformational rearrangements (red lightning bolt in the middle figures). With the agonist still bound, keeping the ligand binding domain in cleft closure formation, a further conformational change makes the channel pore close again (desensitised state, right figures). Adapted from Madden (2002)

1.6.2 NMDA receptors

The heteromeric NMDA receptors consist of the NR1 subunit (Moriyoshi et al., 1991), the NR2 subunit (NR2A-D) (Kutsuwada et al., 1992; Meguro et al., 1992; Monyer et al., 1992; Ishii et al., 1993) and in some cases the NR3 subunit (NR3A and NR3B) (Ciabarra et al., 1995; Sucher et al., 1995; Nishi et al., 2001).

NMDA receptors require the binding of both glutamate at the NR2 subunit as well as glycin (Johnson and Ascher, 1987) as a coactivator at the NR1 subunit. Another characteristic of NMDA receptors is that extracellular Mg^{2+} blocks the ion channel at resting membrane potential. Depolarisation relieves this block

allowing synaptic NMDA receptor activation (Mayer et al., 1984; Nowak et al., 1984).

1.6.3 AMPA receptors

Mammalian AMPA receptors are homo- or heterotetrameric receptors consisting of subunits GluR1-4.

Homomeric AMPA receptors exhibit differences in Ca^{2+} permeability. Homomeric GluR1, GluR3 and GluR4 receptors are Ca^{2+} permeable whereas homomeric GluR2 receptors as well as heteromeric receptors containing the GluR2 subunit lack Ca^{2+} permeability. This effect is caused by a single amino acid change in the pore-forming region generated by posttranscriptional RNA editing (Hume et al., 1991; Verdoorn et al., 1991), in which an adenosine base is deaminated (Seeburg, 2002). Consequently, GluR2 possesses an arginine whereas the other three receptor subunits contain a glutamine at this position. GluR2 subunits appear almost completely in the edited R form (GluR2(R)) and just in low amounts in the Q from (GluR2(Q)). However, GluR2(R) homomers are largely unassembled and retained in the ER, whereas GluR2(Q) subunits are able to form homomeric receptor complexes, which are trafficked to the plasma membrane (Greger et al., 2003).

Furthermore, channel properties are modified by alternative splicing. The second extracellular region of subunits GluR1-4 is spliced as one of two possible variants termed flip and flop; the flop isoform desensitises more rapidly in response to glutamate than the flip isoform does (Sommer et al., 1990).

1.6.3.1 AMPA receptor trafficking and synaptic plasticity

At excitatory synapses changes in neuronal activity can induce long-lasting alterations in synaptic strength thought to be crucial for experience-dependent neuronal plasticity such as learning and memory. Two long lasting forms of synaptic plasticity termed long-term potentiation (LTP) and long-term depression (LTD) have become widely accepted. Both of them are triggered by an increase in the postsynaptic Ca^{2+} concentration as a result of NMDA receptor activation (Malenka, 1994). Ca^{2+} signal properties like magnitude or time course are thought

to induce either LTP or LTD through different postsynaptic signalling pathways (Malenka and Nicoll, 1993). Regulated trafficking of AMPA receptors contributes to changes in synaptic strength during LTP and LTD. In the hippocampus two heteromeric AMPA receptors prevail: those consisting of GluR1 and GluR2 and those containing GluR2 and GluR3. GluR subunits possess unique C-terminal tails mediating interaction with intracellular binding partners. The prominent protein-protein interaction of AMPA receptors is mediated by PDZ-domains (Sheng and Sala, 2001). GluR1 specifically binds to SAP97 via a class I PDZ domain interaction, GluR2 and GluR3 interact through a different kind of PDZ domain with the glutamate receptor interacting protein (GRIP), AMPA receptor binding protein (ABP) and protein interacting with C kinase 1 (PICK1) (Shen et al., 2000; Malinow and Malenka, 2002; Song and Huganir, 2002; Henley, 2003). Interaction with PDZ domain containing proteins appears to be important for AMPA receptor targeting and clustering at specific subcellular regions as well as for stabilising AMPA receptors at synaptic sites and intracellular pools. SAP97 binds GluR1 containing complexes after receptor synthesis in the ER but releases the receptor complex upon arrival at the synapse (Sans et al., 2001). Furthermore, SAP97 provides a linkage to protein kinases via interaction with the kinase anchoring protein AKAP79/150 (Colledge et al., 2000). ABP and GRIP, both contain seven PDZ domains and are present at synaptic membranes and endosomes (Burette et al., 2001). GRIP interacts with GluR2 and GluR3 via PDZ domains 3, 5 and 6 (Dong et al., 1997; Srivastava and Ziff, 1999). The postsynaptic scaffold protein PICK1 binds the C-terminal domains of GluR2 and GluR3 via its PDZ domain (Xia et al., 1999).

Other important non-PDZ domain interactions are mediated by stargazin (see chapter 1.7), the cytoskeletal protein 4.1 (Shen et al., 2000) and NEM-sensitive factor (NSF), an ATPase originally characterised as a factor required for membrane fusion and presynaptic vesicle exocytosis (Rothman, 1994). Protein 4.1 binds to the C-terminal tail of GluR1 and GluR4 and stabilises receptor surface expression (Shen et al., 2000; Coleman et al., 2003). NSF binds to the GluR2 C-terminal region and seems to be important for synaptic AMPA receptor

delivery and/or stabilisation (Malinow and Malenka, 2002; Song and Huganir, 2002). Phosphorylation of the GluR2 C-terminus at Ser880 reduces binding affinities of ABP and GRIP but not for PICK1 (Chung et al., 2000). PICK1 reduces GluR2 surface levels and forms endosome-like clusters with GluR2 (Perez et al., 2001). Furthermore, coassembly of NSF and soluble NSF attachment proteins (SNAPs) to GluR2 causes dissociation of PICK1 (Hanley et al., 2002). Thus NSF is assumed to block PICK1-dependent GluR2 endocytosis (Barry and Ziff, 2002).

Strong evidence supports the notion that LTP involves *de novo* insertion of additional AMPA receptors into the synaptic plasma membrane (Shi et al., 1999; Lu et al., 2001; Pickard et al., 2001). Receptor insertion during LTP is mediated via GluR1 and CaMKII, a protein kinase which is required for triggering LTP (Hayashi et al., 2000). LTP is absent in mice lacking GluR1 (Zamanillo et al., 1999). Whereas AMPA receptor insertion via GluR1 is activity dependent, GluR2/3 containing receptors are proposed to continuously cycle between intracellular pools and the plasma membrane in an activity-independent manner (Malinow and Malenka, 2002; Song and Huganir, 2002). Moreover, AMPA receptor stoichiometry is thought to determine whether a receptor is directly inserted into a synaptic site or indirectly via insertion at an extrasynaptic site followed by lateral diffusion into a synapse (Passafaro et al., 2001; Borgdorff and Choquet, 2002). While LTP exhibits the assembly of AMPA receptors, LTD involves their removal (Lissin et al., 1998).

AMPA receptors are internalised after agonist stimulation in a dynamin- and clathrin-dependent process (Carroll et al., 1999).

Internalisation can be induced via several mechanisms: NMDA receptor activation induces AMPA receptor internalisation through calcium-dependent pathways (Beattie et al., 2000; Daw et al., 2000; Ehlers, 2000) involving GluR2 phosphorylation (Chung et al., 2003) GluR1 dephosphorylation (Ehlers, 2000; Lee et al., 2000; Lee et al., 2003) or depalmitoylation of PSD-95 (El-Husseini Ael et al., 2002).

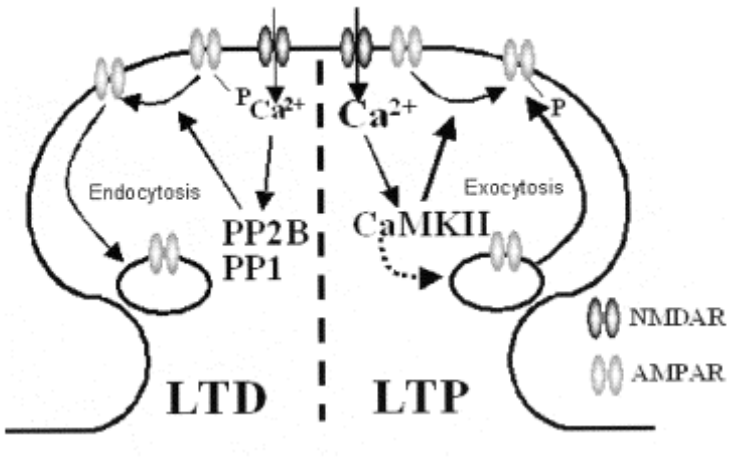

Figure 8 Intracellular pathways involved in LTD and LTP
A modest rise in Ca^{2+} concentration activates protein phosphatase 2B (PP2B) and protein phosphase 1 (PP1). As a result synaptic AMPA receptors are internalised and dephosphorylated. In constrast LTP is induced by a large Ca^{2+} increase activating CaMKII. CAMKII causes AMPA receptor delivery from internal pools to synaptic sites. Adapted from Malenka (2003)

1.6.4 Kainate receptors

Kainate receptors are homo- or hetero-tetrameric receptors consisting of subunits GluR5-7, KA1 and KA2. GluR5-7 exist in different C-terminal splice variants (GluR5a-d, GluR6a-c, GluR7a, b) (Sommer et al., 1992; Gregor et al., 1993; Schiffer et al., 1997; Barbon et al., 2001). Some splice variants differ in regions exhibiting ER retention signals or forward trafficking motifs (Jaskolski et al., 2004). In contrast to NMDA and AMPA receptors which are mainly found at postsynaptic sites kainate receptors have different functions pre- and postsynaptically. At presynaptic sites kainate receptors regulate the release of GABA and glutamate, thereby assisting in presynaptic forms of short- and long-term synaptic plasticity. At postsynaptic sites kainate receptors are involved in synaptic currents of low amplitude and slow decay kinetics (Lerma, 2006; Pinheiro and Mulle, 2006).

1.6.4.1 Kainate receptor trafficking

Surface expression of kainate receptors depends on subunit composition and alternate splicing at the C-terminal domain. KA2 and GluR5c contain a functional ER retention signal which prevents ER exit of homomeric receptors consisting of

these subunits (Ren et al., 2003c; Jaskolski et al., 2004). In addition, KA2 provides a C-terminal di-leucine motif which is supposed to mediate clathrin-dependent endocytosis. Due to the forward trafficking motif CQRRLKHK in their C-terminal domain, GluR6a and GluR7a exhibit high expression levels at the plasma membrane and enable surface expression of other subunits containing an ER retention signal (Jaskolski et al., 2004; Yan et al., 2004; Jaskolski et al., 2005). Through dimerisation the retention signal is sterically masked and thus non-functional. Although kainate receptors possess a PDZ-binding motif at their C-terminus, which mediates interaction with PDZ proteins like PSD-95, SAP97, SAP102 as well as PICK1 and GRIP, ER exit does not depend on PDZ interaction as was shown for GluR5 and GluR6 (Ren et al., 2003b; Jaskolski et al., 2004). In fact, PDZ interaction influences kainate receptor mediated synaptic transmission. Both PICK1 and GRIP interactions are required for the maintenance of kainate receptor mediated synaptic transmission (Hirbec et al., 2003).

1.6.5 The lurcher mutation

The so-called lurcher mutation is a spontaneous mutation, which was found in the orphan receptor GluRδ2 in mice. It results in the change of a highly conserved alanine to a threonine in a region adjanced to the receptor channel pore (Zuo et al., 1997). This single amino acid substitution causes the constitutive channel activation and modified gating kinetics (Kohda et al., 2000).

1.7 Stargazin, a member of the TARP family

The stargazin gene was identified through a spontaneous mutation in the gene locus. Stargazin mutant mice showed ataxic behaviour and moved with their heads held upwards resulting in their baptism as stargazer mice. The protein mutated in those mice was termed stargazin. Stargazin, also referred to as γ-2, is related to the γ-1 subunit of the skeletal muscle voltage-dependent calcium channel (VDCC) (Letts et al., 1998). Surprisingly, it was shown that stargazin

does not cause the mutant phenotype via its involvement with VDCC but via interaction with AMPA receptors. Stargazer mice selectively lack functional AMPA receptors in cerebellar granule cells (Chen et al., 1999; Hashimoto et al., 1999). Indeed three other closely related isoforms of stargazin, termed γ-3, γ-4 and γ-8 are able to substitute for stargazin *in vitro* (Klugbauer et al., 2000; Burgess et al., 2001; Chu et al., 2001). Altogether γ-2, γ-3, γ-4 and γ-8 form the so-called transmembrane AMPA receptor regulatory protein (TARP) family. TARPs in turn belong to a protein superfamily, including among others the γ-1 subunit of VDCC, claudin family tight junction proteins and the peripheral myelin protein (PMP) 22.

1.7.1 Molecular structure

Structurally, TARPs contain four transmembrane domains. The protein's N- and C-terminus are intracellular. The first extracellular loops between the first two transmembrane domains as well as the proximal C-terminal part are known to interact with AMPA receptors. Stargazin regulates AMPA receptors' biophysical properties via its extracellular loop whereas receptor trafficking is regulated via the proximal part of its C-terminal domain (Tomita et al., 2005b; Turetsky et al., 2005). The C-terminal tail can be further subdivided into:

A) a stretch of about 30 amino acids containing 9 serines which can be dynamically phosphorylated in response to NMDA receptor activation during the induction of LTP and LTD (Tomita et al., 2005a),

B) a binding site for nPIST (neuronal isoform of protein-interacting specificially with TC10), a Golgi enriched protein, which is supposed to target the TARP-AMPA complex to PSD-95 at the postsynaptic site (Cuadra et al., 2004) and finally,

C) a PDZ binding motif interacting with PSD-95 which targets TARPs to synapses (Chen et al., 2000a).

1.7.2 AMPA receptor assembly and trafficking

Immunoprecipitation of mouse brain extracts showed that TARPs interact with all AMPA receptor subunits, and not solely a subset of these (Tomita et al., 2003; Tomita et al., 2004; Fukata et al., 2005). However, the presence of individual TARP members throughout different brain regions is non-uniform. Most neuronal cell types, for instance hippocampal pyramidal neurons, express multiple TARP members. On the other hand, cerebellar granule cells solely express stargazin. Loss of stargazin leads to a striking lack of AMPA receptor surface expression both at synaptic and extrasynaptic sites (Chen et al., 1999; Hashimoto et al., 1999; Chen et al., 2000b) suggesting a crucial role of stargazin in AMPA receptor trafficking. Moreover, 40-50% of intracellularly retained AMPA receptors lack mature glycosylation in stargazer mice suggesting a chaperone like role for stargazin (Tomita et al., 2003). Furthermore, even in the hippocampus where several TARPs were identified, the loss of γ-8, the most abundant TARP in this brain region, results in a massive decrease of GluR1 and GluR2/3 subunits. The remaining AMPA receptors are retained somatically in ER and Golgi compartments. Thus, TARPs appearing in the same brain region seem to execute different functions. This thesis is supported by coimmunoprecipitation results in cerebral cortex brain extracts showing that TARP isoforms are strictly segregated (Tomita et al., 2003).

After trafficking AMPA receptors to the cell membrane TARPs bound to PSD-95 target the receptors to postsynaptic sites (Chen et al., 2000b; Schnell et al., 2002). Overexpression of wild type stargazin in cultured hippocampal neurons increased the abundance of extrasynaptic but not synaptic receptors. In contrast, overexpression of PSD-95 caused the opposite effect (Schnell et al., 2002) suggesting that the synaptic presence of TARP complexed AMPA receptors depends on the availability of synaptic PSD-95. PSD-95 is one of the most abundant proteins of the postsynaptic density (Schnell et al., 2002). It interacts with NMDA receptors and stargazin via PDZ interaction and serves as a scaffolding protein for other PSD proteins (Sheng and Pak, 2000). Functionally PSD-95 decreases kainate receptor desensitisation (Garcia et al., 1998) and

increases the open-channel probability of NMDA receptors (Lin et al., 2004). Interestingly, changes in postsynaptic PSD-95 concentration affect synaptic AMPA receptors but not NMDA receptors in neuronal cell culture (El-Husseini Ael et al., 2002).

Although TARPs are believed to be tightly linked to AMPA receptors immunoprecipitation studies with solubilised membrane extracts from cerebral cortex showed dissociation of AMPA receptor subunits GluR1 and GluR2 from γ-3 after AMPA or glutamate treatment, whereas NMDA and GABA treatment had no effect (Tomita et al., 2004). This dissociation of the TARP-AMPA complex is supposed to result in AMPA receptor internalisation or degradation.

As mentioned in chapter 1.6.3.1 besides TARPs other AMPA receptor interacting proteins have been identified to operate subunit-specifically via the C-termini of subunits GluR1 and GluR2 (Song and Huganir, 2002). The majority of the TARPs were shown to be complexed to AMPA receptors in cerebellum, cortex and hippocampus (Tomita et al., 2003; Vandenberghe et al., 2005a). In contrast to TARPs, the C-tail interactors seem to be less “firmly” bound to AMPA receptors, as indicated by coimmunoprecipitation studies (Fukata et al., 2005; Vandenberghe et al., 2005a). Nonetheless, it seems likely that they function in concert with TARPs in regulating AMPA receptors.

1.7.3 Regulation of AMPA receptor ion channel properties

In addition to their involvement in receptor trafficking TARPs modulate the biophysical properties of AMPA receptors. Coexpression of stargazin results in reduced AMPA receptor desensitisation (Priel et al., 2005; Tomita et al., 2005b; Turetsky et al., 2005), enhanced recovery from desensitisation (Priel et al., 2005; Turetsky et al., 2005) and slowed deactivation rates (Priel et al., 2005; Tomita et al., 2005b) in *Xenopus* oocytes and HEK cells. Moreover, the efficiency of the partial agonist kainate is dramatically increased by stargazin, γ-3, γ-4 and γ-8 (Yamazaki et al., 2004; Tomita et al., 2005b; Turetsky et al., 2005).

In cultured hippocampal neurons TARPs are highly clustered at synapses and furthermore colocalise with AMPA receptors. In contrast to other AMPA receptor

interacting proteins, such as GRIP/ABP and PICK1 which occur at excitatory as well as at GABAergic inhibitory synapses (Dong et al., 1999; Wyszynski et al., 1999) and dopaminergic synapses, TARPs are exclusively found at excitatory synapses (Chen et al., 2000b).

1.8 C. elegans SOL-1

Through a genetic screen for modifiers of ionotropic glutamate receptor function in *C. elegans* suppressor of lurcher (sol-1) was identified in a transgenic strain expressing a modified non-NMDA glutamate receptor subunit GLR-1, bearing the lurcher mutation. The *sol-1* gene encodes the 594 amino acid long type I transmembrane protein SOL-1. Almost the entire protein is extracellular and carries four β-barrel forming domains termed CUB-domains. The protein's C-terminus carries the transmembrane domain.

Fluorescence protein fusion constructs of SOL-1 and GLR-1 colocalise in the postsynaptic membrane of transgenic *C. elegans* worms and chemically tagged versions of Sol-1 and GLR-1 coimmunoprecipitate in COS-7 cells (Zheng et al., 2004).

GLR-1 receptors seem to require both SOL-1 and stargazin for functionality. Indeed, GLR-1 is present at the surface of cultured muscle cells from *C. elegans* in the absence of SOL-1 and stargazin. However, only the combination of GLR-1, SOL-1 and stargazin results in measureable glutamate-gated currents (Walker et al., 2006a).

SOL-1 is not required for GLR-1 surface expression but influences GLR-1 receptor gating. In SOL-1 mutants glutamate-gated currents that depend on GLR-1 are almost completely abolished in GLR-1 expressing AVA interneurons of *C. elegans* after pressure application of glutamate. Moreover, kainate-gated currents are completely eliminated, whereas NMDA-gated currents are not affected in SOL-1 mutants (Zheng et al., 2004). Thus, the loss-of-functional mutants of sol-1 and glr-1 exhibit the same electrophysiological phenotype. With the aid of truncated SOL-1 constructs CUB domain 3 was found to be crucial for

SOL-1 function. Although loss of the first three CUB domains does not prevent interaction between SOL-1 and GLR-1, no GLR-1 glutamate-gated currents were recorded in the absence of the first three CUB domains in AVA interneurons (Zheng et al., 2006). As recent studies have shown, SOL-1 has an essential role in GLR-1 desensitisation. On the one hand, the functionality of concanavalin-A (Con-A), a plant lectin known to slow AMPA receptor desensitisation (Partin et al., 1993), depends on the presence of SOL-1. The absence of SOL-1 results in rapid and complete GLR-1 desensitisation as well as in a slowdown of the desensitisation recovery, as was demonstrated in rapid glutamate perfusion experiments in cultured muscle cells from *C. elegans* (Walker et al., 2006a).

1.9 The Drosophila neuromuscular junction

The model organism *Drosophila melanogaster* features many advantages. First of all, *Drosophila* genetics allow efficient manipulation of the genome, which was fully sequenced recently (Adams et al., 2000). Importantly the majority of *Drosophila* genes are evolutionary conserved to vertebrates. Additionally, the short life cycle of *Drosophila* (10 days at 25°C, compare Figure 9) permits quick generation of transgenic and mutant animals. With the aid of the *UAS/Gal4* system the expression of the gene of interest can be controlled in a tissue as well as time specific manner (Brand and Perrimon, 1993). The first part of this system consists of a minimal cassette of the yeast transcription activator galactosidase-4 (*Gal4*), which is inserted in a genetic locus, where it is expressed by surrounding promoters. The choice of the promoter determines the tissue specifity and the point of time of *Gal4* expression. The second part of the expression system consists of a randomly inserted construct encoding the sequence, which shall be expressed. Upstream of this sequence of interest the yeast upstream activating sequence (*UAS*), which is recognised by *Gal4*, is fused. Thus, the gene of interest is only expressed in those tissues and at those points of time, where the *Gal4* cassette itself is expressed.

Last but not least, many mechanisms and processes described in *Drosophila*

were shown to be highly conserved in “higher” organisms. Altogether findings in *Drosophila* form an important step in understanding the function of homologous processes in the vertebrate system.

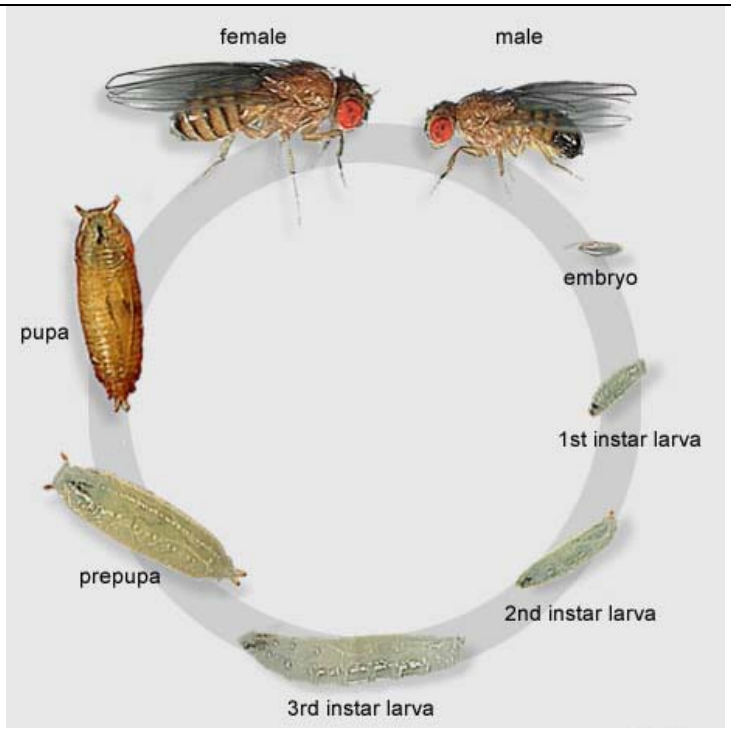

Figure 9 Life cycle of *Drosophila melanogaster*
The embryonic stage lasts roughly 24h and ends with the hatching of the larva. Larvae pass through three stages during which they moult before accomplishing the next larval stage and increase in size. 1st and 2nd instar larval stages last one day each. At the end of the 3rd instar larval stage, lasting two to three days, larvae pupate. Metamorphosis takes four to five days and finishes with the hatching of the adult fly. The duration of the different stages is valid at 25°C. Figure was taken from flymove.uni-muenster.de, compare (Weigmann et al., 2003).

The *Drosophila* NMJ is a favoured model system for the exploration of the synapse. In fact the *Drosophila* NMJ bears a resemblance to excitatory synapses of the vertebrate CNS. Both kinds of synapses are glutamatergic and exhibit homologous glutamate receptors. Synapses at the vertbrate CNS and the *Drosophila* NMJ both display synaptic plasticity. However, the *Drosophila* NMJ displays considerable advantages in comparison to the vertebrate CNS. First of all, the *Drosophila* NMJ is accessible to a variety of techniques such as immunohistochemistry, electrophysiology, electron microscopy and *in vivo* imaging, a powerful tool, which allows the examination of processes like glutamate receptor assembly in the living animal, as was shown in Rasse et al.

(2005). Moreover, the *Drosophila* NMJ is morphologically simple and physiologically well characterised.

Structurally the NMJ of late stage embryos and larvae exhibits a pattern of 30 abdominal muscle cells per hemisphere (Bate et al., 1999) innervated by a number of approximately 36 motoneurons which branch into synaptic varicosities referred to as boutons (Landgraf and Thor, 2006).

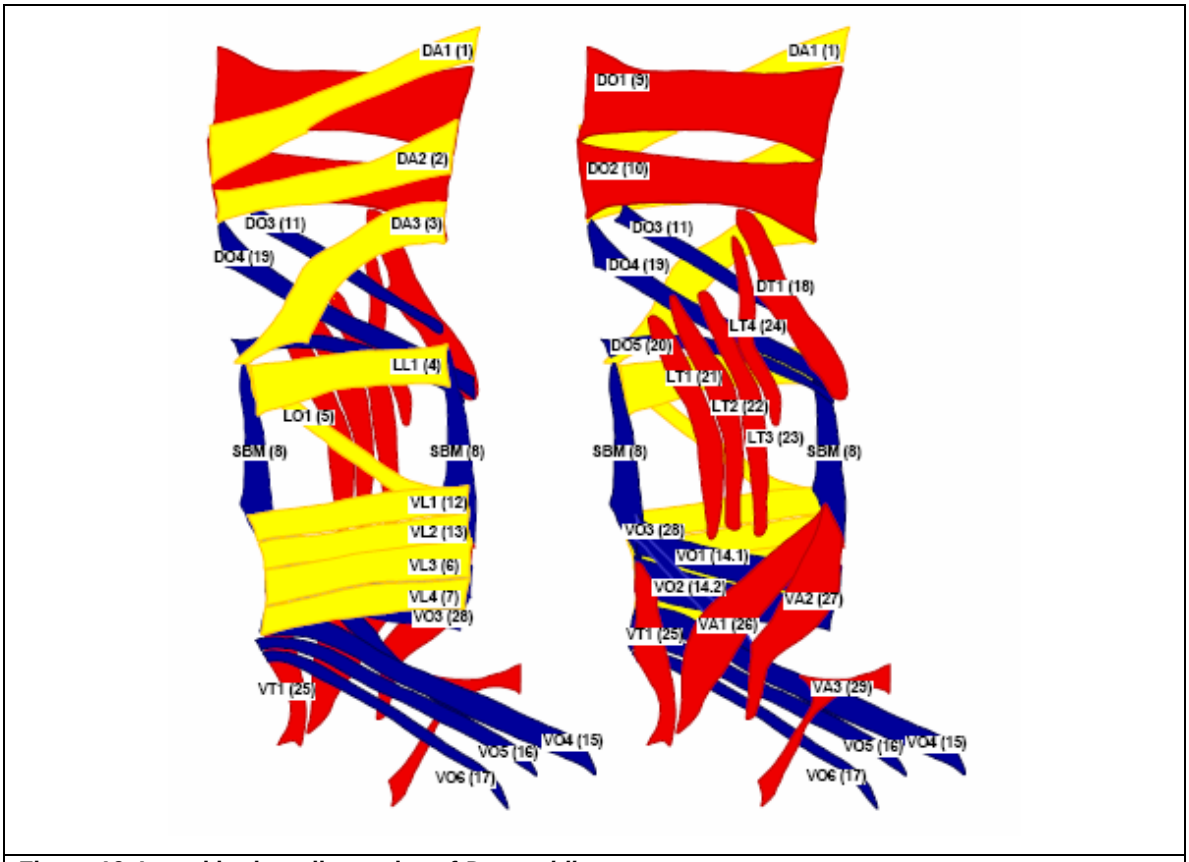

Figure 10 Larval body wall muscles of *Drosophila*
Shown is the set of 30 abdominal muscle cells present in each hemisegment of the *Drosophila* larva. On the left hand the dorsal view, on the right hand the ventral view is displayed. DA, dorsal acute; DO, dorsal oblique; DT, dorsal transverse; LO, lateral oblique; LT, lateral transverse; LL, lateral longitudinal; VA, ventral acute; VO, ventral oblique; VT; ventral transverse; VL, ventral longitudinal; SBM, segment border muscle. Adapted from Bate et al. (1999)

Three different larval bouton types, varying in size, innervation pattern and vesicle composition, can be distinguished. They are termed type I, type II and type III boutons (Gramates and Budnik, 1999), all of which are glutamatergic (Jan and Jan, 1976; Johansen et al., 1989; Broadie and Bate, 1993b, 1993c).

Type I boutons are restricted in their location on the muscle fibre, are up to 8 µm in diameter, and contain mainly clear synaptic vesicles (Rivlin et al., 2004). They

can be further subdivided in Is (small boutons; diameter: 1-3µm) and Ib (big boutons; diameter: 2-8µm) (Rheuben et al., 1999).

In addition to glutamate type II boutons contain the neuropeptide octopamine (Monastirioti et al., 1995) and are often located along the length of the muscle fibre. They are less than 2 µm in diameter and predominantly contain dense core vesicles and few clear vesicles (Rivlin et al., 2004).

Type III boutons contain an insulin-like peptide in addition to glutamate (Gorczyca et al., 1993). They are located only on a single pair of muscles, possess an intermediate size and basically contain dense core vesicles (Rivlin et al., 2004). Neither type II nor type III boutons have been observed to trigger electrical postsynaptic responses (Rheuben et al., 1999).

Embryonic and larval NMJs are similar at the ultrastructural level (Prokop, 1999). Pre- and postsynaptic sites exhibit high electron density when visualised by transmission electron microscopy and are in close proximity to each other just separated by a 10-20nm wide synaptic cleft. The presynaptic compartment is filled with vesicles. Presynaptic active zones feature electron-dense projections referred to as T-bars (Atwood et al., 1993; Zhai and Bellen, 2004). T-bars are linked to the coiled-coil domain active zone protein Bruchpilot (BRP) and were shown to be involved in vesicle release. BRP seems to establish proximity between Ca^{2+} channels and vesicles in order to allow efficient transmitter release and synaptic plasticity. At active zones of BRP mutant larvae, T-bars were entirely lost, Ca^{2+} channel density was reduced, the evoked vesicle release was depressed and short-term plasticity was altered (Kittel et al., 2006). The postsynaptic electron-dense region, the PSD, contains, like its vertebrate homologue in the CNS, among other things the ligand-gated glutamate receptors as well as voltage-gated ion channels and scaffolding molecules (Prokop and Meinertzhagen, 2006). The less electron-dense part of the bouton membrane describes the perisynaptic region and can be visualised by the marker protein Fasciclin II (FasII). One obvious structure in the postsynaptic cell beneath the PSD is the subsynaptic reticulum (SSR) consisting of thin folded extensions of the muscle fibre and harbouring many functionally important proteins in its

membrane (Rheuben et al., 1999). Among those proteins are glutamate receptors, shaker potassium channels, FasII and the scaffolding protein *Discs-large* (DLG).

1.9.1 Development of the *Drosophila* NMJ

Motor neuron growth cones, first observed 10h after egg laying (AEL), extend along the body wall through the developing muscles and form synapic contacts with their target muscle cells via myopodia, specialised muscle processes, 12 to 15h AEL (Broadie et al., 1993; Ritzenthaler and Chiba, 2001). Although the development of functional presynaptic structures seems to be independent of the postsynapse and despite the fact that active zones can form in the absence of muscles, a proper arrangement and localisation requires both a differentiated postsynaptic muscle cell and a close apposition of pre- and postsynapse (Prokop et al., 1996; Prokop, 1999). Stabilisation of the initial synaptic contact is mediated by cell adhesion molecules, one prominent member of which is FasII. During the first contact of motor neuron and muscle, FasII, which is a homologue of the mammalian NCAMs, is strongly expressed on the motor axon surface but only at low levels in the muscle cell (Schuster et al., 1996b). After the contact has stabilised, FasII forms clusters at the membrane both pre- and postsynaptically. At late embryonic stages FasII maintenance is mainly mediated by DLG, a PSD-95 homologue found in *Drosophila* (Thomas et al., 1997; Zito et al., 1997).

Only minutes after the first contact between motor neuron and muscle, glutamate receptors formed clustering starts at the innervation site. Within the first two hours expression of new receptors is initiated. Till the end of embryogenesis the postsynaptic glutamate receptor numbers increase 10 to 20fold (Broadie and Bate, 1993a). In contrast to the vertebrate NMJ, homologues of the heparan sulphate proteoglycan agrin were not found at the *Drosophila* NMJ (Serpinskaya et al., 1999). In fact, like in the vertebrate CNS, a PDZ protein namely DLG is involved in postsynaptic clustering processes, including shaker potassium channels and FasII through a CAMKII phosphorylation dependent manner (Koh et al., 1999). 13-14h AEL the first endogenous currents can be recorded from

ventral NMJs. However, synapses at this state are still immature lacking patterned electrical activity and synaptic current bursts, which are observed 16-20h AEL and after the maturation of the embryonic NMJ including presynaptic branching and bouton enlargement (Broadie and Bate, 1993b).

1.9.2 Non-NMDA type glutamate receptors at the *Drosophila* NMJ

Glutamate receptor subunits at the *Drosophila* NMJ are closely related to mammalian non-NMDA receptors. Five different subunits, termed GluRIIA-E, have been identified so far (Schuster et al., 1991; Petersen et al., 1997; DiAntonio et al., 1999; Marrus et al., 2004; Featherstone et al., 2005; Qin et al., 2005). Mutations deleting either GluRIIA or GluRIIB are viable, whereas the double mutant for GluRIIA and GluRIIB is embryonic lethal (DiAntonio et al., 1999). GluRIIC, GluRIID, GluRIIE are essential subunits and all of them are required for synaptic transmission. In null mutants for GluRIIC, GluRIID or GluRIIE or in the double mutant for GluRIIA and GluRIIB no other glutamate receptor subunits are present at the *Drosophila* NMJ in embryos (Qin et al., 2005). Actually, each single receptor subunit can be rate limiting for synaptic receptor localisation. A genetical reduction of the subunit levels of GluRIIC, GluRIID, GluRIIE or GluRIIA in the complete absence of GluRIIB results in a simultaneous reduction of the remaining glutamate receptor subunits at the *Drosophila* NMJ (Marrus et al., 2004; Featherstone et al., 2005; Qin et al., 2005). Thus the experimental data so far suggest a potential tetrameric receptor complex comprising subunits GluRIIC-E and either GluRIIA or GluRIIB (Qin et al., 2005). However, the precise subunit stoichiometry of that receptor complex is still unsolved.

Null mutants of either GluRIIA or GluRIIB still develop functional receptor complexes at the NMJ. However, the ion channels of GluRIIA null mutants differ in their biophysical properties from the ion channels of GluRIIB null mutants. Patch clamp recordings using outside-out patches from muscle membrane of *Drosophila* larvae show a 10-fold faster desensitisation in mutants containing GluRIIB but missing GluRIIA in comparison to wild type animals (DiAntonio et al., 1999), whereas receptor complexes containing GluRIIA but lacking GluRIIB show

no difference in desensitisation compared to the wild type situation. A loss of either GluRIIA or GluRIIB does not change the glutamate receptor single channel amplitude.

Both, overexpression of the GluRIIA subunit as well as increased larval locomotion, result in an increase in active zones and the number of synaptic boutons which is coupled to a decrease of perisynaptic FasII (Sigrist et al., 2000; Sigrist et al., 2002; Sigrist et al., 2003). Conversely this synaptic strengthening is suppressed by downregulation of the GluRIIA receptor level or upregulation of the GluRIIB receptor level implicating antagonistic roles for GluRIIA and GluRIIB at the *Drosophila* NMJ.

Glutamate receptor numbers are further regulated by other synaptic components. First of all, nonvesicular presynaptic glutamate release regulates postsynaptic glutamate receptor numbers. In this way glutamate acts as a negative regulator on postsynaptic receptor field size and function (Featherstone et al., 2002). Proteins involved in the regulation of synaptic glutamate receptor levels are the p21-associated kinase (PAK) and FasII (Schuster et al., 1996a; Sone et al., 2000; Albin and Davis, 2004).

GluRIIA and GluRIIB subunits were shown not to tolerate the addition of a chemical or a fluorescence tag at their very N- or C-terminus. However, a functional receptor subunit was obtained by EGFP insertion into the middle of the C-terminus of GluRIIA (Rasse et al., 2005) and GluRIIB (unpublished data). Through *in vivo* imaging of the larval NMJ a direct correlation between synaptic GluRIIA entry and synapse growth was shown. Glutamatergic PSDs form *de novo* and not via partitioning from already existing synapses at the *Drosophila* NMJ. Almost all newly formed GluRIIA receptor fields were shown to be in thíght association with presynaptic active zone markers after 10h of maturation (Rasse et al., 2005). Although neither presynaptic active zone formation nor initial PSD assembly depend on the presence of glutamate receptors, PSD maturation does (Prokop et al., 1996; Schmid et al., 2006). In the absence of glutamate receptors complexes small nascent synapses are established but fail to reach mature size (Schmid et al., 2006).

1.9.3 Studies of invertebrate TARP family members

Recently invertebrate homologues of stargazin have been identified in several species. The open reading frames C18D1.4 in *Caenorhabditis elegans* (*C. elegans*), XM 397021 in *Apis mellifera* (honey bee) and CG33670 in *Drosophila* display weak sequence identities to vertebrate stargazin. The predicted proteins share 21% (C18D1.4), 24% (XM 397021) and 25% (CG33670) amino acid sequence identities with the vertebrate stargazin protein. These proteins were refered to as *C. elegans* stargazin, *Apis* stargazin and *Drosophila* stargazin by Walker et al. (2006b).

In *C. elegans* AMPA receptors consisting of the GLR-1 subunit are trafficked to the cell membrane even in the absence of *C. elegans* stargazin (Walker et al., 2006b), indicating that invertebrate stargazin might primarily perform a functional role. Indeed, the presence of *C. elegans* stargazin increases GLR-1 receptor surface expression 3-fold in *Xenopus* oocytes but neuronal distribution of *C. elegans* stargazin does not completely overlap with that of GLR-1 indicating the existence of other important AMPA receptor interactors in *C. elegans*. In *Xenopus* oocytes functional homomeric GLR-1 receptors require coexpression of both *C. elegans* stargazin and SOL-1 (see chapter 1.8).

Stargazin homologues can partially substitute for each other. *Xenopus* oocytes coinjected with GLR-1, SOL-1 and either *C. elegans*, *Apis mellifera*, *Drosophila* or vertebrate stargazin all exhibit glutamate-gated currents. However, gating kinetics are different depending on what kind of stargazin is expressed (Walker et al., 2006b).

1.9.4 Drosophila SOL-1

In *Drosophila* the sequence CG31218 was found to be homologous to *C. elegans* SOL-1. Indeed, the predicted Drosophila protein shares 25% amino acid identity with to *C. elegans* SOL-1 and exhibits the characteristic 4 CUB domains as well as the C-terminal transmembrane domain. It was shown that this protein, reffered to as *Drosophila* SOL-1, can functionally substitute *C. elegans* SOL-1 when coexpressed with *C. elegans* stargazin and GLR-1 in *Xenopus* oocytes (Walker et al., 2006a).

2 Materials and methods

2.1 Chemicals

All chemicals used were from Sigma (St. Louis, USA), Roth (Karlsruhe, Germany) or Merck (Darmstadt, Germany) if not stated otherwise. Enzymes for molecular biology like T4 DNA ligase, alkaline phosphatase, Taq polymerase and the majority of restriction endonucleases were purchased from Roche (Mannheim, Germany). The restriction endonuclease *Asc*I was purchased from New England Biolabs (Beverly, USA).

2.2 Buffer solutions

Barth's solution

88mM NaCl, 1.1mM KCl, 2.4mM $NaHCO_3$, 0.3mM Ca(NO)3, 0.4mM CaCl2, 0.8mM $MgSO_4$, 15mM HEPES, pH adjusted to 7.6 with NaOH

Barth's solution, Ca^{2+}-free

88mM NaCl, 1.1mM KCl, 2.4mM $NaHCO_3$, 0.8mM $MgSO_4$, 15mM HEPES, pH adjusted to 7.6 with NaOH

HL-3

70mM NaCl, 5mM KCl, 20mM $MgCl_2$, 10mM $NaHCO_3$, 5mM trehalose, 115mM sucrose, 5mM HEPES, pH adjusted to 7.2

Normal frog Ringer's solution (NFR)

115mM NaCl, 2.5mM KCl, 1.8mM CaCl2, 10mM HEPES, pH adjusted to 7.2 with NaOH

NTEP buffer

0.5% NP-40,150mM NaCl, 50mM Tris/HCl (pH 7.9), 5mM EDTA, 10mM iodacetamide, 1mM PMSF

PBS

8g NaCl, 0,2g KCl, 0.2g KH_2PO_4, 1.15g $NaH_2PO_4 \cdot 2H_2O$

PBS/Tween

0,05% (w/v) Tween 20 in PBS

SDS-electophoris buffer

25mM Tris/HCl, 3.5mM SDS, 192mM glycine pH 8.3

SDS sample buffer

50mM TRIS/HCl pH 6.8, 2% SDS, 10% (v/v) glycerol, 0.1% bromphenol-blue, 2% β-mercaptoethanol

Squishing buffer

10mM Tris/HCl pH 8.2, 1mM EDTA, 25mM NaCl, 200µg/ml proteinase K

Transfer buffer

25mm Tris/HCl, 192mM glycine, 20% (v/v) methanol, pH 8.3

2.3 Molecular biology

Molecular cloning was executed using standard molecular biology methods (Sambrook et al., 1989). Cloned DNA constructs were double strand sequenced (MWG Biotech, Ebersberg, Germany; Qiagen, Hilden, Germany). Sequencing results were analyzed with MacVector™ (Accelrys, San Diego, USA).

2.3.1 Overlap Extension PCR

Overlap extension PCR (see Figure 11) was performed as described in the Elongase® kit protocol (Invitrogen, Karlsruhe, Germany). A schematic overview is shown in Figure 11.

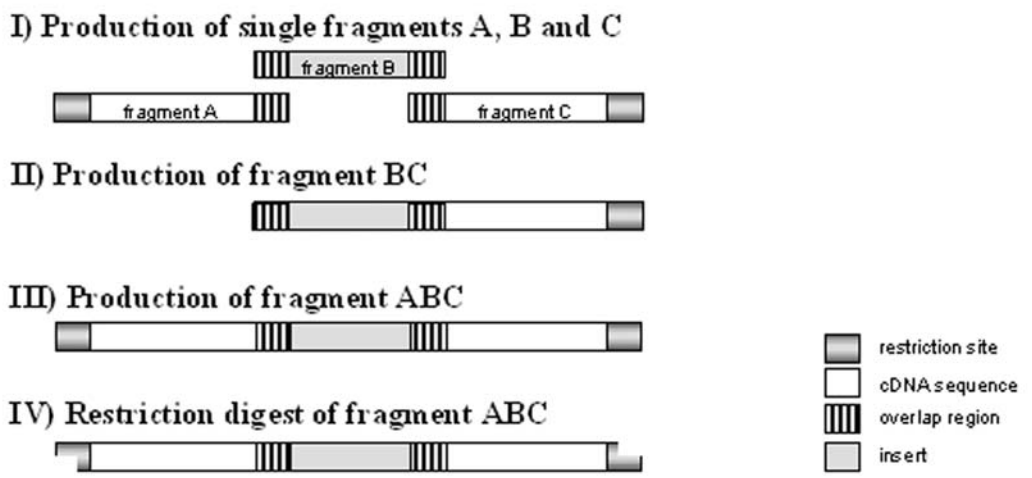

Figure 11 Overlap extension PCR
In the first step the three subfragments A, B and C are created by PCR with Vent DNA-polymerase. The N-terminus of fragment B shares base overlap regions of 23 basepairs with the C-terminus of fragment A, the C-terminus of fragment B shares base overlap regions of 25-36 basepairs with the N-terminus of fragment C. In the second step fragments B and C are linked by Elongase® overlap extension PCR. In the third step the full length fragment is formed again via Elongase® overlap extension PCR. In the last step the full length PCR product is digested at the 5' and 3' restriction site and applied to ligation into the target vector.

2.3.2 Cloning of GluRII constructs

pSL1180 3xHA

A three time repetitive haemaglutinine tag (3xHA) was amplified via PCR from source vector pCFB-EGSH (Stratagene, La Jolla, CA, USA)

PCR-primers:

3xHA: fw: 5'-GTCAGGCGCGCCGGCAGCGTAGTCAGGTACGTCGTAAGG-3'

rv: 5'-GTCAGGCGCGCCAGCTTACCCATATGACGTTCCAGACTACG-3'

The purified PCR product was cut at *Asc*I sites, which were introduced by the primers, and ligated into pSL1180 which was linearised with *Asc*I previously.

pSL1180 5xmyc

A five time repetitive myc tag (5xmyc) was cut with restriction enzymes *Spe*I and *Nhe*I from source vector pSL1180 5xmyc (donated by Alf Herzig, department of molecular biology, MPI for Biophysical Chemistry Göttingen).
A specific linker with flanking *Asc*I-sites and an internal *Xba*I-site was constructed by oligonucleotide annealing of 5′-CGCGCCGAGCAAGTCTAGAGG-3′ (oligo A) and 5′-CGCGCCTCTAGACTTGCTCGG-3′ (oligo B). With the exception of the first five bases both oligonucleotid sequences are complementary resulting in a double stranded cDNA linker with *Asc*I-specific overhangs. For oligonucleotide annealing 20µM of each oligonucleotide was used in buffer solution containing 25mM TRIS/HCl pH 8.0 and 10mM $MgCl_2$. The annealing protocol included five minute incubation at 95°C followed by slow cooling to 30°C.
The purified linker was ligated into target vector pSL1180 which was linearised with *Asc*I previously. The ligation product was linearised with *Xba*I in the middle of the linker region and ligated with 5xmyc (*Spe*I/*Nhe*I) (*Xba*I overhangs are compatible to both *Spe*I-overhangs and *Nhe*I-overhangs).

2.3.2.1 GluRII cDNA constructs

All used tags (EGFP, 3xHA and 5xmyc) are flanked by *Asc*I containing linkers at both ends. In general EGFP was first inserted into the receptors via overlap extension PCR. Once introduced 3xHA and 5xmyc containing constructs were introduced through *Asc*I digest replacing EGFP. The only exception is GluRIIA which contains internal *Asc*I sites.

pFastbac1 GluRIIA

restriction cut:	*Xba*I / *Xho*I		
insert:	GluRIIA	source:	pUAST GluRIIA
vector:	pFastbac1		

pFastbac1 GluRIIB

restriction cut: *Xba*I / *Hind*III
insert: GluRIIB source: pUAST GluRIIB
vector: pFastbac1

pFastbac1 GluRIIC

restriction cut: *Xba*I
insert: GluRIIC source: pUAST GluRIIC
vector: pFastbac1

pFastbac1 GluRIID

restriction cut: *Not*I / *Xba*I
insert: GluRIID source: pUAST GluRIID
vector: pFastbac1

pFastbac1 GluRIIE

restriction cut: *Not*I / *Xba*I
insert: GluRIIE source: pUAST GluRIIE
vector: pFastbac1

pFastbac1 GluRIIA EGFP

restriction cut: *EcoR*I / *Xho*I
insert: GluRIIA EGFP source: pSL GluRIIA EGFP (constructed by Tobias Rasse)
vector: pFastbac1

pUAST GluRIIA EGFP

restriction cut: *EcoR*I / *Xho*I
insert: GluRIIA EGFP source: pSL GluRIIA EGFP (constructed by Tobias Rasse)

vector: pUAST

pFastbac1 GluRIIA 3xHA, pFastbac1 GluRIIA 5xmyc

GluRIIA contains an internal *Asc*I site. 5xmyc and 3xHA inserts were subcloned into precursor constructs of pSL GluRIIA termed pSL GluRIIA N-term and pFastbac1 GluRIIA ΔN-term (constructed by Tobias Rasse). pFastbac GluRIIA ΔN-term, pSL1180 3xHA and pSL1180 5xmyc were digested *Asc*I. 3xHA inserts and respectively 5xmyc inserts were ligated into the linearised pFastbac GluRIIA ΔN-term forming pFastbac GluRIIA ΔN-term 3xHA and pFastbac GluRIIA ΔN-term 5xmyc. pFastbac GluRIIA ΔN-term 3xHA, pFastbac GluRIIA ΔN-term 5xmyc were cut *BamH*I / *Xho*I and ligated into a previously via *BamH*I / *Xho*I linearised pSL GluRIIA N-term forming pSL GluRIIA 3xHA and pSL GluRIIA 5xmyc. Finally GluRIIA 3xHA and GluRIIA 5xmyc were transferred into pFastbac1 via *EcoR*I / *Xho*I digestion.

pUAST GluRIIA 3xHA

restriction cut: *Bgl*II / *Kpn*I
insert: GluRIIA 3xHA source: pSL GluRIIA 3xHA
vector: pUAST

pUAST GluRIIA 5xmyc

restriction cut: *Bgl*II / *Kpn*I
insert: GluRIIA 5xmyc source: pSL GluRIIA 5xmyc
vector: pUAST

pFastbac1 GluRIIB EGFP

This construct was generated by overlap extension PCR (compare 2.3.1) was applied. pFastbac1 GluRIIB served as template vector. The following primer pairs were used:

Fragment A:
forward:
5'-GCAAGGGTACCTATGCCTTCC-3'
reverse:
5'-GGCGCGCCAGATGTGTATAAGAGACATGTAATTTGCTCCAGCGATGAGTAAC-3'
Fragment B:
forward:
5'-CTCTTATACACATCTGGCGCGCCGAGCAAGGGCGAGGAGCTGT-3'
reverse:
5'-TCTGTCTCTTATACACATCTGCCCGGGCGCGCCGCCCTTGTACAGCTGCTCCATGCC-3'
Fragment C:
forward:
5'-
GGCGGCGCGCCCGGGCAGATGTGTATAAGAGACAGAATTACAAGTGCTTCCAGTGCGAAAA-3'
reverse:
5'-CCTCTACAAATGTGGTATGGCTG-3'
Fragment BC:
forward: fragment B forward, reverse: fragment C reverse
Fragment ABC:
forward: fragment A forward, reverse: fragment C reverse
restriction digest: *Kpn*I / *Hind*III
vector: pFastbac1 GluRIIB insert: PCR fragment ABC

pUAST XL+ GluRIIB EGFP

pFastbac1 GluRIIB EGFP was linearised via *Hind*III, pUAST XL+ was linearised via *Xho*I. Both linearised vectors were subjected to a Klenow reaction in order to produce blunt ends. pFastbac1 GluRIIB EGFP (*Hind*III, blunt) and pUAST XL+ (*Xho*I, blunt) were further digested with *Not*I. GluRIIB EGFP (*Not*I / *Hind*III, blunt) was ligated into pUAST XL+ (*Not*I / *Xho*I, blunt).

pFastbac1 GluRIIB 3xHA

restriction cut: *Asc*I
insert: 3xHA source: pSL1180 3xHA
vector: pFastbac1 IIB EGFP

pUAST XL+ GluRIIB 3xHA

restriction cut: *Pme*I
insert: GluRIIB 3xHA (*Stu*I / *Hind*III blunt)
source: pFastbac1 GluRIIB 3xHA
vector: pUAST XL+

pFastbac1 GluRIIB 5xmyc

restriction cut: *Asc*I
insert: 5xmyc source: pSL1180 5xmyc
vector: pFastbac1 IIB EGFP

pUAST XL+ GluRIIB 5xmyc

restriction cut: *Pme*I
insert: GluRIIB 5xmyc (*Stu*I / *Hind*III blunt)
source: pFastbac1 GluRIIB 5xmyc
vector: pUAST XL+

pFastbac1 GluRIIC EGFP

For the generation of this construct overlap extension PCR (compare 2.3.1) was applied. pFastbac1 GluRIIC served as template vector. The following primer pairs were used:

Fragment A:

forward:

5’-GATCTCCAAAATGGACTGGGAG -3’

reverse:

5’-GGCGCGCCAGATGTGTATAAGAGACAGCTCGACTTGGGAGTGCGG-3’

Fragment B:

forward:

5’-CTCTTATACACATCTGGCGCGCCGAGCAAGGGCGAGGAGCTGT-3’

reverse:

5’-TCTGTCTCTTATACACATCTGCCCGGGCGCGCCGCCCTTGTACAGCTGCTCCATGCC-3’

Fragment C:

forward:

5’-CGGGCAGATGTGTATAAGAGACAGAATTACACGCCGAGTTGTCATCGGG-3’

reverse:

5’-CCTCTACAAATGTGGTATGGCTG-3’

Fragment BC:

forward: fragment B forward, reverse: fragment C reverse

Fragment ABC:

forward: fragment A forward, reverse: fragment C reverse

restriction cut: *Xho*I

vector: pFastbac1 GluRIIC insert: PCR fragment ABC

insert orientation was checked with primer 5′-CCAAAATGGACTGGGAGAAC-3′

pUAST GluRIIC EGFP

restriction cut: *Xba*I

insert: GluRIIC EGFP

source: pFastbac1 GluRIIC EGFP

vector: pUAST

pFastbac1 GluRIIC 3xHA

restriction cut: *Asc*I

insert: 3xHA source: pSL1180 3xHA

vector: pFastbac1 IIC EGFP

pUAST GluRIIC 3xHA

restriction cut: *Xba*I
insert: GluRIIC 3xHA
source: pFastbac1 GluRIIC 3xHA
vector: pUAST

pFastbac1 GluRIIC 5xmyc

restriction cut: *Asc*I
insert: 5xmyc source: pSL1180 5xmyc
vector: pFastbac1 IIC EGFP

pUAST GluRIIC 5xmyc

restriction cut: *Xba*I
insert: GluRIIC 5xmyc
source: pFastbac1 GluRIIC 5xmyc
vector: pUAST

pFastbac1 GluRIID EGFP

For the generation of this construct overlap extension PCR (compare 2.3.1) was applied. pFastbac1 GluRIID served as template vector. The following primer pairs were used:
Fragment A:
forward:
5'-GAAACCACAGAAGGCTCCAC-3'
reverse:
5'-GGCGCGCCAGATGTGTATAAGAGACATGAATTCCGACTGCGAGAG-3'
Fragment B:

forward:

5’-CTCTTATACACATCTGGCGCGCCGAGCAAGGGCGAGGAGCTGT-3’

reverse:

5’-TCTGTCTCTTATACACATCTGCCCGGGCGCGCCGCCCTTGTACAGCTGCTCCATGCC-3’

Fragment C:

forward:

5’-CGGGCAGATGTGTATAAGAGACAGAATTACATCTCAGTCCATAGAGTCCCTG-3’

reverse:

5’-CCTCTACAAATGTGGTATGGCTG-3’

Fragment BC:

forward: fragment B forward, reverse: fragment C reverse

Fragment ABC:

forward: fragment A forward, reverse: fragment C reverse

restriction digest: *Pst*I

vector: pFastbac1 GluRIIC insert: PCR fragment ABC

insert orientation was checked with primer 5′-TATTGTCCGCGTGCTGAGAG-3′

pUAST GluRIID EGFP

restriction cut: *Not*I / *Xba*I

insert: GluRIID EGFP

source: pFastbac1 GluRIID EGFP

vector: pUAST

pFastbac1 GluRIID 3xHA

restriction cut: *Asc*I

insert: 3xHA source: pSL1180 3xHA

vector: pFastbac1 IID EGFP

pUAST GluRIID 3xHA

restriction cut: *Not*I / *Xba*I
insert: GluRIID 3xHA
source: pFastbac1 GluRIID 3xHA
vector: pUAST

pFastbac1 GluRIID 5xmyc

restriction cut: *Asc*I
insert: 5xmyc source: pSL1180 5xmyc
vector: pFastbac1 IID EGFP

pUAST GluRIID 5xmyc

restriction cut: *Not*I / *Xba*I
insert: GluRIID 5xmyc
source: pFastbac1 GluRIID 5xmyc
vector: pUAST

pFastbac1 GluRIIE EGFP

restriction cut: *EcoR*I / *Xba*I
insert: GluRIIE EGFP
source: pUAST GluRIIE EGFP (constructed by Gang Qin)
vector: pFastbac1

pFastbac1 GluRIIE 3xHA

restriction cut: *Asc*I
insert: 3xHA source: pSL1180 3xHA
vector: pFastbac1 IIE EGFP

pUAST GluRIIE 3xHA

restriction cut: *EcoR*I / *Xho*I
insert: GluRIIE 3xHA
source: pFastbac1 GluRIIE 3xHA
vector: pUAST

pFastbac1 GluRIIE 5xmyc

restriction cut: *Asc*I
insert: 5xmyc source: pSL1180 5xmyc
vector: pFastbac1 IIE EGFP

pUAST GluRIIE 5xmyc

restriction cut: *EcoR*I / *Xho*I
insert: GluRIIE 5xmyc
source: pFastbac1 GluRIIE 5xmyc
vector: pUAST

pSGEM GluRIIA

restriction cut: *EcoR*I / *Xho*I
insert: GluRIIA source: pFastbac1 GluRIIA
vector: pSGEM

pSGEM GluRIIB

restriction cut: *BamH*I / *Hind*III
insert: GluRIIB source: pFastbac1 GluRIIB
vector: pSGEM

pSGEM GluRIIC

restriction cut: *Xba*I

insert: GluRIIC source: pFastbac1 GluRIIC
vector: pSGEM

pSGEM GluRIID

restriction cut: *Not*I / *Xba*I
insert: GluRIID source: pUAST IID
vector: pSGEM

pSGEM GluRIIE

restriction cut: *EcoR*I / *Xho*I
insert: GluRIIE source: pFastbac1 GluRIIE
vector: pSGEM

pSGEM GluRIIE 3xHA

restriction cut: *EcoR*I / *Xho*I
insert: GluRIIE 3xHA source: pFastbac1 GluRIIE 3xHA
vector: pSGEM

pUAST GluRIIF

Cloning of pUAST GluRIIF was accomplished on basis of two different cDNA clones termed RE13419 and RE56017. Sequences of RE13419 and RE56017 are identical except an additional base at the N-terminal region of IIF resulting in an N-terminal frame shift and an N-terminal shortened GluRIIF version. RE56017 and a variety of other sequenced cDNA clones of this region show a prolonged N-terminus compared to RE56017. The RE13419 cDNA was amplified by PCR and cloned into pUAST via *Not*I / *Kpn*I digestion (performed by Gang Qin). In the following cloning steps the N-terminal sequence was exchanged from RE13419 to RE56017. Two PCR fragments were generated, the first from the RE56017 template sequence with primers 5'-GCTAGATCTGTGCTTTTTTCTTTCCATCAACTG G-3' and 5'-CTTGAACACCTGCTTCCAACTGAC-3', the second one from pUAST

RE13419 construct with primers 5'-GTCAGTTGGAAGCAGGTGTTCAAG-3'and 5'-TTGGTCGGAGGTGCAGGATA-3'. Subsequently both PCR products were combined via an overlap extension PCR step (compare Figure 11 step II). The combined product was digested *Bgl*II / *Asp*I and ligated into a previously *Bgl*II / *Asp*I linearised pUAST RE13419.

pUAST GluRIIF RNAi

pUAST GluRIIF RNAi construct was obtained by PCR with primer pairs.
fw: 5'-GCGAGAATTCCTGGTATTCGGTTATCCGTGTT-3' (icluding an *EcoR*I site) and
rv: 5'-GCTATCTAGAGCTTTCGCGTTCATCTTCC-3' (including a *Xba*I site)
using pUAST GluRIIF as template. The PCR products was digested with *EcoR*I and ligated to form a hairpin construct. The hairpin construct was cut with *Xba*I and ligated into the pUAST vector previously linearised via *Xba*I restriction cut.

2.4 Cell culture

2.4.1 Sf9 cell cultivation

Sf9 cells (Smith et al., 1985) were cultured in 75 mm^2 flasks (Nunc GmbH & Co. KG, Wiesbaden, Germany) in 10ml of supplemented TC-100 medium (Invitrogen, Karlsruhe, Germany) [supplements: 10% foetal calf serum (FCS) (Biochrom AG, Berlin, Germany) and 1% penicillin/streptomycin (PS) (Invitrogen, Karlsruhe, Germany)] at 29°C. For cell passage cells were scraped from the flask in 6ml freshly supplemented TC-100 medium. 2ml of cell suspension were transferred to a new 75 mm^2 flask containing 8ml supplemented TC-100 medium.

2.4.2 Recombinant GluRII baculovirus generation

The baculovirus system allows efficient overexpression of functional proteins in Sf9 cells. Recombinant baculoviruses were generated with the help of the Bac-toBac® Expression System as described in Anderson et al. (1996) (for a procedural scheme see Appendix Figure 34). The gene of interest is cloned behind the strong viral polyhedrin promoter. Both promoter and coding region can

be mobilised through Tn7 transposon sites (see Appendix Figure 31). DH10Bac competent cells (Invitrogen, Karlsruhe, Germany), which contain a parental bacmid with a *lac*Z-mini-attTn7 as well as a helper plasmid providing transposition proteins, were transformed with the pFastbac1 plasmid containing the particular glutamate receptor construct. The transposition proteins mobilise the region on pFastbac1 between the two Tn7 sites which is inserted into the Bacmid at the mini-*att*Tn7 target site disrupting the *lac*Z gene. Transposition success was checked by white/blue screening on X-Gal containing plates (2YT Agar containing gentamycin (7µg/ml), tetracyclin (10µg/ml), kanamycin (50µg/ml), IPTG (40µg/ml), X-Gal (100µg/ml)). Bacmid DNA of lacZ negative clones was used for Sf9 cell transfection with Cellfectin transfection reagent (Invitrogen, Karlsruhe, Germany). Sf9 cells were transferred to 35mm cell culture dishes (Nunc GmbH & Co. KG, Wiesbaden, Germany) in a concentration of $8 \cdot 10^5$cells/dish the day before transfection. The Cellfectin reagent was diluted 1 to 100 in the serum-free TC-100 medium. To 100 µl aliquot of diluted Cellfectin 200 ng bacmid DNA diluted in 100 µl of serum-free TC-100 medium was added. After incubation for 30min at room temperature, 900 ml of supplemented TC-100 medium was added, and the DNA/Cellfectin mixture was applied to the prepared Sf9 cells in 35mm dishes. After 4 hours incubation the transfection mixture was replaced by 2 ml of supplemented TC-100 medium. One week after transfection, the baculovirus–containing culture media was collected. After removal of cell debris by centrifugation for 10 min at 4000rpm the virus stock was obtained. The virus stock was used for virus maxi stock generation.

2.4.3 Virus maxi stock generation

Sf9 cells at a number of $5 \cdot 10^5$ were incubated with 30µl virus stock in 1ml supplemented TC-100 medium in a 75 mm^2 flask for one hour at 29°C. Afterwards virus containing medium was removed and replaced by 10ml supplemented TC-100 medium. After 5 days incubation at 29°C the medium was removed from the flask and stored as virus maxi stock.

2.4.4 Virus infection of Sf9 cells

The total number of 10^6 Sf9 cells was transferred in a 35mm cell culture dish. Cells remained for reattachment for one hour at 29°C. Afterwards medium was removed and 200µl virus stock or 30µl virus maxi stock plus 170µl supplemented TC-100 medium was added. After incubation at 29°C for 1h virus solution was replaced by supplemented TC-100 medium. Infected cells were incubated 38 to 40h at 29°C.

2.5 Biochemistry

2.5.1 Coimmunoprecipitation

Infected Sf9 cells were harvested in 1ml PBS 38 to 42 hours after infection and transferred into an Eppendorf cup. Cells were centrifuged for 2min at 3000rpm resuspended in PBS and pelletised again. The cells of two 35mm cell culture dishes were pooled and resuspended in 1ml NTEP buffer. Cell lysis in NTEP buffer was done for 45min on ice. Cell debris was spun down at 13200rpm for 20min. Afterwards the supernatant was divided into three equal volumes the first of which was was incubated with HA antibody, the second with c-myc antibody and the third with an unspecific IgG fraction [IgG, heavy chain, Ab-1, rabbit (Dianova, Hamburg, Germany)] for immunoprecipitation at 4°C for two hours on a shaker (for antibody specifications see chapter 2.5.2.1). Subsequently 40µl resuspended Protein-A Sepharose CL-4B (Sigma, St. Louis, USA) was added. Samples were incubated for 2h at 4°C on a shaker. The protein-antibody-sepharose complex was spun down at 10000rpm for 2min and washed at least four times with 1ml NTEP buffer. After each washing step the complex was pelleted again at 10000rpm for 2min. After the last washing step the supernatant was removed and the sepharose pellet resuspended in 30µl 1xLaemmli buffer. Samples were boiled for 5min, spun down at 13200rpm for 10min, divided into 2x15µl which both were loaded on different lanes of a 7.5% polyacrylamide gel for western blot analysis (compare chapter 2.5.2). The first of the two samples of the three different precipitates (anti-myc, anti-HA or anti-IgG) was probed with the

c-myc antibody the second one with the HA antibody.

2.5.2 Western Blot analysis

20µl protein samples in 1xLaemmli buffer were loaded on a 7.5% polyacrylamide gel. Electrophoresis was performed at 80V (stacking gel period) and furthermore at 120V. After electrophoresis the polyacrylamide gel and a nitrocellulose membrane (0.2 µm pore diameter) (Amersham Biosciences, GE Healthcare, Munich, Germany) were preincubated in transfer buffer for 30min. Semi-dry transfer was performed at 3mA/cm^2 membrane for 2h. Afterwards the nitrocellulose membrane was blocked in 5% (w/v) blocking agent (Amersham Biosciences, GE Healthcare, Munich, Germany) for 2 h at 4°C. After blocking the primary antibody in PBS/Tween was added for overnight incubation at 4°C (for primary antibody dilutions compare chapter 2.5.2.1). The membrane was washed three times for 30 min in PBS/Tween. For Secondary antibody incubation horseradish peroxidase coupled antibody directed against mouse or rabbit (Amersham Biosciences, GE Healthcare, Munich, Germany), depending on the origin of the primary antibody, was added in a 1:2000 dilution in PBS/Tween. Incubation was performed for one hour at 4°C. The blot was washed as described before. For band visualisation western blotting detection reagent or AceGlow detection reagent were added (Amersham Biosciences, GE Healthcare, Munich, Germany or PEQLAB Biotechnologie GMBH, Erlangen, Germany). Bands were visualised on a Kodak-X-OMAT AR photo film (Kodak, Stuttgart, Germany) or by cooled CCD-chip analysis with the Chemi-Smart 5000 (PEQLAB Biotechnologie GMBH, Erlangen, Germany). Band intensity quantification was performed with BIO-1D software (Vilber Lourmat, Torcy Z.I., France). Band intensities were normalised via an α-tubulin control.

2.5.2.1 Primary antibodies

Antibody	WB dilution
rabbit anti-GluRIIC (Qin et al., 2005)	1:500
mouse anti-c-myc (9E10) (Santa Cruz Biotechnology, Santa Cruz, CA, USA)	1:1000
mouse anti-HA: HA-probe (F-7) (Santa Cruz Biotechnology, Santa Cruz, CA, USA)	1:1000
Mouse, monoclonal anti-α-tubulin (Sigma, St. Louis, USA)	1 :2000

2.6 Two electrode voltage clamp measurements in Xenopus oocytes

The following techniques and preparations were performed in the laboratory of Prof. Dr. Michael Hollmann in the Department of Biochemistry I – Receptor Biochemistry at the Ruhr University Bochum.

Practically in the voltage-clamp method the membrane potential (V_m) of a cell is "clamped" to a certain value by an amplifier, called command potential (V_{cmd}). Each deviation from V_{cmd} caused by current flux through the membrane, in particular due to ion channel opening, is opposed by the induction of an equal current of inverted polarity. This compensatory current is taken as the dimension of current flow through the membrane.

2.6.1 The *Xenopus laevis* oocyte expression system

Oocytes from *Xenopus laevis* are a common heterologous expression system for ion channel proteins. External mRNA injected into the oocyte is translated with high efficiency and resulting proteins are subjected to modifications like phosphorylation and glycosylation (Gurdon et al., 1971; Coleman, 1984; Dascal, 1987). Voltage and ligand activated ion channels can be expressed functionally and subsequently characterised by two electrode voltage clamp (TEVC) (Miledi and Sumikawa, 1982; Gundersen et al., 1983; Barnard et al., 1987). In contrast to expression systems depending on cell transfection, coexpression of multiple

proteins is feasible in X*enopus* oocytes. The oocyte's size of about 1mm facilitates the handling of procedures like injection and the application of TEVC on the one hand. On the other hand the big size prevents the temporal resolution of fast current components since agonist cannot be applied to all receptor channels simultaneously (Goldin, 1991).

2.6.2 Oocyte preparation

Adult *Xenopus laevis* (Nasco, Fort Atkinson, WI) were anesthetised with 3-amino-benzoic acid ethylester (1.5 g/l; Sigma, Taufkirchen, Germany). Frog oocytes of stage V or VI were surgically removed from the ovaries and incubated in clusters of about 20 oocytes with 4mg/ml collagenase typeI (Worthington Biochemicals, Freehold, NJ) in Ca^{2+}-free Barth's solution for 1.5h at 20°C shaking slowly in order to remove the follicular cell layer. Afterwards oocytes were extensively washed with Barth's solution and kept in Barth's solution containing 100µg/ml gentamycin, 40µg/ml streptomycin and 63 µg/ml penicillin.

2.6.3 cRNA synthesis

cRNA synthesis was performed as described in (Hollmann et al. 1994). Template DNAs were linearised with *Nhe*I. 1µg linearised cDNA was applied to *in vitro* transcription using an *in vitro* transcription kit (MBI Fermentas). In a modified standard protocol 800µM of each of the ribonucleotides (Amersham Biosciences, GE Healthcare, Munich, Germany) (except rGTP which was used at 200µM) and 800µM GpppG (Amersham Biosciences, GE Healthcare, Munich, Germany) for capping were used and the total incubation time with T7 polymerase was prolonged to three hours. [α-^{32}P] UTP (Amersham Biosciences, GE Healthcare, Munich, Germany) was utilised for trace labeling in order to quantify cRNA yields and to estimate *in vitro* transcription quality via agarose gel electrophoresis.

2.6.4 cRNA injection

Sharp injection tips were created out of glass capillaries (WPI, Sarasota, FL, USA) in a PIP5 vertical puller (HEKA, Lambrecht/Pfalz, Germany) and afterwards mechanically broken. In two separate approaches 2ng and 10ng of each single

cDNA was injected into oocytes 24h after oocyte preparation with the aid of a nanoliter injector (WPI, Sarasota, FL, USA). Injected oocytes were stored three to six days in Barth's solution at 17°C.

2.6.5 TEVC measurements

Three to seven days after injection oocytes were applied to TEVC measurements in NFR as bath solution. The TEVC setup consisted of a microscope (Stemi 2000, Zeiss), a measurement chamber (constructed at the MPI for Experimental Medicine, Göttingen, Germany), a TurboTec 10CX amplifier (NPI Electronic GmbH, Tamm, Germany), an analog/digital transducer (ITC16 Computer Interface, Instrutech Corp., Long Island, NY, USA).

Voltage clamp measurements were performed at a holding potential of -70mV controlled by Pulse software (HEKA, Lambrecht/Pfalz, Germany). Electrodes were produced from borosilicate glass (Hilgenberg, Malsfeld, Germany) with the aid of a PIP5 vertical puller (HEKA, Lambrecht/Pfalz, Germany) and filled with 3M KCl. The resistance was between 1 to 4 MΩ for the voltage electrodes and between 0.1 to 1.5 MΩ for the current electrode. 6mM glutamate in NFR was applied through a flow system involving 60ml syringes which were connected to the measurement chamber via an eight-way valve (Hamilton, Reno, NV, USA) for a total duration of 20s. Current amplitude size was measured by Pulse software.

2.7 Drosophila melanogaster: cultivation, genetics and techniques

2.7.1 Fly cultivation

Fly strains were held at 25°C in plastic bottles (Greiner Bio-one, Kremsmünster, Austria) containing nutrition medium (ingredients: 195g agar, 200g soy flour, 360g yeast, 1600g corn flour, 440g beet syrup, 1600g malt, 30g nipagine, 126ml propionic acid, filled up to 18l with H_2O). For embryo collections plastic cylinders with a grid at their top were placed on apple agar plates (1l apple juice, 100g saccharose, 85g agar, 40ml nipagine (15%), filled up to 3l with H_2O).

2.7.2 Fly transgenics

An Eppendorf InjectMan (Hamburg, Germany) was used to perform *Drosophila* germ line transformation which was described in Rubin and Spradling, (1982). 300ng/µl of the P-element DNA (pUAST) containing the transgene was injected together with 100ng/µl of a helper plasmid (pΔ2-3) containing transposase. The genetic background of the transgenic animals was w1 (Castiglioni, 1951) (genetics described in 2.7.3).

2.7.3 Fly genetics

GluRIIA/GluRIIB double mutant background was generated by crossing *df(2L)cl*^{h4} (Petersen et al., 1997) to *df(2L)gluRIIA&IIB*^{SP22} (Petersen et al., 1997; DiAntonio et al., 1999; Qin et al., 2005), GluRIIC mutant background by crossing *df(2L)ast*^{2} to *gluRIII*^{1} (Marrus et al., 2004) and GluRIID mutant background by crossing *pBac{RB}01443* to *df(3R)gluRIID&IIE*^{E3} (Qin et al., 2005). *df(2L)cl*^{h4} and *df(2L)gluRIIA&IIB*^{SP22} are deficiencies for GluRIIA and GluRIIB, *df(2L)ast*^{2} is a deficiency for GluRIIC and *df(3R)gluRIID&IIE*^{E3} is a defiency for GluRIID and GluRIIE.

name	**genetics**
w1	$\frac{w-}{w-};\frac{+}{+};\frac{+}{+}$
AB- (embryo)	$\frac{w-}{w-};\frac{df(2L)gluRIIA\&IIB^{SP22}}{df(2L)gluRIIA\&IIB^{SP22}};\frac{+}{+}$
AB- (larvae)	$\frac{w-}{w-};\frac{df(2L)cl^{h4}}{df(2L)gluRIIA\&IIB^{SP22}};\frac{+}{+}$
AB-, IIAEGFP	$\frac{w-}{w-};\frac{df(2L)cl^{h4}}{df(2L)gluRIIA\&IIB^{SP22}};\frac{UASgluRIIA^{GFP893}}{+}$
AB-, IIBEGFP	$\frac{w-}{w-};\frac{df(2L)cl^{h4}}{df(2L)gluRIIA\&IIB^{SP22}};\frac{UASgluRIIB^{GFP897}}{+}$
IIA^{hypo}	$\frac{w-}{w-};\frac{df(2L)cl^{h4},UASgluRIIA^{hypo}}{df(2L)gluRIIA\&IIB^{SP22}};\frac{+}{+}$

C- (embryo)	$\frac{w-}{w-};\frac{gluRIII^{1}}{gluRIII^{1}};\frac{+}{+}$
IIC^{hypo}	$\frac{w-}{w-};\frac{df(2L)ast^{2},UASgluRIICcDNA}{gluRIII^{1}};\frac{+}{+}$
D- (embryo)	$\frac{w-}{w-};\frac{+}{+};\frac{pBac\{RB\}e01443}{pBac\{RB\}e01443}$
IID^{hypo}	$\frac{w-}{w-};\frac{UASgluRIID}{+};\frac{df(3R)gluRIID\ \&\ IIE^{E3}}{pBac\{RB\}e01443}$
DE- (embryo)	$\frac{w-}{w-};\frac{+}{+};\frac{df(3R)gluRIID\ \&\ IIE^{E3}}{df(3R)gluRIID\ \&\ IIE^{E3}}$
IIERNAi	$\frac{w-}{w-};\frac{UASgluRIIERNAi}{+};\frac{24B-Gal4}{+}$
IIFRNAi	$\frac{w-}{w-};\frac{UASgluRIIFRNAi}{+};\frac{24B-Gal4}{+}$

Table 1 Fly genetics
Genetics of all phenotypes used for fly biochemistry and immunohistochemistry. Shown are X, 2nd and 3rd *Drosophila* chromosomes.

The GluRIIE RNAi construct (IIERNAi) was described in Qin et al. (2005).

In IIC^{hypo} (and IID^{hypo}) animals a single transgene copy of *UASgluRIIC* (or *UASgluRIID*) in the absence of *Gal4*, thus expressed in reduced amounts, is sufficient to rescue embryos null for GluRIIC (C-) (or null for GluRIID (D-)).

For the generation of IIA^{hypo} a genomic fragment of GluRIIA, comprising the promoter region and the complete open reading frame but missing most of the 3' untranslated region (3'-UTR), was used. This transgene still produces full-length GluRIIA, however, in dramatically reduced amounts because of a loss of message stability (G. Qin and S. Sigrist, unpublished observations). This 3'-UTR construct was expressed from *pUAST* under the control of the endogenous *GluRIIA* promoter. A single transgene copy rescues embryos null for both *GluRIIA* and *GluRIIB* (Qin et al., 2005).

2.7.4 P-element imprecise excision screen

In the *Drosophila* genome transposable elements called P-elements which can be mobilised via an enzyme termed transposase occur naturally. The transposase encoding sequence is situated between inverted terminal repeats in the P-element. Stable inserted P-elements lack the transposase encoding sequence but carry genetic markers showing for instance a certain eye or body colour. These stable inserted P-elements can be mobilised with a probability of 11-13% (Karess and Rubin, 1984) by crossing in a transposase expressing chromosome. The majority of the P-elements will jump out precisely removing just the P-element from its insertion site. However a minority of the P-elements removes a random part of the adjacent genomic regions when mobilised in a process termed imprecise excision. In a genetic screen animals carrying a P-element in the gene of interest are exposed to transposase and the next generation is screened for animals lacking the genetic P-element marker. Stargazin deletion mutants were generated by the use of a fly line carrying the P-element P{SUPor-P}CG11566^{KG10455} [BDGP Gene Disruption Project (Bellen et al., 2004)] located in the first intron of CG33670 on the X-chromosome. For P-element mobilisation a fly line carrying the Δ2-3 Transposase on the second chromosome was used. Adult male flies from lines in which P{SUPor-P}CG11566^{KG10455} was mobilised were tested for imprecise excision events via genomic PCR.

2.7.5 Genomic PCR

Genomic PCR was performed on single flies according to (Gloor et al., 1993). In short, a single fly was mashed with a pipette tip, containing 50µl squishing buffer, without intentionally expelling any liquid. After mashing the remaining tip content was expelled on the mashed fly and subsequently incubated for 30in at room temperature followed by a 2min incubation step at 95°C for proteinase K inactivation.

The following primers were used to determine the deletion region's extent:

Primer pair 1	Deletion primer 1 forward	5′-AGAAGTGGCAGCCAGGATAC-3′
	Deletion primer 1 reversed	5′-GCGGCTAGAACAGATGAAGA-3′
Primer pair 2	Deletion primer 2 forward	5′-CATACACATACACTTGCACGC-3′
	Deletion primer 2 reversed	5′-GCGGCCTGTAGAGTTCGTA-3′
Primer pair 3	Deletion primer 3 forward	5′-GATACGAACTCTACAGGCCGC -3′
	Deletion primer 3 reversed	5′-CACCGAAGGATAATCCCTCAT-3′
Primer pair 4	Deletion primer 4 forward	5′-ATGAGGGATTATCCTTCGGTG-3′
	Deletion primer 4 reversed	5′-GAGTGTTGCTGGTGGTGGTG-3′
Primer pair 5	Deletion primer 5 forward	5′-CACCACCACCAGCAACACTC-3′
	Deletion primer 5 reversed	5′-GGCTGCAACAGGTGTGATGA-3′
Primer pair 6	Deletion primer 6 forward	5′-GAGTCTGCGGTTGGCAACTT-3′
	Deletion primer 6 reversed	5′-TGTCCTGGTGGCTCCTGTAA-3′
Primer pair 7	Deletion primer 7 forward	5′-GCCAAGTTGCTGCAATTC-3′
	Deletion primer 7 reversed	5′-CCATTGGCTTTGGCTACA-3′
Primer pair 8	Deletion primer 8 forward	5′-TAGCACCACCATAGCGTATC-3′
	Deletion primer 8 reversed	5′-TATCGCAGCCATGAGTTG-3′
Primer pair 9	Deletion primer 9 forward	5′-GTGCGGCTTGTAGGCATT-3′
	Deletion primer 9 reversed	5′-TCTCTGATGCGTCACTCC-3′
Primer pair 10	Deletion primer 10 forward	5′-GGTTGTTCGGATGCTTCACT-3′
	Deletion primer 10 reversed	5′-GGCAACTCTATCGGTGAATG-3′
Primer pair 11	Deletion primer 11 forward	5′-CCAATGTAGGCGGTTGTA-3′
	Deletion primer 11 reversed	5′-CGCGTAGTCACAAGTGCT-3′
Primer pair 12	Deletion primer 11 forward	5′-AGCTTCGTACGCATGTGT-3′
	Deletion primer 11 reversed	5′-CAGAGACTGGACTTGGTGTACT-3′

An overview for primer position and P-element location on the stargazin locus is given in Figure 12.

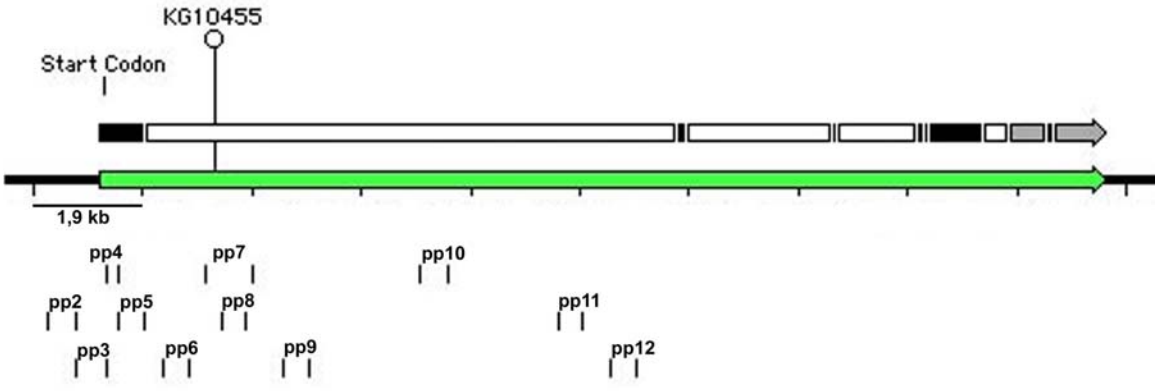

Figure 12 P-element and primer position for stargazin imprecise excision screen
Shown in green is the genetic region of the predicted *Drosophila* stargazin protein published by Walker et al. (2006b) on the X-chromosome. Exons encoding for this predicted protein are depicted in black, non coding exons in grey and introns in white. The P-element P{SUP or -P}CG11566^{KG10455} is shown as hollow circle (KG10455). The start codon position is shown above the intron-exon sequence. The pairs of lines beneath the gene region represent the 11 of the 12 primer pairs (pp2-pp12) used in genomic PCR to determine the deletion size (for primer sequences see above).

2.7.6 Quantitative real-time PCR

Real-time PCR was performed in order to estimate the expression levels of the *Drosophila* homologous proteins for SOL-1 and stargazin as well as for GluRIIF in somatic muscles and CNS tissue. Total RNA was extracted from entire 3rd instar larvae, larval or adult heads and larval or adult torsi with the RNeasy mini kit (Qiagen, Hilden, Germany). 2µg extracted RNA was used in reverse transcription reaction with the TaqMan reverse transcription kit (Applied Biosystems Foster City, CA, USA). The synthesised cDNA together with specific primer pairs were applied to real-time PCR reaction using QuantiTect SYBR Green PCR master mix (Applied Biosystems Foster City, CA, USA). Quantitative real-time PCR was performed utilising the GeneAmp 5700 Sequence Detection System (Applied Biosystems Foster City, CA, USA). Ct values were calibrated against total cDNA levels of the TaT binding protein-1 (tbp-1), which was used as internal control. Transcript levels were normalised to the level of wild type transcript. For the comparison of transcript levels in heads and torsi, head transcript levels were used for normalisation. Data were analised with Excel (Microsoft Corporation, Redmond, USA).

The following primer pairs were used for real-time PCR experiments in this

thesis:

SOL-1 1	fw primer	5′-GTGCCTACAAGTTGATTGGTCG-3′
	rv primer	5′-ATGTGAGCGGATTCTGCGTC-3′
SOL-1 2	fw primer	5′-GTCTACAATAGCAGCGAGCG-3′
	rv primer	5′-GCACAACTCTTTCGTCACTTGC-3′
Stargazin 1	fw primer	5′-GCAGGGAGGCATCAGCAACAT-3′
	rv primer	5′-GTAGTTGGCATTGGGCAGCTTCTC-3′
Stargazin 2	fw primer	5′-TCCAATGAGGGTTATCAGCCG-3′
	rv primer	5′-CCAGCAGCCAGGAAAATAGGA-3′
Stargazin 3	fw primer	5′-AGCAACACTCGCCCTATGC-3′
	rv primer	5′-GGAATGCTGCCAGAGATCG-3′
Stargazin 4	fw primer	5′-CCACTTGCTCGCATCAAAAC-3′
	rv primer	5′-CGATTTCCGCCTTCAGTATTG-3′
GluRIIF	fw primer	5′-CGTAATTTCTAATGCCTTGCCCC-3′
	rv primer	5′-GCAGATTCAATACTGCTTTCGCG-3′
1st transcript	fw primer	5′-CAGAAATGGCAGAGGAACTTCG-3′
	rv primer	5′-GCAACTTCGTTTTCGCGGT-3′
2nd transcript	fw primer	5′-ATTCTTACGCCAAGGATCTGGAC-3′
	rv primer	5′-GCGAATGGAGCAATGAAGGAG-3′
tbp-1	fw primer	5′-AAGCCCGTGCCCGTATTATG-3′
	rv primer	5′-AAGTCATCCGTGGATCGGGAC-3′

2.7.7 Immunohistochemistry

2.7.7.1 Larval body-wall preparation, fixation and staining

2.7.7.1.1 Preparation

3rd instar larvae were attached to a rubber dissection pad with fine steel insect pins (0.1*10mm, Thorns, Göttingen, Germany) and covered by a drop of cold HL-3 solution (Stewart et al., 1994). The larvae were cut open dorsally along the midline from posterior to anterior with dissection spring scissors (FST, Vancouver, Canada). The epidermis was stretched and pinned down by the use

of two insect pins on each side. All internal organs and the central nervous system were removed with fine forceps (FST, Vancouver, Canada).

2.7.7.1.2 Fixation and staining

Preparations were fixed for 10 minutes with 4% paraformaldehyde (PFA) in phosphate-buffered saline (PBS). Afterwards the larval preparations were transferred in a blocking solution containing 5% NGS in PBT (PBS containing 0,05% Triton TX100) for 30 min. Blocking solution war removed and replaced by blocking solution containing the primary antibody. The dissection was incubated over night at 4°C. The next morning the samples were washed three times for 5 minutes and afterwards three times for 20 min with PBT. Fluorescence-labeled secondary antibodies were added 1:500 in PBT containing 5% NGS and incubated at room temperature for 2 hours following washing steps as described before. The preparations were mounted on an object slide in VectaShield Mounting Medium for fluorescence (Vector Laboratories, Burlingame, USA).

2.7.7.2 Primary antibody concentrations

mouse anti-GluRIIA (8B4D1; Developmental Studies Hybridoma Bank, Iowa City, USA)	1:100
rabbit anti-GluRIIC (Qin et al., 2005)	1:500
rabbit anti-GluRIID (Qin et al., 2005)	1:500
mouse anti-NC82 (gift of E. Buchner, University of Würzburg, Germany)	1:100
mouse anti-c-myc (9E10) (Santa Cruz Biotechnology, Santa Cruz, CA, USA)	1:500
mouse anti-HA: HA-probe (F-7) (Santa Cruz Biotechnology, Santa Cruz, CA, USA)	1:500
goat anti-HRP cyanine 5 (Dianova, Hamburg, Germany)	1:200

2.7.7.3 Fluorescence microscopy, image acquisition and analysis for quantitatve fluorescence measurements

Immunostainings of *Drosophila* larval body muscle preparations were examined with the wide field fluorescence light microscope Axioscope 2 equipped with an Axiocam camera MOT (Zeiss, Jena, Germany). Pictures were produced through a 100x oil immersion objective (numerical apperture 1.4) or alternatively a 40x oil immersion objective (numerical aperture 1.3) with the Axiovision software (Zeiss, Jena, Germany).

For fluorescence signal quantification images of PSDs at body wall muscles 6/7 were acquired at a fixed illumination time allowing the comparison of the fluorescence intensity information of two different images. Image analysis was performed with Image J (NIH, Bethesda, USA). For each picture a cumulative intensity histogram starting from the gray value 255 was generated. In order to assure signal specificity the gray value for the 1000th brightest pixel was determined and used for intensity estimation.

Results were transferred to and further processed in Excel (Microsoft Corporation, Redmond, USA), statistical analysis was performed in GraphPad Prism 4 (GraphPad Software, San Diego, USA). For statistical analysis the nonparametric Mann-Whitney rank sum test was applied.

2.7.8 Preparation of embryonic and larval samples

Embryos were collected and dechorionated 18h AEL. 3rd instar larval body wall preparations were done as described in 2.7.7.1.1. A total number of 60 embryos or 20 larval preparations was transferred into 50µl 2%SDS solution including 10µl 5x concentrated SDS sample buffer. Subsequently embryonic and larval samples were mechanically homogenised with an Eppendorf pastille and centrifuged at 13200 rpm for 5min. Homogenisation and centrifugation was repeated once more. Afterwards the homogenate was denatured at 95°C for 10min following a 10min centrifugation step at 13200 rpm. 20µl of embryonic or larval samples were loaded on a 7.5%SDS gele.

2.7.9 TEVC measurements at the *Drosophila* larval NMJ

(Measurements were performed by Andreas Fröhlich)

TEVC measurements were performed at the ventral-longitudinal muscle 6 of the anterior abdominal segments A2 and A3 in male late 3rd instar larvae at 22°C. Larval body wall preparations were done as described in chapter 2.7.7.1.1. In addition the CNS was removed by cutting through the segmental near the ventral nerve chord. The larval fillet preparations were washed with HL-3 solution supplemented with 1 mM Ca^{2+} and subsequently transferred to the recording chamber where the larval NMJ was detected with the help of a fixed-stage upright microscope (BX51WI; 40x water-immersion lens (Olympus, Hamburg, Germany).

Miniature amplitude and evoked postsynaptic currents were recorded with an AxoClamp 2B amplifier (Axon Instruments, USA). Sharp micropipettes made of borosilicate glass (with filament, 1.5 mm outer diameter) were filled with 3 M KCL were used as for voltage and current electrodes. The electrode resistances were between 10 and 20 MΩ, holding potential was set to -60mV.

3 Results

3.1 Overview

At the *Drosophila* NMJ five different subunits, GluRIIA-E, have been identified so far (Schuster et al., 1991; Petersen et al., 1997; DiAntonio et al., 1999; Marrus et al., 2004; Featherstone et al., 2005; Qin et al., 2005). Null mutants for the essential subunits GluRIIC, GluRIID or GluRIIE or a double mutant for GluRIIA and GluRIIB result in the absence of any glutamate receptor subunit at the *Drosophila* NMJ (Qin et al., 2005). Furthermore, by reducing the levels of subunits GluRIIA, GluRIIC, GluRIID or GluRIIE, the other glutamate receptor subunits are concomitantly reduced (Marrus et al., 2004; Featherstone et al., 2005; Qin et al., 2005). These data suggest that ionotropic glutamate receptors at the *Drosophila* NMJ form as heteromultimeric complexes requiring four distinct subunits. However, the exact receptor stoichiometry remains unknown. Vertebrate glutamate receptors are perhaps composed of four subunits, with each receptor tetramer established as dimer of dimers (Mayer and Armstrong, 2004). Assuming a tetrameric receptor complex for glutamate receptors at the *Drosophila* NMJ, this tetrameric complex would include the three essential subunits as well as either GluRIIA or GluRIIB. However, a strict receptor stoichiometry requiring four different subunits has not been described for ionotropic glutamate receptors before. The maximum number of different subunits in a ionotropic glutamate receptor complex has been identified in vertebrate NMDA receptors so far. Coexpression of NR1, NR2 and NR3 results in a functional receptor, which displays a decrease in glutamate-induced currents compared to NMDA receptor complexes consisting of subunits NR1 and NR2 (Sucher et al., 1995; Nishi et al., 2001).

In this thesis, coimmunoprecipitation experiments were performed in Sf9 cells in order to identify differences in the strength of subunit-subunit interactions for heteromeric receptors consisting of various combinations of two GluRII subunits (chapter 3.4).

In *GluRIIA&IIB* double mutant embryos as well as in the *GluRIID* mutant embryos synaptic transmission is completely abolished at the *Drosophila* NMJ (Featherstone et al., 2005; Yoshihara et al., 2005). To learn more about the total protein levels of GluRII subunits in the absence of one essential subunit in embryos western blot analysis was performed (chapter 3.6). The reduction of one GluRII subunit results in the reduction of all GluRII subunits at the *Drosophila* NMJ (Marrus et al., 2004; Featherstone et al., 2005; Qin et al., 2005). In order to examine the influence of the reduction of GluRII subunits on the protein levels of the only biochemically accessible subunit GluRIIC western blot analysis was performed in 3rd instar larvae displaying hypomorphic expression levels of one GluRII subunit (chapter 3.6).

Furthermore, it was attempted to reconstitute functional glutamate receptor complexes of *Drosophila* muscles by recombinant expression. The requirement of both four different *Drosophila* NMJ glutamate receptor subunits and accessory proteins for the formation of a functional receptor complex was examined in *Xenopus* oocytes via TEVC measurements (chapter 3.7).

Among several accessory proteins of glutamate receptor complexes, members of the TARP family have been suggested to be key factors in AMPA receptor trafficking, synaptic insertion and, furthermore, to alter AMPA receptor ion channel properties (Chen et al., 2000b; Cuadra et al., 2004; Tomita et al., 2004; Tomita et al., 2005b; Turetsky et al., 2005; Vandenberghe et al., 2005b). Genetic tools available in *Drosophila* might allow a particularly thorough analysis of TARP function. In this thesis, a potentional *Drosophila* stargazin homologue was examined through immunohistochemical and biochemical experiments (chapter 3.8).

As already mentioned above, so far, five different non-NMDA type receptor subunits have been identified at the *Drosophila* NMJ. In fact this thesis demonstrates a sixth glutamate receptor subunit at the *Drosophila* NMJ. In this thesis, immunohistochemical data suggest that in fact GluRIIF is also expressed within PSDs of larval neuromuscular synapses. Furthermore, the interdependency of GluRIIF and the other GluRII subunits was examined through

immunhistochemical and electrophysiological experiments (chapter 3.9).

3.2 In vivo tagging of Drosophila muscle expressed glutamate receptor subunits

Based on the model of Ayalon and Stern-Bach glutamate receptors assemble first as dimers and tetramerisation occurs by formation of a dimer of dimers. Here it was attempted to identify differences in subunit-subunit interactions using coimmunoprecipitation experiments between *Drosophila* muscle GluRII subunits recombinantly coexpressed in insect cells (Sf9). In order to allow efficient precipitation, *Drosophila* glutamate receptor subunits were equipped with tags allowing precipiation. Receptor tagging was unavoidable because, despite substantial efforts, antibodies allowing Western blot detection of *Drosophila* GluRII subunits are still very limited (see chapter 3.5, below). Glutamate receptor subunits GluRIIA to GluRIIE were tagged with multiple repeats of HA and myc, for which antibodies with high affinity exist. GluRIIA already was functionally tagged with EGFP before in our lab (Rasse et al., 2005). Systematic variation of tagging sites showed just one position in GluRIIA, namely in the middle of the C-terminal tail, at which EGFP did not interfere with receptor functionality and PSD incorporation. In order to tag subunits GluRIIB-GluRIIE an EGFP tag was inserted at exactly this postion in the middle of the subunits C-termini. Since the EGFP sequence was equipped with flanking restriction sites, EGFP could be easily replaced with a 3xHA and a 5xmyc tag. Subsequently, the tagged receptor subunits were tested for in vivo PSD incorporation after transgenesis.

Under the influence of the *Mhc-Gal4* driver *UAS* constructs of the 3xHA and 5xmyc tagged GluRII receptor subunits were expressed in somatic muscles. The tagged receptor subunits were visualised via immunohistochemistry at the *Drosophila* NMJ of 3rd instar larval body wall preparations with the anti-HA antibody or the anti-c-myc antibody. In fact, all receptor subunits tagged with either 3xHA or 5xmyc were targeted to the PSDs (data not shown). An overview of the tagged subunits cloned and transgenically introduced into the fly genome is given in Figure 13.

Receptor subunit	EGFP tag	5xmyc tag	3xHA tag
GluRIIA	++	+	++
GluRIIB	++	+	++
GluRIIC	-	++	++
GluRIID	++	+	++
GluRIIE	++	+	++

Figure 13 Fluorescence inensity signal of tagged glutamate receptor subunits at the *Drosophila* NMJ
Shown is an overview of all *UAS*GluRII subunit constructs carrying an EGFP tag, a 5xmyc tag or a 3xHA tag in the middle of their C-terminus at a position, which was shown to maintain GluRIIA receptor functionality after insertion of EGFP (Rasse et al., 2005). The *UAS*GluRII constructs were expressed in somatic muscles. Expression was regulated by the *Mhc-Gal4* driver. The presence of each GluRII construct at the *Drosophila* NMJ was tested via immunohistochemistry. EGFP constructs, which were used as precursor constructs for the generation of the 3xHA and 5xmyc constructs, were probed with the anti-GFP antibody, 5xmyc constructs were probed with the anti-c-myc antibody and 3xHA constructs with the anti-HA antibody. All constructs but the GluRIIC EGFP construct were identified in PSDs at the *Drosophila* NMJ. ++: strong PSD signal; +: weak PSD signal; -: no PSD signal

3.3 Expression of 3xHA and 5xmyc tagged glutamate receptor subunits in Sf9 cells

The tagged receptors were applied to Baculovirus infection of Sf9 cells an insect cell line derived from the ovary of the butterfly *Spodoptera frugiperda*. Because of their closer relationship to *Drosophila* compared to other common mammalian cell lines, Sf9 cells were considered being more likely to provide the expressed receptors with interactor, transport and scaffolding proteins required for receptor maturation and proper localisation. Moreover, the baculovirus expression system used for Sf9 cell infection was shown to efficiently express recombinant receptor proteins (Mouillac et al., 1992; Ponimaskin et al., 1998; Ponimaskin et al., 2001; Ponimaskin et al., 2002).

Indeed high expression levels of recombinantly expressed *Drosophila* NMJ glutamate receptors could be verified in Sf9 cells by immunoprecipitation and western blot analysis (compare Figure 14, Figure 15).

3.4 Addressing glutamate receptor subunit composition by coimmunoprecipitation in Sf9 cells

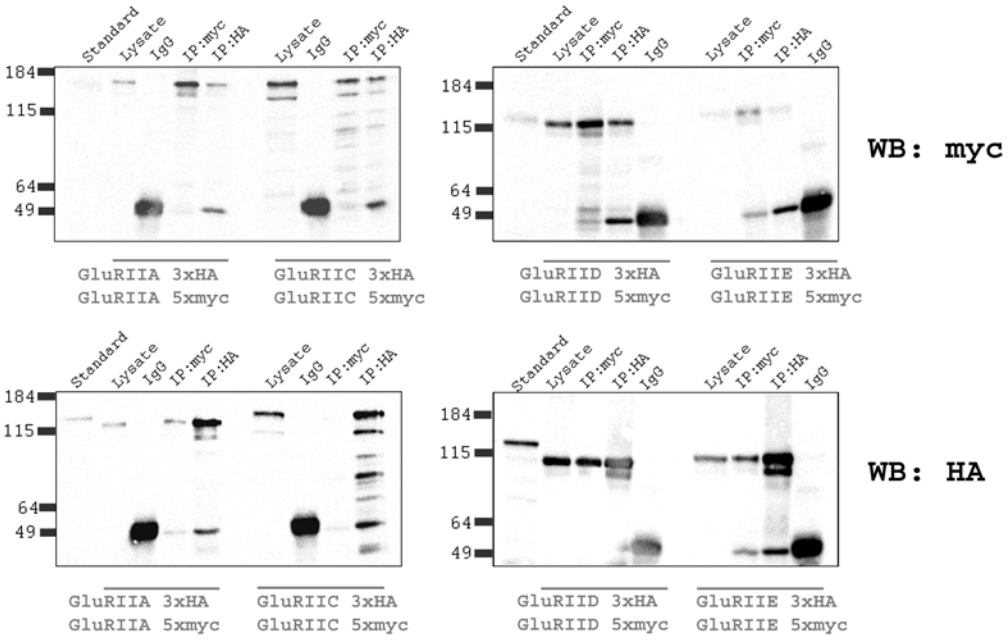

Figure 14 Coimmunoprecipitation experiments of homomeric 3xHA and 5xmyc tagged glutamate receptor subunit pairs from Sf9 cell lysates
3xHA and 5xmyc tagged versions of one single glutamate receptor subunit were coexpressed in Sf9 cells. Coimmunoprecipitation of the 3xHA and 5xmyc tagged version was performed for receptor subunits GluRIIA, GluRIIC, GluRIID and GluRIIE. Both antibody combinations for immunoprecipitation (IP) and western blot (WB) (IP: anti-myc, WB: anti-HA or IP: anti-HA, WB: anti-myc) were tested. On each blot the following samples are shown: the input control (Lysat) taken after cell lysis, a control IP (IgG) in which IgG in the absence of an antibody was used to show unspecific precipitation, an IP performed with c-myc antibody (IP: myc) and an IP performed with HA antibody (IP: HA). The upper two blots were probed with the myc antibody, the lower two blots with the HA antibody. Numbers on the left part of each blot indicate the molecular weight in kDa.

For interaction studies, two differently tagged receptor subunits, the first carrying a 3xHA tag, the second carrying a 5xmyc tag, were coexpressed in Sf9 cells.

First of all homomeric receptor subunit pairs were tested in coimmunoprecipitation experiments. The receptor complexes were precipitated from Sf9 cell lysates with antibodies directed against their myc or HA tag. Consecutively both precipitates were probed against both the myc tagged as well as the HA tagged subunit using western blotting. Combinations of monomeric

GluRIIA, GluRIIC, GluRIID or GluRIIE receptors were tested. For each combination tested, coprecipitation for both possible combinations for immunoprecipitation (IP) and western blot (WB) (IP: anti-myc, WB: anti-HA or IP: anti-HA, WB: anti-myc) was found (compare Figure 14). Precipitation due to unspecific protein binding to the antibody – Protein-A sepharose complex was excluded through a control in which an unspecific IgG antibody fraction coupled to sepharose A was incubated in Sf9 cell lysates containing the tested tagged glutamate receptor subunit combination (compare IgG lanes in Figure 14 and Figure 15). Thus, these first experiments indicated a potential for homotypic interaction between subunits GluRIIA-IIE.

Next, coimmunoprecipitation experiments for heteromeric complexes consisting of two different subunits showed no striking difference compared to homomeric complexes. Coprecipitation could be shown for the tested combinations for at least one of the two possible immunoprecipitation/western blot antibody combinations (Figure 15). However, the coexpression of the combination of GluRIID 5xmyc and the serotonin receptor 5HT1A from mouse carrying an HA tag, which was used as a negative control, resulted in coprecipitation, too, just faintly visible for IP: anti-myc, WB: anti-HA conditions but obvious under IP: anti-HA, WB: anti-myc conditions (Figure 15 bottom right blots). While a specific interaction between serotonin receptors and glutamate receptors cannot be excluded in the moment, non-physiological interactions between GluRII subunits are likely to have been contributed to coimmunoprecipitation here.

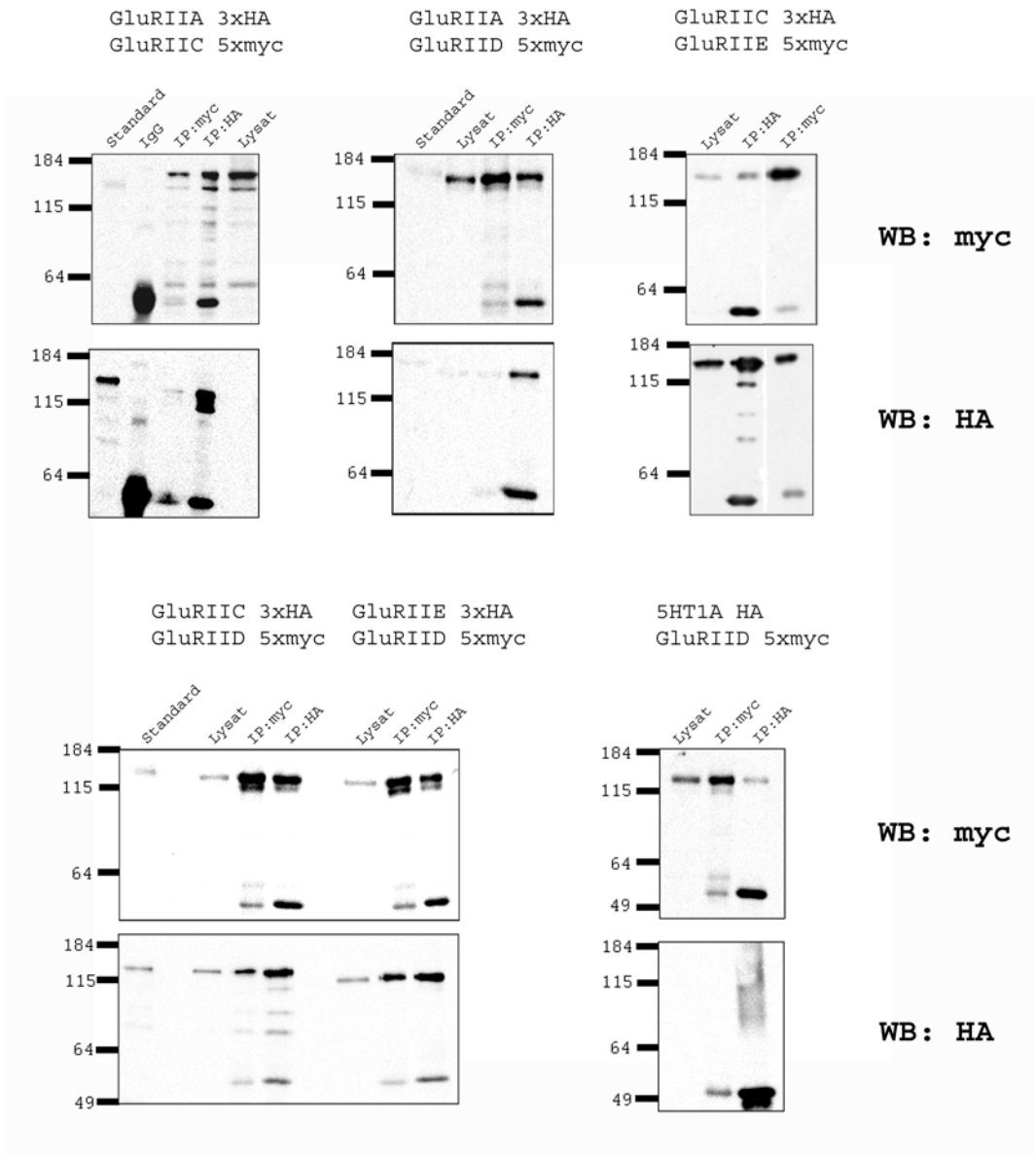

Figure 15 Coimmunoprecipitation experiments of heteromeric 3xHA and 5xmyc tagged glutamate receptor subunit pairs from Sf9 cell lysates

The 3xHA tagged version of one glutamate receptor subunit was coexpressed with the 5xmyc tagged versions of a different glutamate receptor subunit in Sf9 cells. Coimmunoprecipitation was performed for the following receptor subunit combinations, the first one 3xHA tagged, the second one 5xmyc tagged: GluRIIA+GluRIIC, GluRIIA+GluRIID, GluRIIC+GluRIIE, GluRIIC+GluRIID and GluRIIE+GluRIID. In addition 5HT1A HA, a HA tagged murine serotonin receptor was coexpressed with GluRIID 5xmyc as a negative control for non-specific receptor interactions. Both antibody combinations for immunoprecipitation (IP) and western blot (WB) (IP: anti-Myc, WB: anti-HA or IP: anti-HA, WB: anti-Myc) were tested. Coexpressed subunits are shown above each blot. On the presented blots the following samples are shown: Standard: Sf9 cell lysat containing subunits GluRIID 5xmyc and GluRIIE 3xHA, Lysat: input control taken after cell lysis, IgG: a control IP in which IgG in the absence of an antibody was used to show unspecific precipitation, IP: myc: an IP performed with myc antibody, IP: HA: an IP performed with HA antibody. In each case the upper of the two blots on top of each other was probed with the myc antibody, the lower one with the HA antibody. Numbers on the left part of each blot indicate the molecular weight in kDa.

Taken together, Sf9 cell expression did not appear suited to explore physiological subunit-subunit interactions between GluRII subunits.

3.5 Detection of endogenously expressed GluRIIC using western blot analysis

In immunohistochemical studies antibodies directed against GluRIIA, GluRIIB, GluRIIC and GluRIID were shown to label the receptor subunits at the *Drosophila* NMJ (Marrus et al., 2004; Qin et al., 2005). However, the only antibody, which reliably results in visible bands in western blot analysis, is the polyclonal GluRIIC antibody from rabbit [(Qin et al., 2005), Figure 16].

3.6 Examination of the dependence of GluRIIC subunit expression levels on the presence of other receptor subunits

As already mentioned before, single knockout mutations of glutamate subunits GluRIIC, GluRIID or GluRIIE as well as a double knockout mutation for subunits GluRIIA&GluRIIB are embryonic lethal (DiAntonio et al., 1999; Qin et al., 2005). *GluRIIA&GluRIIB* double mutant embryos as well as *GluRIID* mutant embryos do not display synaptic transmission at the *Drosophila* NMJ (Featherstone et al., 2005; Yoshihara et al., 2005). Additionally, hypomorphs expressing reduced levels of GluRIIC (IIC^{hypo}), GluRIID (IID^{hypo}), GluRIIA in the absence of GluRIIB (IIA^{hypo}) or GluRIIE (IIERNAi) (for details on genetics of these genotypes compare Methods chapter 2.7.3) display a reduced amount of the remaining glutamate receptor subunits at the *Drosophila* NMJ of 3rd instar larvae (Marrus et al., 2004; Featherstone et al., 2005; Qin et al., 2005). However, whether the reduction of one subunit induces degradation of the other subunits or whether the other subunits are stabilised in internal pools, unable to traffick further to the PSDs, is not known.

In order to examine the effect of losing an essential subunit or subunit combination on the protein levels of a remaining subunit western blot analysis was performed in late stage embryos of *GluRIIA&GluRIIB* double mutants (AB-),

GluRIIC null mutants (C-), *GluRIID&GluRIIE* double mutants (DE-) (for details on genetics of these genotypes see Methods chapter 2.7.3). Western blots were probed with the GluRIIC antibody.

To further analyse the protein levels in 3rd instar larvae, displaying residual levels of one receptor subunit, western blot analysis was performed in 3rd instar larval body wall preparations of IIA^{hypo}, IIC^{hypo}, IID^{hypo}, or IIERNAi. Again, western blots were probed with the GluRIIC antibody.

In AB-, C-, D- and DE- embryos, GluRIIC protein levels were strongly reduced when compared to wild type animals (Figure 16 A). However, the remaining GluRIIC levels detected in the null mutants were approximately one third of the GluRIIC levels in wild type animals. Loss of GluRIIC itself did not completely abolish the GluRIIC band in embryos. Band quantification and normalisation to tubulin levels showed a decrease of the IIC signal to a residual 12% when compared to wild type animals. This basal band intensity is most likely due to the nature of the $G\mathit{luRIII}^{1}$ background. $G\mathit{luRIII}^{1}$ is no deletion mutant of GluRIIC but a random point mutant generated through ethyl methanesulfonate (EMS) treatment (Marrus et al., 2004). Although $G\mathit{luRIII}^{1}$ results in embryonic lethality when crossed over $\mathit{df(2L)ast}^{2}$ the GluRIIC protein levels are not gone for this GluRIIC mutant. These findings indicate that this allele is a functional null mutant but no protein null mutant.

In IIC^{hypo}, IID^{hypo}, or IIERNAi 3rd instar larvae reduced GluRIIC protein levels in comparison to wild type larvae were detected. Strikingly, IIA^{hypo} conditions were sufficient to retain GluRIIC protein levels to an amount comparable to wild type animals (Figure 16 B).

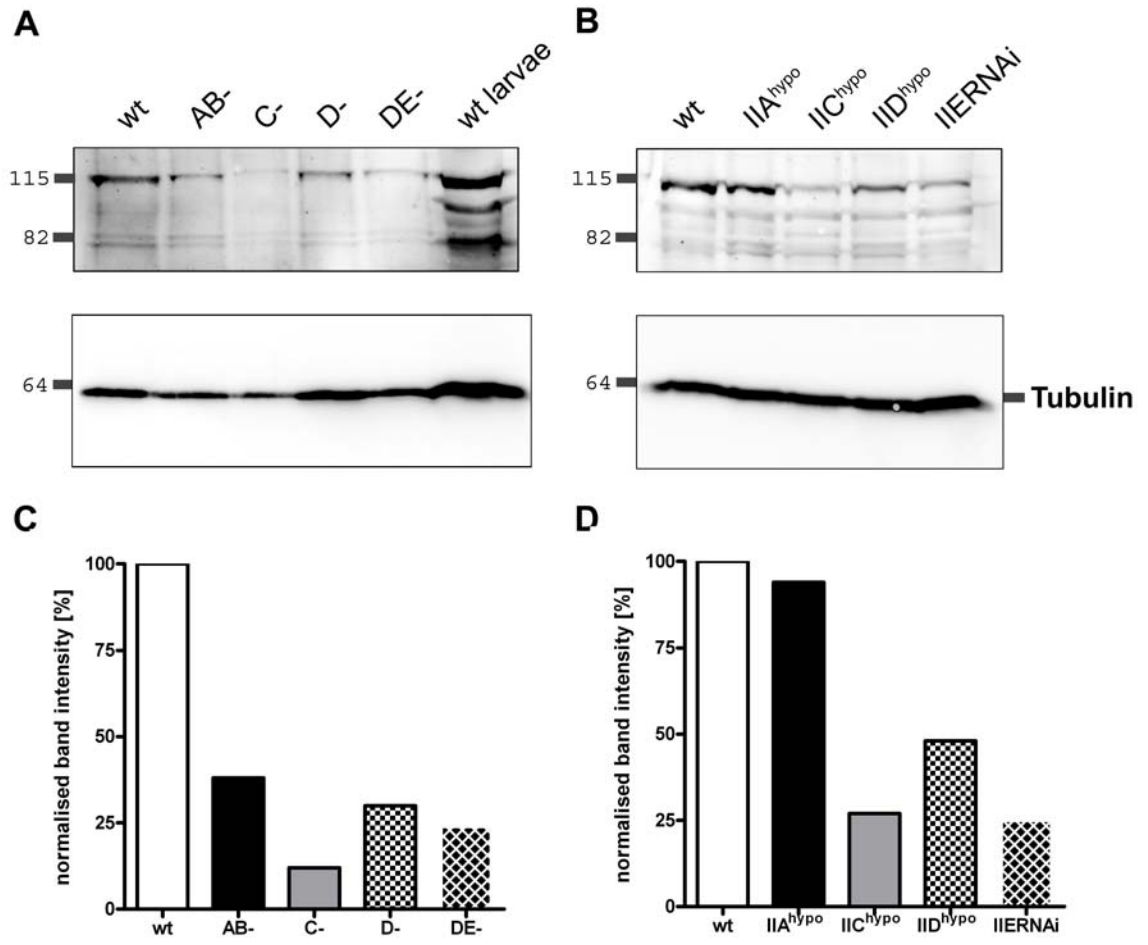

Figure 16 Determination of GluRIIC protein levels in GluRII subunit mutant embryos and GluRIIA, GluRIIC and GluRIID hypomorphic larvae
Shown are western blot analyses of **A)** late stage embryos of receptor subunit null mutants and of **B)** 3rd instar larvae expressing low levels of a particular single receptor subunit. The upper two blots were probed with the GluRIIC antibody and the lower two blots with the α-tubulin antibody as a loading control for band intensity normalisation. Band intensities normalised to the tubulin control were compared to wild type (wt) band intensities. **C)** Shown are the normalised band intensities in embryos. Protein levels are reduced for embryos missing subunits GluRIIA+GluRIIB (AB-) (normalised band intensity: 38% of wt), those missing subunit GluRIID (D-) (normalised band intensity: 30% of wt) and those missing subunits GluRIID+GluRIIE (DE-) *(*normalised band intensity: 24% of wt). Embryos missing the GluRIIC subunit (C-) show a residual signal (normalised band inensity: 12% of wt). **D)** Shown are the normalised band intensities in 3rd instar larvae. Low levels of GluRIIA (IIA^{hypo}) retain wt like GluRIIC levels (normalised band intensity: 94% of wt) whereas low levels of GluRIIC, GluRIID and GluRIIE still show a clear reduction of GluRIIC protein levels (IIC^{hypo} normalised band intensity: 27% of wt; IID^{hypo} normalised band intensity: 48% of wt; IIERNAi normalised band intensity: 25% of wt). The numbers on the left part of the blot show the molecular weight in kDa.

Immunohistochemical results showed no visible synaptic glutamate receptor levels at the NMJ of embryos missing one of the essential subunits (Featherstone et al., 2005; Qin et al., 2005). Moreover, just very faint synaptic

levels of glutamate receptor subunits were deteceted at the *Drosophila* NMJ for IIA^{hypo}, IIC^{hypo}, IID^{hypo}, or IIERNAi larvae (Marrus et al., 2004; Featherstone et al., 2005; Qin et al., 2005). In contrast to these findings, GluRIIC protein levels in embryos or in 3rd instar larval body wall preparations were reduced to a far lesser degree as indicated by immunohistochemistry. Embryos missing an essential glutamate receptor subunit display approximately one third of the protein levels found in wild type animals while hypomorphs of an essential receptor subunit in 3rd instar larvae show GluRIIC protein amounts at least 25% the size of wild type animals. These results indicate that internal pools still contain a considerable amount of GluRIIC containing complexes, which are stabilised and thus not destined for degradation. However, this GluRIIC containing complexes fail to assemble as synaptic receptor complexes. Interestingly low amounts of GluRIIA in the absence of GluRIIB raise GluRIIC levels to almost 100% compared to the wild type situation without increasing the numbers of functional receptors at the PSDs. These findings indicate that GluRIIA in the absence of GluRIIB mediates a stabilising effect on GluRIIC levels during glutamate receptor formation and processing. However, GluRIIA levels in IIA^{hypo} are not sufficient to increase synaptic receptor numbers at the *Drosophila* NMJ.

In contrast to IIA^{hypo} larvae, which display no reduction in GluRIIC levels, IID^{hypo} and IIERNAi larvae showed decreased GluRIIC protein levels, probably due to increased GluRIIC degradation. This observation indicates an involvement of either GluRIID or GluRIIE or both in proper receptor trafficking.

Worth mentioning, GluRIIC bands in embryos slightly differ in size compared to larval GluRIIC bands, which appear a little bit smaller in size (compare Figure 16 A lanes 1-5 contra lane 6). This size shift can reflect a different glycosylation pattern as a means for receptor maturation during different developmental stages in *Drosophila*. Immature glycosilation of vertebrate glutamate receptor subunits was shown to block ER exit (Greger et al., 2002). However, since a size shift is also visible when comparing wild type embryos with wild type larvae, a possible difference in the glycosylation pattern rather influences other receptor properties than ER/Golgi trafficking.

3.7 TEVC measurements of heterologously expressed Drosophila NMJ glutamate receptors in Xenopus oocytes

3.7.1 TEVC measurements of different *Drosophila* glutamate receptor subunit combinations expressed in *Xenopus* oocytes

After glutamate receptors are trafficked to the cell membrane and inserted into the synapse they are accessible for electrophysiological experiments. Electrophysiological measurements at the *Drosophila* NMJ displayed the indispensability of subunits GluRIIC and GluRIID and the subunit pair GluRIIA+GluRIIB for the formation of functional receptors at the NMJ (Marrus et al., 2004; Featherstone et al., 2005; Qin et al., 2005). However, so far no heterologously expressed glutamate receptor has been found to be functional. As previously mentioned, the combined data on GluRII subunits suggests a heteromeric glutamate receptor complex consisting of either subunits GluRIIA,C,D,E or GluRIIB,C,D,E. But does coexpression of these subunit combinations effectively result in functional glutamate receptors? To answer this question glutamate receptor subunits were expressed in *Xenopus laevis* oocytes which were applied to two electrode voltage clamp (TEVC) measurements.

A simultaneous expression of multiple constructs is difficult in cell culture. Although western blot analysis may identify all transfected constructs in the whole cell batch, just a subset of cells express all constructs simultaneously. In contrast *Xenopus* oocytes are known as a heterologous expression system, displaying both coexpression of multiple proteins within one cell and high expression levels. cRNA of the constructs of interest can be directly injected into oocytes ensuring that all constructs are within one cell simultaneously.

In first TEVC experiments, combinations of GluRIIA,C,D,E and GluRIIB,C,D,E, the E subunit tagged with 3xHA respectively, were tested. No current response could be detected after application of glutamate in different concentrations ranging from 300µM to 6mM. Moreover, single oocyte western blot experiments displayed no detectable expression of the tagged receptor subunit.

In addition oocytes injected with GluRIIA,C,D,E and GluRIIB,C,D,E cRNA combinations, which contained the non tagged GluRIIE subunit, did not show glutamate evoked currents on the application of 6mM glutamate as well. Although the chemical tag is not likely to be responsible for the subunits not to form a functional receptor complex, the following experiments were performed with non tagged subunits.

3.7.2 CG17793, CG31218 and CG4940 together encode for a SOL-1 homologue in *Drosophila*

In the last years the importance of several non-receptor subunit proteins for glutamate receptor function was demonstrated. Among those proteins stargazin plays a key role in mammals and is referred to as an accessory subunit for glutamate receptors. Recently Walker et al. (2006b) identified stargazin homologues in *Caenorhabditis elegans*, *Drosophila melanogaster* and *Apis mellifera* (compare chapter 3.8).

Another important protein for glutamate receptor function, called SOL-1, was identified in *C. elegans* recently (Zheng et al., 2004; Walker et al., 2006a; Zheng et al., 2006). A homologous protein of SOL-1 exists in *Drosophila*, in the following refered to as *Drosophila* SOL-1. A subset of three adjanced genes, namely CG 17793, CG31218 and CG4940, encodes for *Drosophila* SOL-1. The *Drosophila* SOL-1 protein shares a sequence homology of about 25% with *C. elgans* SOL-1 (Walker et al., 2006a) (compare sequence alignment in Figure 17). In order to determine, if *Drosophila* SOL-1 transcripts are abundant in somatic muscles and the CNS of adult flies real-time PCR experiments were performed. Two different primer pairs were used, one binding within the 3rd exon of CG31218, in a region encoding for CUB domain 2, the other binding the 2nd exon of CG4940, which encodes for CUB domain 4 (compare Figure 17 B). Real-time PCR experiments showed, that *Drosophila* SOL-1 RNA is present both in adult heads, mainly consisting of the CNS, and in adult torsi, mainly representing somatic muscles.

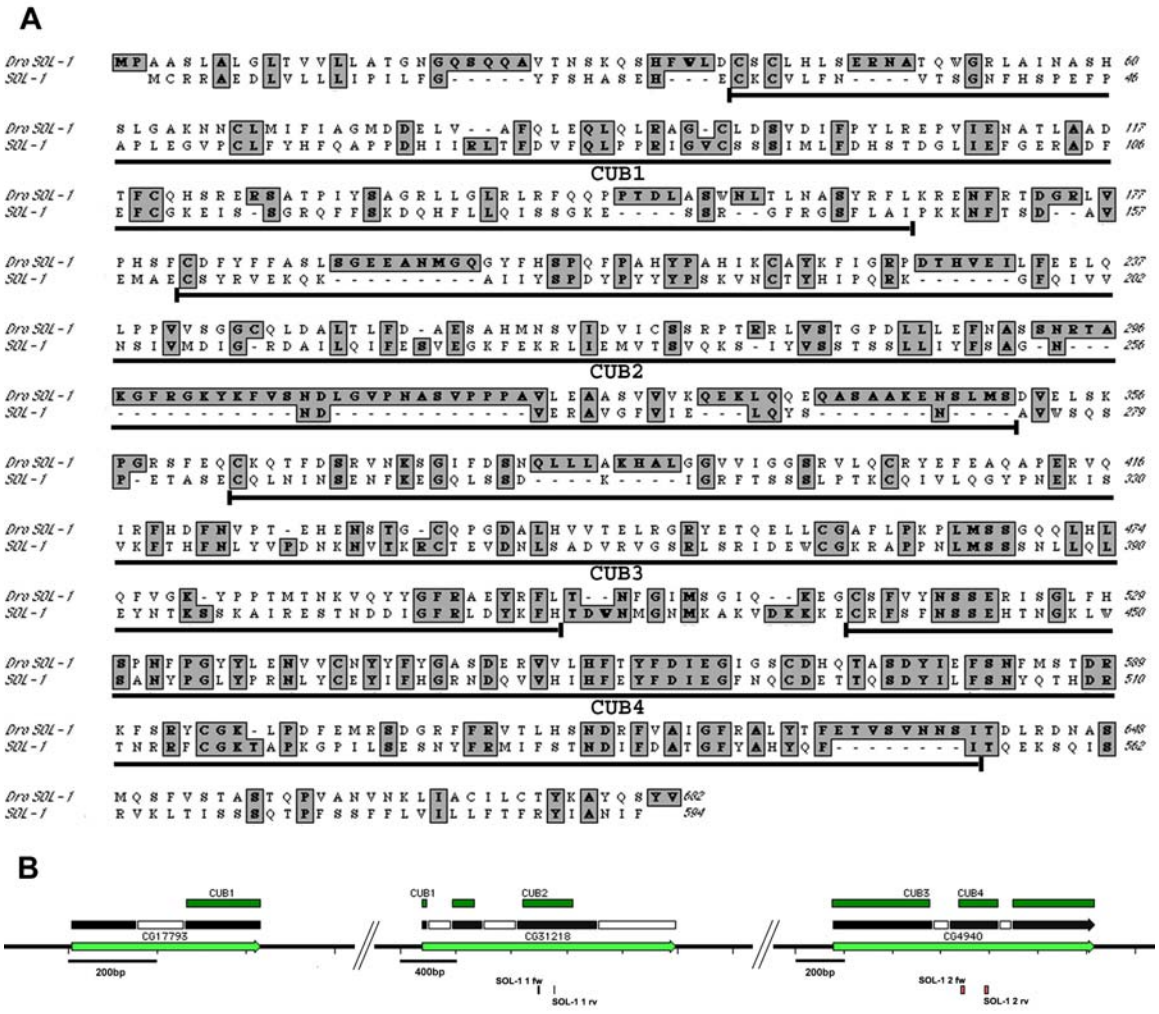

Figure 17 Sequence analysis of SOL-1
A) Shown are the amino acid sequences of *C. elegans* SOL-1 (SOL-1) and the SOL-1 homologous protein identified in *Drosophila* (Dro SOL-1). Amino acid similarities are shown in grey shaded boxes; the four CUB domains (CUB1 – CUB4) are shown beneath the alignment. **B)** Shown in light green are the three gene loci (CG17793, CG31218 and CG4940) encoding for the SOL-1 homologous protein in *Drosophila* on the 3rd chromosome. Exons are depicted in black, introns in white. Above the intron exon mapping the location of regions encoding for CUB domains are shown in dark green. The 2nd exon of CG17793 as well as the first two exons of CG31218 encode for CUB domain 1, the 3rd exon of CG31218 encodes for CUB domain 2, the 1st exon of CG4940 encodes for CUB domain 3 and the last two exons of CG4940 encode for CUB domain 4.The pairs of lines beneath the gene region represent primer pairs used for real-time PCR.

However, SOL-1 RNA displays a stronger enrichment in muscles than in the adult CNS, since the RNA levels in the torso are, depending on the accounted amplicon, more than four times the RNA levels detected in adult heads (Figure 18).

	tbp-1	SOL-1 1	SOL-1 2
C_t adult head	20,78	22,61	22,36
C_t adult torso	21,77	21,54	20,26
NTC	40	39,01	37,46
Normalised ratio torso/head		4,17	8,55

Figure 18 Real-time PCR data for *Drosophila* SOL-1
Real-time PCR was performed with mRNA from adult heads and adult torsi. Two different amplicons (SOL-1 1 and SOL-1 2) were tested. The binding sites of the primer pair for SOL-1 1 are situated in the exon encoding for CUB domain 2; the binding sites of the primer pair for SOL-1 2 are situated in the exon encoding for CUB domain 4 (compare Figure 17 B). The internal control tbp-1 was used for C_t value normalisation. The normalised ratio torso/head reflects the distribution of SOL-1 RNA levels in adult torsi compared to adult heads. fw: forward; rv: reversed

3.7.3 Examining the influence of a SOL-1 homologous protein on glutamate receptor functionality

C. elegans SOL-1 was found to be essential for the measurement of glutamate evoked currents for homomeric glutamate receptors consisting of the GLR-1 subunit in *Xenopus* oocytes. A Con-A mediated slowdown of GLR-1 desensitisation kinetics depends on the presence of *C. elegans* SOL-1 (Walker et al., 2006a). In the absence of SOL-1 GLR-1 desensitisation is too fast to be resolved via TEVC in *Xenopus* oocytes. Besides SOL-1 the presence of *C. elegans* stargazin was essential to obtain current responses from GLR-1 receptors on the application of glutamate (Walker et al., 2006a). However, GLR-1 functionality could be maintained by replacing *C. elegans* stargazin with one of its homologues from vertebrates, *Apis* or *Drosophila* (Walker et al., 2006b). In order to examine, if the presence of *Drosophila* SOL-1 is necessary for the functionality of *Drosophila* NMJ glutamate receptors, *Drosophila* SOL-1 cRNA, alone or in combination with cRNA of the stargazin homologue from *Apis*, was added to the previously tested cRNA mix consisting of the combinations GluRIIA,C,D,E and GluRIIB,C,D;E.

Coinjection of subunit combinations GluRIIA,C,D,E or GluRIIB,C,D,E with *Drosophila* SOL-1 and *Apis* stargazin did not result in current responses. However, additional oocyte preincubation in a solution including 100µM Con-A,

which is known to slow AMPA receptor desensitisation, led to a current response to the application of 6mM glutamate for the combination of GluRIIB,C,D,E + *Drosophila* SOL-1 + *Apis* stargazin. Currents 50±15nA in size (n=6) were obtained after application of 6mM glutamate solution (Figure 19 A). Further experiments suggested that the presence of *Apis* stargazin is non-obligate for a glutamate evoked current response. Oocytes expressing GluRIIB,C,D,E + *Drosophila* SOL-1 after preincubation with 100µM Con-A responded to 6mM glutamate with currents of 44±12nA in size (n=5) (Figure 19 B). Non injected oocytes pretreated with 100µM Con-A displayed current responses the size of 5,1±1,7nA (n=10). Oocytes injected with the cRNA combination GluRIIA,C,D,E + *Drosophila* SOL-1 did not show any significant current response under the same conditions, no matter if *Apis* stargazin was present or not (6,5±0,9nA, n=5).

Noteworthy just about 25% of the measured oocytes displayed a significant current response in all cases when a current signal was detectable. Within an oocyte batch the expression levels for the injected cRNAs seem to fluctuate explicitly. The observed current response to 6mM glutamate observed for oocytes injected with GluRIIB,C,D,E + *Drosophila* SOL-1 is significant but small in size (Figure 19 C). Hence it is most likely that currents could only be obtained from those oocytes having the highest expression levels within the batch.

In addition to a 6mM glutamate solution a 300µM glutamate solution was applied. The reduced glutamate concentration resulted in smaller current responses (see Figure 19 A). Oocytes injected with GluRIIB,C,D,E + *Drosophila* SOL-1 + *Apis* stargazin and preincubated with 100µM Con-A responded with currents 14±4nA in size (n=4), those injected with GluRIIB,C,D,E + *Drosophila* SOL-1 and preincubated with 100µM Con-A with currents 5±1nA in size (n=4). However those current values are not significantly larger in size than current values obtained from non injected oocytes (5,1±1,7nA).

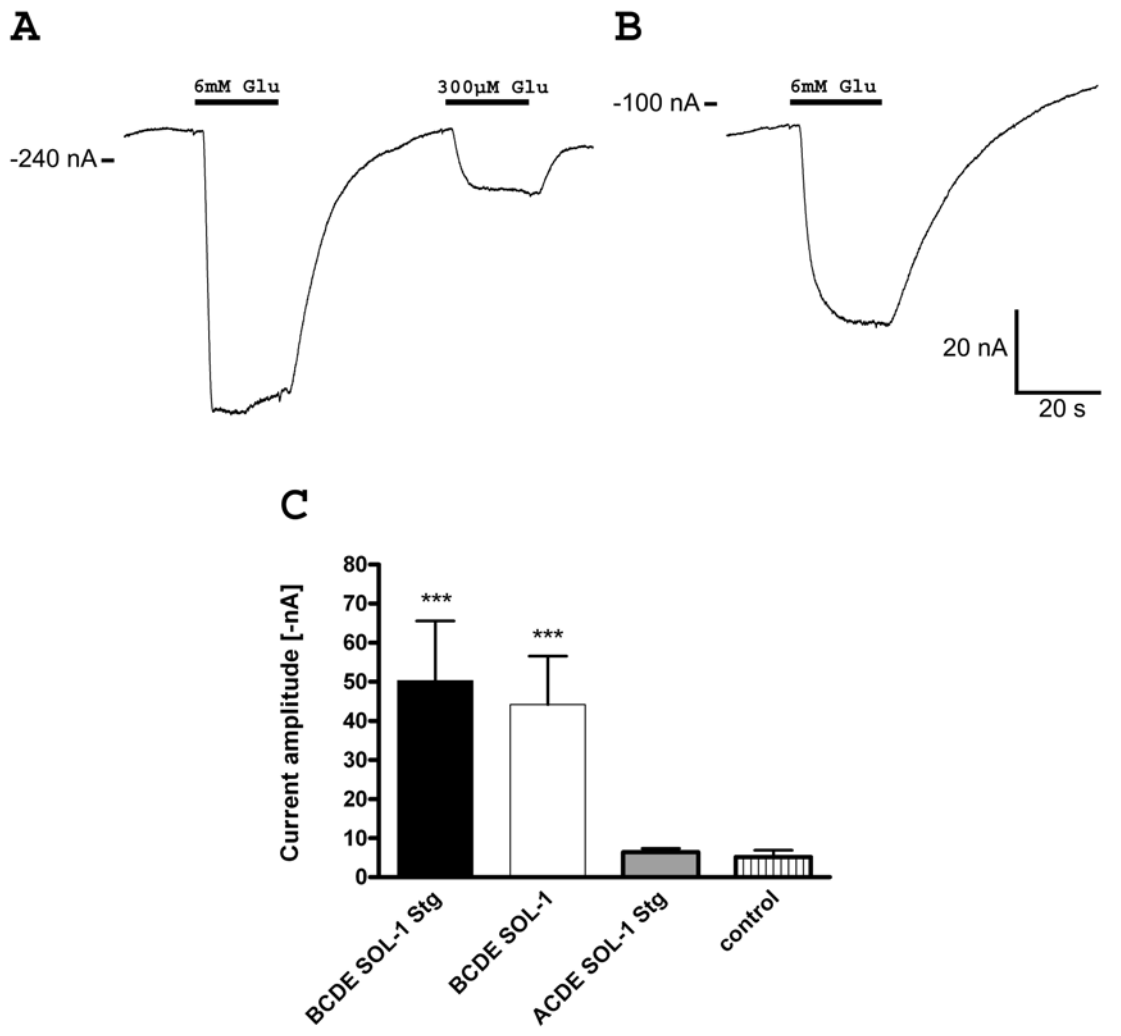

Figure 19 TEVC measurements from *Xenopus* oocytes
A) Currents recorded from *Xenopus* oocytes injected with the cRNA combination of GluRIIB, GluRIIC, GluRIID, GluRIIE, *Drosophila* SOL-1 and *Apis* stargazin and preincubated with 100µM concanavalin-A in response to the application of 6mM (6mM Glu) and 300µM (300µM Glu) glutamate. **B)** Currents recorded from *Xenopus* oocytes injected with the cRNA combination GluRIIB, GluRC, GluRD, GluRE and *Drosophila* Sol-1 and preincubated with 100µM concanavalin A in response to the application of 6mM glutamate. The duration of the application corresponds to the length of the lines above the current trace. Oocytes were voltage clamped at a holding potential of -70mV. **C)** Shown are the mean current amplitudes in response to the application of 6mM Glu. Oocytes were preincubated with 100µM concanavalin-A. The mean current amplitude for oocytes injected with the cRNA combination GluRIIB, GluRIIC, GluRIID, GluRIIE, *Drosophila* SOL-1 and *Apis* stargazin (BCDE SOL-1 Stg) and for oocytes injected with the cRNA combination GluRIIB, GluRIIC, GluRIID, GluRIIE and *Drosophila* SOL-1 (BCDE SOL-1) are five times (BCDE SOL-1 Stg: 50,3±15,3nA [mean value±SEM] n=6 ***p=0,0005) and four times respectively (BCDE SOL-1: 44,1±12,5nA n=5 ***p=0,0005) larger in size compared to non injected oocytes [(control): 5,2±1,7nA n=10]. The size of the mean current amplitude for oocytes injected with the cRNA combination GluRIIA, GluRIIC, GluRIID, GluRIIE, *Drosophila* SOL-1 and *Apis* stargazin [(ACDE SOL-1 Stg): 6,5±0,9nA n=5 p=0,165] does not differ from non injected oocytes. n: number of measured oocytes; p: P value of a nonparametric Mann-Whitney rank sum test.

Summarising, a functional glutamate receptor complex was identified through TEVC measurements in *Xenopus* oocytes. Glutamate-induced currents were measured for the subunit combination GluRIIB,C,D,E coexpressed with *Drosophila* SOL-1 and preincubated with 100µM Con-A. The applied glutamate concentration was 6mM.

3.8 Examination of a potential Drosophila stargazin homologue with immunohistochemical and biochemical methods

3.8.1 The predicted *Drosophila* stargazin homologue shows structural homology to vertebrate stargazin

The sequence of a stargazin homologue in *Drosophila*, as recently published in Walker et al. (2006b), describes a protein sharing 25% amino acid sequence identity with vertebrate stargazin (compare sequence analysis in Figure 20). CG33670, the gene encoding for the homologous stargazin protein in *Drosophila*, includes seven exons and six introns (compare Figure 12) and is located on the X-chromosome. The first five exons encode for the sequence published in Walker et al. (2006b). According to Walker et al. (2006b) this vertebrate stargazin homologue in *Drosophila* is refered to as *Drosophila* stargazin in the following.

In real-time experiments the presence of *Drosophila* stargazin RNA in adult heads as well as in adult torsi was displayed. In contrast to *Drosophila* SOL-1, RNA of *Drosophila* stargazin displays a stronger enrichment in the adult CNS than in the somatic muscles, since the RNA levels in the torso were at least just 13% of the RNA levels detected in adult CNS (Figure 21).

A comparison of SOL-1 RNA levels with stargazin RNA levels indicates that in the brain both proteins are present in comparable amounts while in muscles SOL-1 numbers dominate over stargazin numbers.

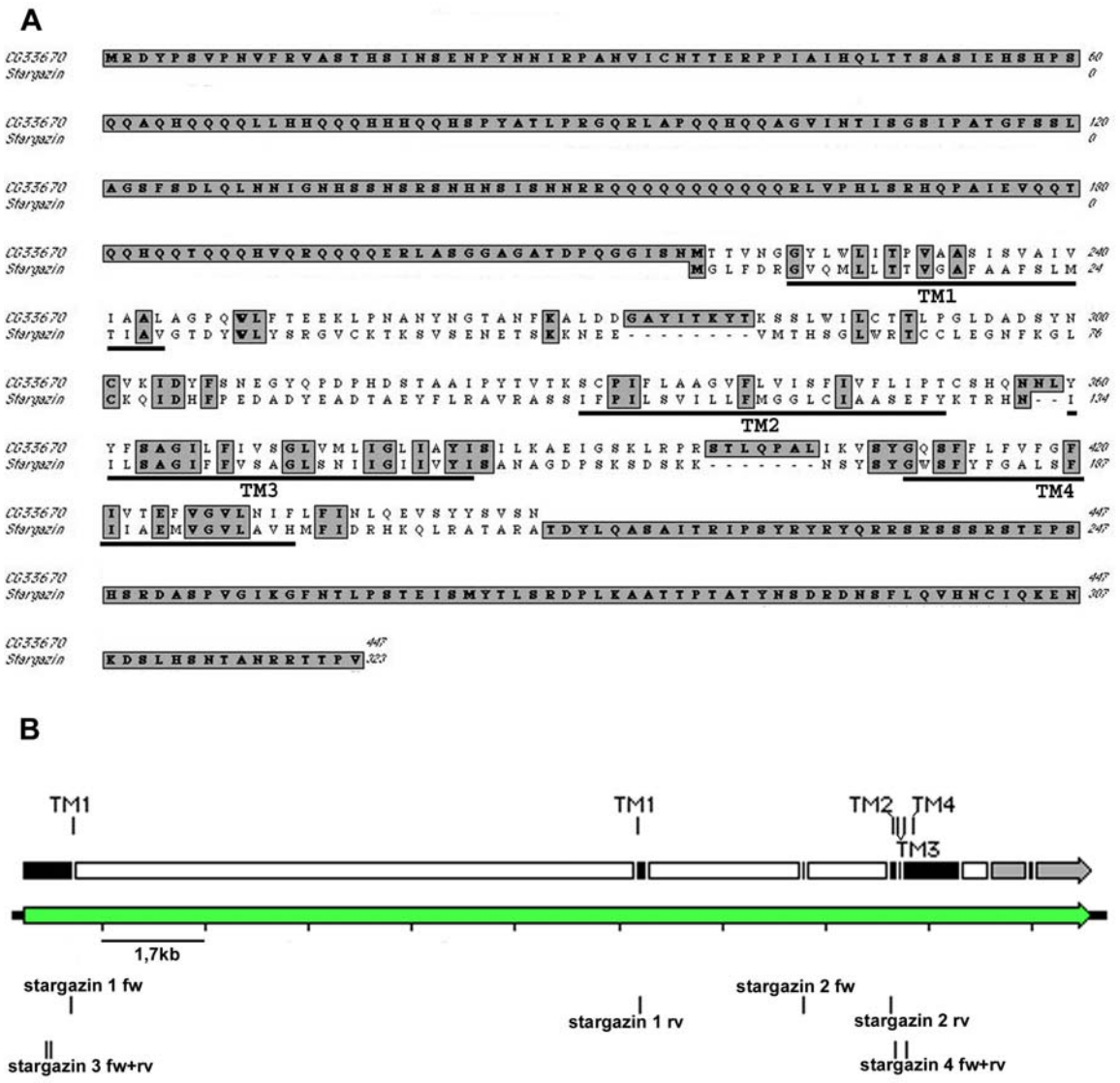

Figure 20 Sequence analysis of stargazin
A) Shown are the amino acid sequences of vertebrate stargazin (Stargazin) and the stargazin homologous protein identified in *Drosophila* (CG33670). Amino acid similarities are shown in grey shaded boxes; the four transmembrane domains (TM1 – TM4) are shown beneath the alignment. **B)** Shown in light green is the gene locus of CG33670, which encodes for the stargazin homologous protein in *Drosophila* on the X-chromosome. Exons coding for the predicted *Drosophila* stargazin protein from Walker et al. (2006b) are depicted in black, non-coding exons in grey and introns in white. Above the intron-exon mapping the location of regions encoding for TM1 – TM4 are shown. Exons 1 and 2 encode for TM1, exon 4 encodes for TM2, exons 4 and 5 encode for TM3. Finally the message for TM4 is also encoded on exon 5. The pairs of lines beneath the gene region represent primer pairs used for real-time PCR. fw: forward; rv: reversed

Stargazin has been shown both in vertebrates and in *C. elegans* to be a crucial factor for the functionality of glutamate receptors at the postsynapse. In order to examine a potential role for *Drosophila* stargazin in glutamate receptors trafficking and function at the *Drosophila* NMJ, it was attempted to generate a

specific mutant in CG33670.

	tbp-1	stargazin 1	stargazin 2
C_t adult head	20,78	22,26	23,08
C_t adult torso	21,77	26,20	28,05
NTC	40	35,03	34,44
Normalised ratio torso/head		0,13	0,06

Figure 21 Real-time PCR data for *Drosophila* stargazin
Real-time PCR was performed with mRNA from adult heads and adult torsi. Two different amplicons (stargazin 1 and stargazin 2) were tested. The binding sites of the primer pair for stargazin 1 are situated at the ending of t exon 1 and the beginning of exon 2. This region encodes for TM1. The binding sites of the primer pair for stargazin 2 are situated at the ending of exon 3 and at the beginning of exon 4 (compare Figure 20 B). The internal control tbp-1 was used for C_t value calibration. The normalised ratio torso/head reflects the distribution of stargazin RNA levels in adult torsi compared to adult heads.

3.8.2 An N-terminal deletion mutant of *Drosophila* stargazin obtained by P-element imprecise excision

The P-element P{SUPor-P}CG11566^{KG10455} located at the beginning of intron 1 of CG33670, 1,2kb downstream of the first exon, was mobilised by transposase in an imprecise excision screen (for more details compare chapter 2.7.4). Single candidate flies were checked for a deletion around the P-element insertion site via genomic PCR. From a total number of 464 candidate fly lines 131 (28%) showed imprecise excision after P-element mobilisation and 3 lines (0,9%) (line #148, #174, #181) showed large deletion regions including the complete first exon, parts of the 5'UTR and the N-terminal part of the first intron (compare Figure 22 A, B). The deletions contained the parts of the stargazin gene encoding for the protein's whole N-terminal region as well as a small part of the first transmembrane domain (compare Figure 22 C). Those three lines are referred to as 1st exon deletion mutant lines in this thesis. One line (0,2%) (line #131) contained a deletion removing the N-terminal part of the first stargazin intron but leaving the first exon untouched (compare Figure 22 A, B). This line is referred to as 1st intron deletion mutant line further on. Lines #148, #174 and #181 are homozygous viable.

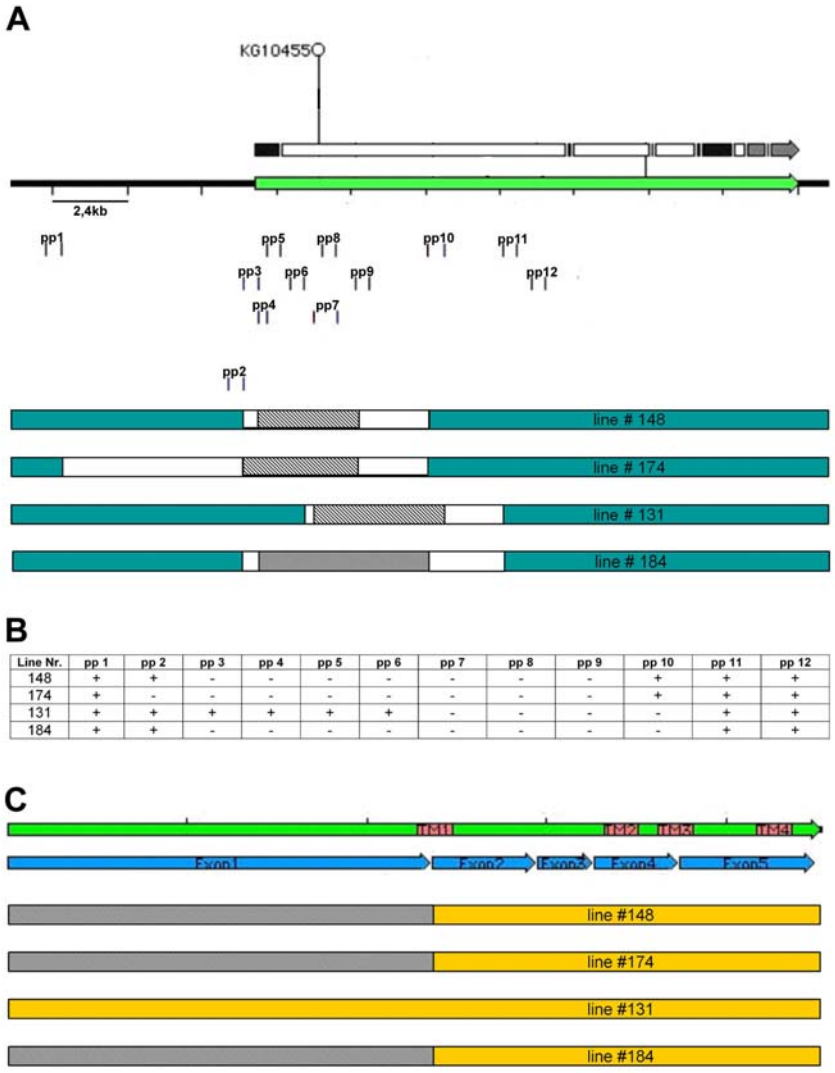

Line Nr.	pp 1	pp 2	pp 3	pp 4	pp 5	pp 6	pp 7	pp 8	pp 9	pp 10	pp 11	pp 12
148	+	+	-	-	-	-	-	-	-	+	+	+
174	+	-	-	-	-	-	-	-	-	+	+	+
131	+	+	+	+	+	+	-	-	-	-	+	+
184	+	+	-	-	-	-	-	-	-	-	+	+

Figure 22 Stargazin deletion mutants

A) Shown in green is the genetic region of the predicted *Drosophila* stargazin protein published by Walker et al. (2006b) on the X-chromosome. Exons encoding for this predicted protein are depicted in black, non coding exons in grey and introns in white. The P-element P{SUP or -P}CG11566^{KG10455} is shown as hollow circle (KG10455). The pairs of lines beneath the gene region represent the 12 primer pairs (pp1-pp12) used in genomic PCR to determine the deletion size in lines #148, #174, #131 and #184. Underneath the four deletion mutant lines obtained from the imprecise excision screen are listed. The black and white shaded box represents the confirmed deletion region. Since the absence of a PCR product can be due to the loss of one of the two primer binding sites or both of them, the endings of a deleted gene region cannot be precisely defined. Thus regions which could not be excluded from belonging to the deletion region are shown in white and gene regions unaffected by the deletion are shown in blue. **B)** Table of the results of the 12 genomic PCRs performed for each of the four mutant lines. PCR reactions resulting in an amplicon are marked with "+", those PCR reactions generating no amplicon are marked with "-". **C)** Shown in green is the stargazin amino acid sequence published by Walker et al. (2006b). Transmembrane domain positions (TM1-4) are shown in red. Below the corresponding exon regions are marked in blue. Underneath the four deletion mutant lines obtained from the imprecise excision screen are listed. For a better clarification deletion positions were transferred from transcriptional to translational level under the assumption that all but the deleted exon regions of the stargazin locus are still translated. Deleted protein regions are depicted in black and white shaded boxes. The deletion of line #131 does not touch an exon region; hence, no deletion is shown.

Line #131 is heterozygous viable solely. Homozygous 3rd instar larvae can be selecetd but just those female adult flies carrying the 1st intron deletion hatch heterozygously.

It shall be mentioned that the deletion mutant schemes in Figure 22 C are not meant to represent the real mutant proteins which are most likely absent due to the fact that the start codon is missing in the 1st exon mutants.

3.8.3 Mutants deleting the expression of a complete first transmembrane domain of *Drosophila* stargazin

To test whether mRNA transcripts display the deletions shown on genomic level and whether mRNA transcript levels of non deleted regions of the stargazin transcript are altered compared to wild type conditions, real-time PCR was performed with mRNA isolated from 3rd instar larvae from the four mutant lines. Two different primer pairs were used for real-time PCR experiments. The first primer pair has its binding site located at the 1st exon of *Drosophila* stargazin, which is missing in the 1st exon mutants. The second primer pair binds at the intersection of exons 4 and 5 (compare Figure 20 B). Real-time PCR performed with the 1st exon primer pair showed no RNA message for the 1st exon mutants, whereas the 1st intron mutant #131 displayed RNA levels almost the size of wild type RNA levels (Figure 23 A). The levels for the amplicon at the intersection of exon 4 and 5 were not comparably reduced for the 1st exon mutants. RNA levels at this position were either slightly reduced in comparison to wild type RNA levels (compare “% of normalised wt levels” for mutants #148, #174 and #131 in Figure 23 B) or appeared unchanged (compare “% of normalised wt levels” for mutant #184 in Figure 23 B).

Although parts of the 5’UTR are missing in the 1st exon deletion mutants it seems like the endogenous stargazin promoter has not been damaged severly, providing the mutant flies with a truncated stargazin mRNA. Probably, in the 1st exon mutans the stargazin protein is not translated because the original start codon is missing or it might be translated as a truncated protein due to an alternative start codon. In the case of the 1st intron deletion mutant the shortened

intron could result in a wrongly spliced mRNA. However, primer pairs flanking the 1st intron still gave the same amplicon size for isolated 1st intron mutant RNA as they do for RNA isolated from wild type flies (data not shown), suggesting that the first intron is spliced correctly. The first intron is 9kb in size. It cannot be excluded that so far uncharacterised alternative exons are included into this region, which might be disrupted by mutant #131. In any case, the 1st intron mutant and the 1st exon mutants cause the same glutamate receptor phenotype.

A)	**C_t tbp-1 (internal control)**	**C_t stargazin 3 (1st exon primer pair)**	**% of normalised wt levels for stargazin 3**
wt	**20,70**	**27,63**	**100,00 %**
#148	**20,32**	**35,41**	**0 %**
#174	**20,87**	**36,49**	**0 %**
#184	**20,42**	**34,53**	**0 %**
#131	**20,37**	**26,68**	**90,33 %**
NTC	**35,70**	**34,25**	

B)	**C_t tbp-1 (internal control)**	**C_t stargazin 4 (4th to 5th exon primer pair)**	**% of normalised wt levels for stargazin 4**
wt	**26,87**	**25,00**	**100%**
#148	**27,98**	**25,78**	**44,75%**
#174	**27,53**	**25,98**	**56,64%**
#184	**25,70**	**24,62**	**106,44%**
#131	**25,77**	**24,89**	**85,66%**
NTC	**40,00**	**30,24**	

Figure 23 Real-time PCR data for *Drosophila* stargazin deletion mutants
Real-time PCR was performed with mRNA from 3rd instar larvae. Shown are the C_t values for two independent real-time PCR experiments with two different primer pairs. The binding site of the primer pair is located in the 1st exon (stargazin 3); the binding site of the second primer pair is located at the intersection from the 4th to the 5th exon (stargazin 4) (compare Figure 20 B). **A)** For the 1st exon deletion mutants #148, #174 and #184 the RNA message in the first exon is abolished, whereas for intron mutant #131 the message is almost unchanged compared to wild type (wt) control animals. In the right column C_t values for stargazin 3 were normalised to the tbp-1 internal control and compared to wt RNA levels. **B)** At the exon 4/5 intersection the amplicon levels are still detectable for all four stargazin deletion mutants. In the right column C_t values for stargazin 4 were calibrated to the tbp-1 internal control and normalised to wt RNA levels. NTC: non template control.

3.8.4 Drosophila stargazin deletion mutants show an increased amount of glutamate receptors at the NMJ

Mammalian stargazin as well as the *C. elegans* stargazin homologue were shown to be essential for glutamate receptor functionality (Tomita et al., 2005b; Turetsky et al., 2005; Walker et al., 2006b). While a lack of stargazin results in a massive reduction of AMPA receptor levels both at synaptic and extrasynaptic sites (Chen et al., 1999; Hashimoto et al., 1999; Chen et al., 2000b) GLR-1 containing glutamate receptors are well expressed on the surface of *C. elegans* transgenic body wall cells even in the absence of *C. elegans* stargazin (Walker et al., 2006a).

How do the deletion mutants generated for *Drosophila* stargazin effect receptor levels at the neuromuscular junction? Are the total receptor subunit protein levels altered? In order to answer those questions the stargazin mutant flies were applied to immunohistochemistry as well as to western blot analysis.

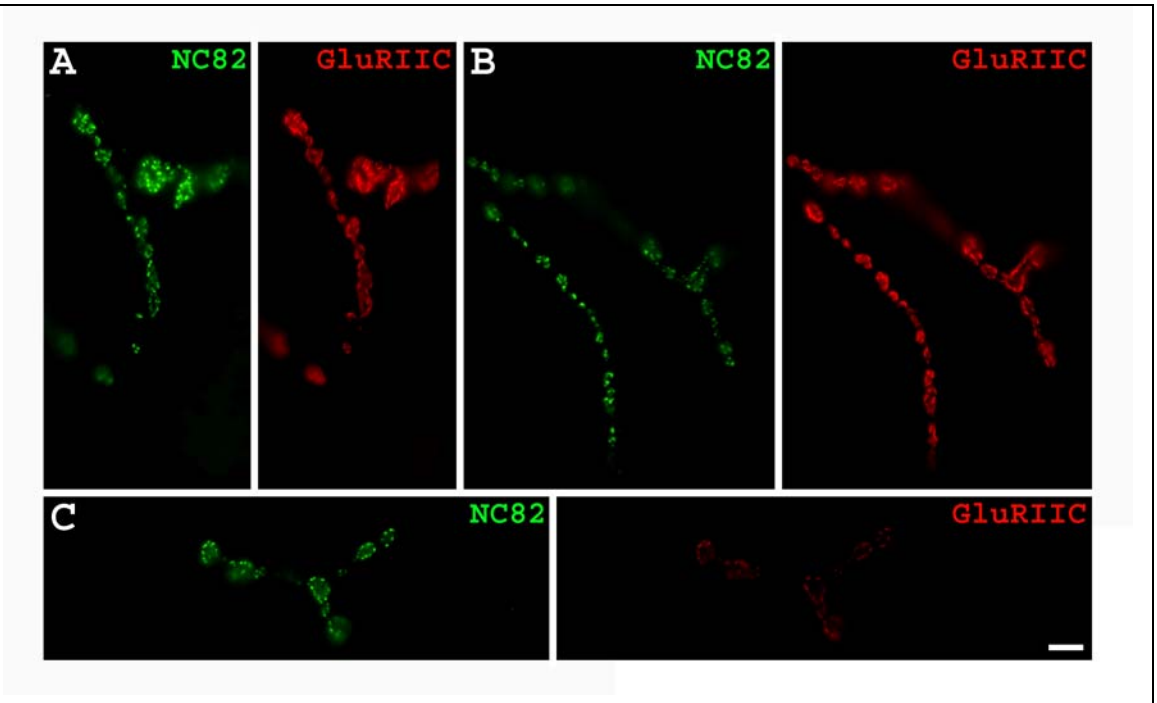

Figure 24 Glutamate receptor levels are enhanced in *Drosophila* stargazin mutant flies
Shown are epifluorescence pictures of *Drosophila* larval NMJs from **A)** 1st intron deletion mutant #131 flies, **B)** 1st exon deletion mutant flies and **C)** wild type flies, stained with antibodies against NC82 (green channel) and GluRIIC (red channel). All images were taken at a constant illumination time for both green and red channels. The illumination time for the GluRIIC staining was adjusted the way that just faint fluorescence signals were visible for the wild type background. Scale bar represents 5µm.

3rd instar larvae from the three stargazin 1st exon deletion mutant lines #148, #174 and #184 as well as from the 1st intron deletion mutant line #131 were stained with antibodies against the GluRIIC subunit or against the GluRIID subunit and in both cases in combination with the NC82 antibody, which was shown to label the presynaptic active zones (Heimbeck et al., 1999; Wucherpfennig et al., 2003). For all lines the postsynaptic receptor fluorescence intensity signal of the stained receptor subunits was increased significantly at all body wall muscles in the stargazin deletion mutant in comparison with wild type animals, while the presynaptic NC82 fluorescence signal was not significantly changed (compare representative pictures for lines #131 and #184 in Figure 24). Quantification of the fluorescence intensities after anti-GluRIIC immunostaining was performed at muscles 6/7 for wild type larvae, the mutant line #184, the intron mutant line #131, the source P-element line P{SUPor-P}CG11566^{KG10455} used for imprecise excision screen and a line obtained from the imprecise excision screen featuring a very small deletion around the P-element insertion site in the 1st stargazin intron. Whereas no significant difference in GluRIIC dependent fluorescence intensity was found comparing the wild type line to the P-element line and to the small imprecise excision deletion line (Figure 25 A) fluorescence intensity of mutant #184 was increased to 124±5% and in case of mutant #131 to 129±4% when compared to wild type animals (Figure 25 B).

In addition to the GluRIIC receptor levels the GluRIID receptor levels were significantly increased, too, as was shown by quantification of 3rd instar larvae stained with antibodies against the GluRIID subunit (Figure 25 C). Fluorescence intensity was 115±4% for mutant #184 larvae and 113±4% for mutant #131 larvae compared to wild type animals.

In another experiment 3rd instar larval body wall preparations from homozygous stargazin deletion mutants were applied to western blot analysis. The blot was probed with the GluRIIC antibody and with the anti-tubulin antibody for normalisation. Western blot band quantification showed an increase in GluRIIC protein levels to 141% for mutant #131 and 164% for mutant #184 when compared to wild type animals (Figure 25 D).

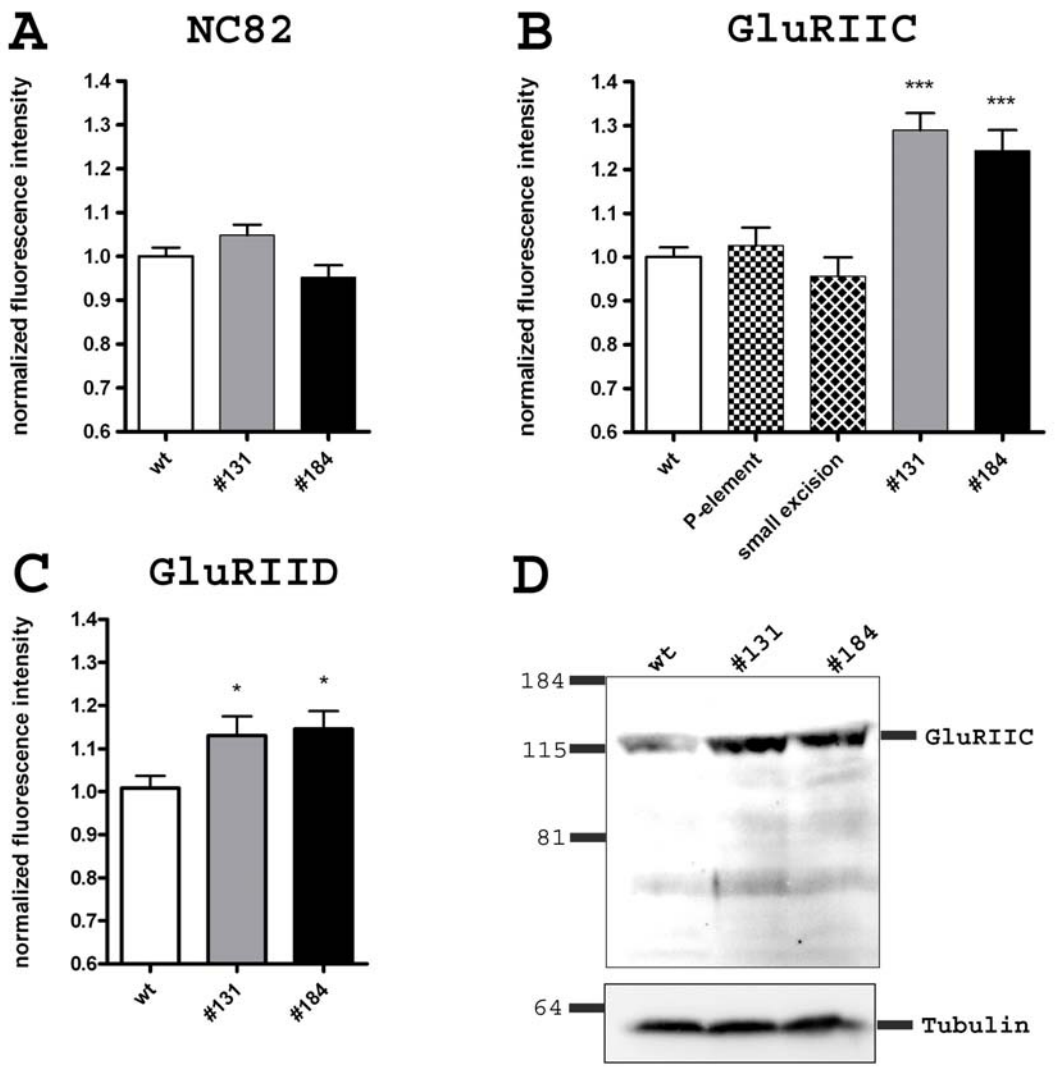

Figure 25 Stargazin mutants increase the glutamate receptor levels at the *Drosophila* NMJ
A, **B** and **C** Shown is the fluorescence intensity signal at muscles 6/7 at the NMJ of 3rd instar larvae normalised to the fluorescence intensity values of wild type larvae. While for the presynaptic active zone marker NC82 no significant fluorescence intensity difference is observed (mean values + SEM: wt: 1,00±0,02 n=52; #131: 1,05±0,02 n=49, #184: 0,95±0,03, n=48) (**A**), the intensity is significantly increased for the GluRIIC fluorescence signal (mean values + SEM: wt: 1,00±0,02 n=43, #131: 1,29±0,04 n=39, *** p<0,0001, #184: 1,24±0,05 n=39, *** p<0,0001) (**B**) as well as for the GluRIID fluorescence signal (mean values + SEM: wt:1,00± 0,03 n=12, #131: 1,13±0,04 n=10, * p=0,019, #184: 1,14±0,04 n=11, * p=0,012) (**C**). The location of the P-element P{SUPor-P}CG11566^{KG10455} in the first intron (P-element: 1,03±0,04 n=28,) as well as a small imprecise excision at the P-element insertion site (small excision: 0,96±0,04 n=11) do not alter receptor fluorescence intensity significantly (**C**). **D** Western blot analysis of 3rd instar larval body wall preparations probed with the GluRIIC antibody shows an increase in GluRIIC protein levels in stargazin mutants #131 (normalised band intensity: 141%) and #184 (normalised band intensity: 164%) compared to wild type animals. The input level was 10 3rd instar larval body wall preparations per lane. Band intensities were normalised to tubulin levels. The numbers on the left part of the blot show the molecular weight in kDa. wt: wild type, #131: 1st intron deletion mutant, #184: 1st exon deletion mutant line #184, P-element: line P{SUPor-P}CG11566^{KG10455}, small excision: intron mutant carrying a small deletion around the P-element insertion site of P{SUPor-P}CG11566^{KG10455}. n: number of analyzed NMJs; p: P value of a nonparametric Mann-Whitney rank sum test.

To sum it up, the loss of the 1st *Drosophila* stargazin exon as well as the loss of a large part of the 1st *Drosophila* stargazin intron results in an increase of GluRIIC and GluRIID protein levels at NMJs as was shown by immunohistochemistry. The increase of GluRIIC levels was additionally confirmed by western blot analysis.

These results suggest a role for *Drosophila* stargazin on glutamate receptor functionality similar to the one described for the stargazin proteins in mouse and *C. elegans*. Loss of *Drosophila* stargazin, which is the effect most likely caused by the mutants obtained from the imprecise excision screen, or at least the expression of a non functional truncation of the stargazin protein, which is the alternative effect caused by the deletion mutants, results in a compensatory increase in glutamate receptor levels in order to maintain a functional glutamatergic neurotransmission at the *Drosophila* NMJ.

3.9 GluRIIF: a novel glutamate receptor subunit found at the Drosophila NMJ

3.9.1 GluRIIF shares similarities with kainate receptors

CG11155 in the following referred to as GluRIIF was first mentioned by its Celera transcript number CT30863 in Littleton and Ganetzky (2000) as a glutamate receptor structurally related to the kainate family. Recently, it was shown that the transcriptional expression levels of GluRIIF among a variety of other transcripts of the *Drosophila* nervous system are modulated depending on the synaptic activity pattern (Guan et al., 2005).

Sequence analysis of GluRIIF cDNA clones, discovered in 2005, resulted in two different transcripts, which are probably generated due to alternative splicing. The CG11155 gene region consists of 16 coding exons. Both transcripts share the first 11 exons. The first transcript misses exons 12 and 14; the second

transcript misses exons 15 and 16 (compare Figure 26 A). Strikingly the first transcript encodes an intact glutamate receptor (compare Figure 27 A), whereas the second transcript results in a truncated glutamate receptor possessing an additional stretch of 165 amino acids in between transmembrane domains 2 and 3 but lacking a fourth transmembrane domain (see supplementary Figure 35).

A

B

	C_t (body wall preparation)	C_t (larval head preparation)	NTC
GluRIIF	20,68	20,17	32,46
1st transript	23,48	22,10	35,77
2nd transcript	25,09	23,54	39,10
tbp-1 (internal control)	21,65	20,75	34,85

Figure 26 GluRIIF transcript exon – intron structure
A) Exons are shown as green, blue or red boxes, introns are shown as thick black lines. Two different transcripts have been found for the GluRIIF gene CG11155. The first transcript consists of the green and red exons with a total number of 14 exons. The second transcript consists of the green and the blue exons exhibiting a sum of 14 exons. **B)** Real-time PCR results show the expression of both transcripts. For RNA isolation 3rd instar larvae body wall preparations without the CNS and larval heads containing the CNS were used. Primer pairs against regions both transcripts have in common (GluRIIF) as well as transcript specific primer pairs (1st transcript, 2nd transcript) were used for real-time PCR analysis. tbp-1 mRNA levels were utilised as internal control. NTC: non template control.

The intact GluRIIF receptor isoform encodes a glutamate receptor subunit sharing a higher similarity with mammalian kainate receptor subunits (36-43% amino acid sequence identity) than with the other glutamate receptor subunits GluRIIA – GluRIIE found at the *Drosophila* NMJ (26-34% sequence identity,

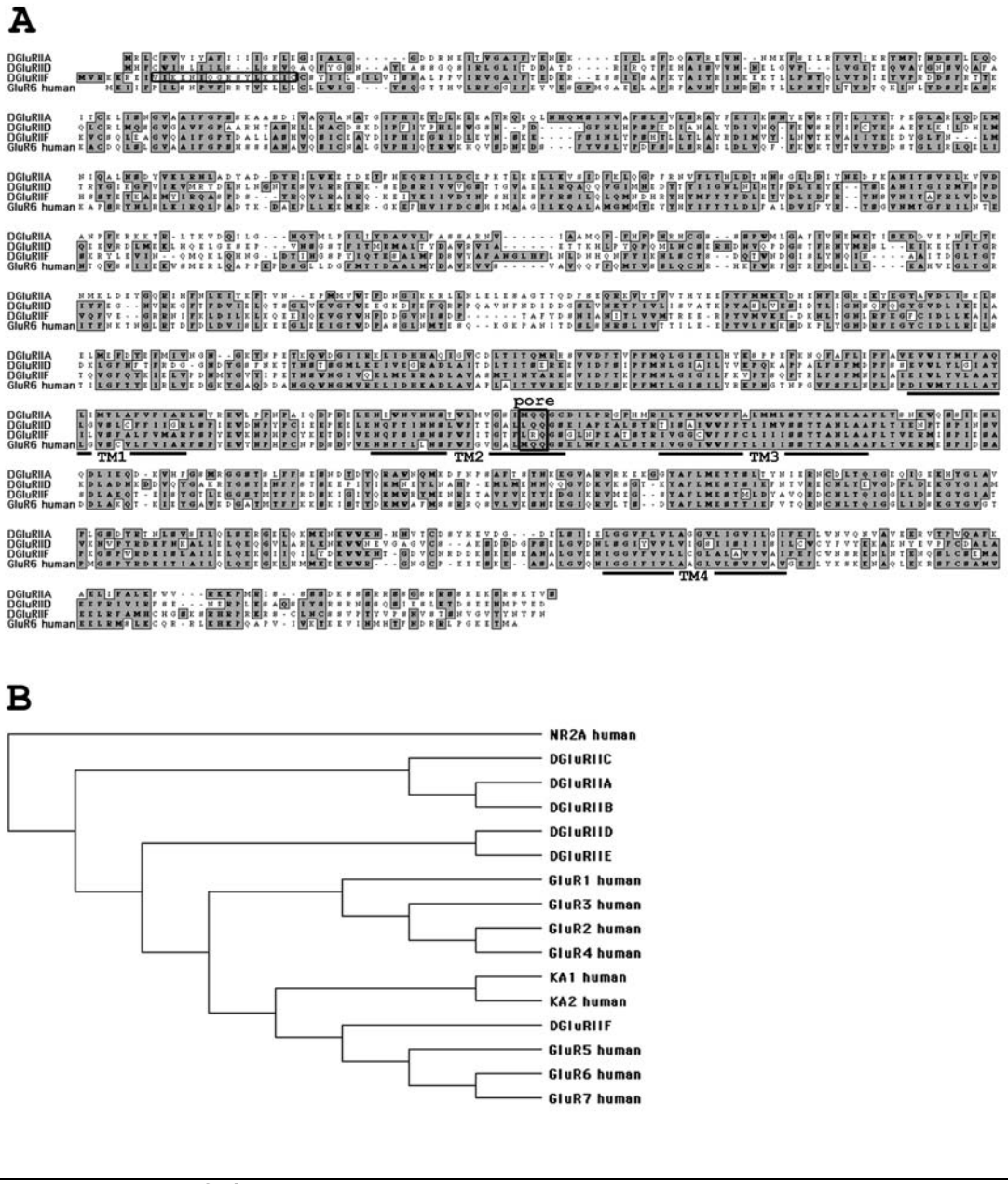

Figure 27 Sequence of GluRIIF

A) Sequence alignment of the predicted amino acid sequences of (from top to bottom) GluRIIA, GluRIID, GluRIIF and the human kainate receptor subunit GluR6. Amino acid similarities are shown in grey shaded boxes; transmembrane domains (TM1 – TM4) are shown below, the ion channel pore region (pore) above the sequence alignment. In the N-terminal region of GluRIIF the peptide sequence used for rabbit immunisation is marked in a box. **B)** Dendrogram analysis comparing the GluRIIF amino acid sequence with sequences of the *Drosophila* NMJ glutamate receptors (DGluRIIA – DGluRIIE) as well as a human NMDA receptor subunit (NR2A), human AMPA receptor subunits (GluR1 – GluR4) and human kainate receptors (GluR5 – GluR7, KA1 and KA2). GluRIIF is closely related to kainate receptors. Dendrogram was generated with the help of the MacVector software (Accelrys, San Diego, CA). Sequence identities obtained after ClustalW alignment: GluRIIA – GluRIIF: 32%; GluRIIB – GluRIIF: 27%; GluRIIC – GluRIIF: 26%; GluRIID – GluRIIF: 34%; GluRIIE – GluRIIF: 33%; NR2A – GluRIIF: 16%; GluR1 – GluRIIF: 37%; GluR2 – GluRIIF: 35%; GluR3 – GluRIIF: 36%; GluR4 – GluRIIF: 37%; GluR5 – GluRIIF: 43%; GluR6 – GluRIIF: 43%; GluR7 – GluRIIF: 41%; KA1 – GluRIIF: 37%; KA2 – GluRIIF: 36%.

(compare Figure 27 B). Among the *Drosophila* NMJ glutamate receptor subunits GluRIID and GluRIIE, which also display similarities to kainate receptors, share a higher relationship with GluRIIF than subunits GluRIIA – GluRIIC.

In order to verify the presence of both transcripts real-time PCR was performed with primer pairs specific for just one of the two transcripts (Figure 26 B). In fact RNA levels of both transcripts were detected in RNA isolation from 3rd instar larval body wall preparations lacking the CNS as well as in RNA isolation from 3rd instar larvae heads containing the larval CNS. The C_t value obtained from a primer pair directed against the N-terminal region of GluRIIF, which both transcripts have in common, is definitely smaller compared to the C_t values for ampplicons specific for one of the two transcripts in both body muscle enriched as well as CNS enriched samples. These findings indicate that both transcripts are expressed in both muscles and CNS at leasts as the dominant transcripts.
These real-time PCR results are consistent with recent studies performed in our laboratory (personal communication with Gang Qin and Stephan Sigrist) showing GluRIIF expression in the CNS as well as in body wall muscles via *in situ* hybridisation experiments. Those experiments showed GluRIIF mRNA expression in embryonic CNS while in larvae mRNA was found in body wall muscles. Furthermore, GluRIIF RNA enrichment in muscles was shown by an Affymetrix *Drosophila* Genome array, in which RNA expression profiles from 3rd instar epidermis preparations, mainly consisting of body wall somatic muscles but lacking the CNS, were compared to those of total 3rd instar larvae. In fact the average fold increase of GluRIIF RNA found in epidermis samples compared to total larvae samples is higher (3,8 fold increase) than the increase found for RNA levels of GluRIID (3,2 fold increase), a subunit which was shown to be essential for glutamatergic transmission at the NMJ (Qin et al., 2005).
Although both GluRIIF transcripts were verified, a glutamate receptor subunit missing one of its four transmembrane domains is a so far uncommon feature.

3.9.2 An antibody directed against the GluRIIF N-terminus identifies a protein at the PSD

As already mentioned above antibodies directed against GluRIIA, GluRIIB, GluRIIC and GluRIID were shown to specifically label the receptor subunits at the *Drosophila* NMJ in immunohistochemical studies (Marrus et al., 2004; Qin et al., 2005). In order to examine the location of GluRIIF at the *Drosophila* NMJ the peptide VIKENIQGRSYLKKIC, which represents a short stretch of the GluRIIF N-terminus (compare Figure 27 A) was applied to rabbit immunisation for the production of a polyclonal antibody directed against GluRIIF. This antibody, from now on refered to as GluRIIF antibody, displayed a GluRIIF staining at all NMJs in 3rd instar wild type larvae.

In synaptic boutons expression of GluRIIF was confined to typical punctae (Figure 28 A). These punctae were found in direct opposition to the label of the presynaptic marker Nc82 (Figure 29 B). Moreover, costaining with the GluRIIF and the GFP antibody in larvae expressing a transgenic GluRIIB-EGFP in the AB- background (AB-, IIBEGFP; compare chapter 2.7.3) showed a precise overlap for the glutamate receptor subunits GluRIIF and GluRIIB-EGFP (Figure 29 A, C). Transgenic expressed GluRIIB-EGFP was shown to be fully functional (unpublished data). Thus it can be concluded that GluRIIF specifically localises to the PSD region of individual synaptic sites at the *Drosophila* NMJ. The localisation of GluRIIF at PSDs is further supported by the finding, that larvae reared at 29°C exhibited a staining pattern including ring like structures (compare Figure 28), which were already reported for the GluRIIA subunit in larvae reared at 29°C (Sigrist et al., 2003).

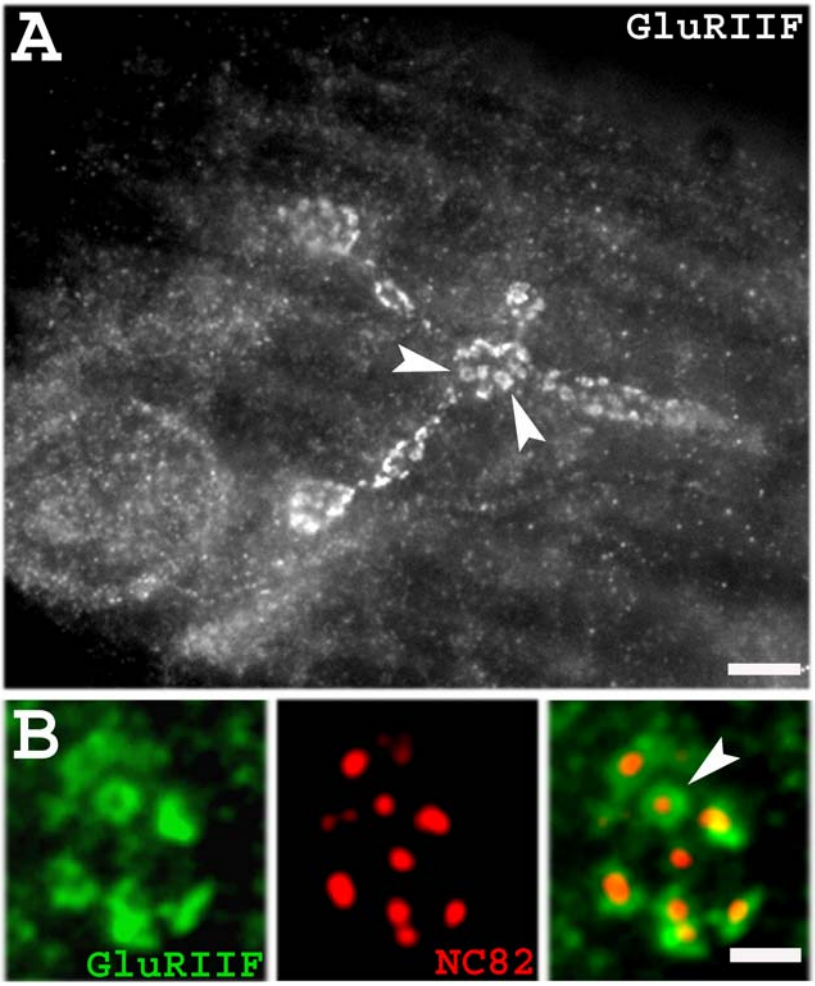

Figure 28 Glutamate receptors containing the GluRIIF subunit encircle active zones at the *Drosophila* NMJ
Shown are epifluorescence images of the NMJ of 3rd instar larval body wall preparations from wild type animals which were grown at 29°C. **A)** GluRIIF staining shows single larger receptor assemblies forming circle like structures (arrowheads). Scale bar represents 5µm. **B)** Enlargement of a single synaptic bouton stained against GluRIIF (green channel) and NC82 (red channel). The GluRIIF circles surround the presynapitc active zone marker (NC82) signal (arrowhead). Scale bar represents 1µm.

The reduction of essential GluRII subunits results in a reduction of the levels of the remaining subunits at the *Drosophila* NMJ as was shown by immunohistochemical experiments (Marrus et al., 2004; Featherstone et al., 2005; Qin et al., 2005) and western blot analysis (compare chapter 3.6).

To show if GluRIIF containing receptors depend on the abundance of other subunits, anti-GluRIIF immunostaining was performed in flies completely missing or just sporadically expressing one single subunit. The complete loss of either

GluRIIA or GluRIIB does not result in embryonic lethality. GluRIIA-EGFP or GluRII-BEGFP both shown to be fully functional (Rasse et al., 2005) were expressed in AB- background (AB-, IIAEGFP or AB-, IIBEGFP) (for details on genetics of these genotypes compare chapter 2.7.3). 3rd instar larval body wall preparations were stained against GluRIIF and GFP. In both AB-, IIAEGFP and AB-, IIBEGFP larvae the GluRIIF signal colocalised with the GFP signal at the PSDs.

When GluRIIA was missing (AB-, IIBEGFP) GluRIIF staining appeared unaltered when compared to wild type situation (Figure 29 C and B). However, loss of GluRIIB (AB-, IIAEGFP) apparently caused a reduction in the GluRIIF signal (Figure 29 D).

The removal of GluRIIC leads to embryonic lethality but the expression of basal GluRIIC levels (IIC^{hypo}) is sufficient for larval growth. In IIC^{hypo} larvae the GluRIIC protein levels were decreased (compare chapter 3.6). Moreover, the synaptic levels of GluRIIA, GluRIIB and GluRIIC were shown to be reduced almost to zero (Marrus et al., 2004). Consistent with these results GluRIIF staining was no longer detectable at the NMJ of 3rd instar larval body wall preparations while the presynaptic NC82 levels remained unchanged (Figure 29 F). The same effect could be observed for animals exhibiting reduced GluRIIE levels through RNAi (IIERNAi) (Figure 29 E), a situation which was shown to result in a decrease of GluRIIC protein levels in muscles (compare chapter 3.6) and in a massive reduction of GluRIIC and GluRIID levels at the *Drosophila* NMJ (Qin et al., 2005).

Taken together, immunohistochemical results indicate that the presence of GluRIIF at the *Drosophila* NMJ depends on the abundance of the essential muscle glutamate receptor subunits. GluRIIF receptor levels, just like the levels of GluRIIC, GluRIID and GluRIIE, are present at the NMJ when either GluRIIA or GluRIIB subunits are missing but the GluRIIF containing receptor numbers are drastically reduced when just residual amounts of subunits GluRIIC or GluRIIE are expressed at the *Drosophila* NMJ. Consequently the GluRIIF subunit extends the number of glutamate receptor subunits found at the *Drosophila* NMJ from five to six.

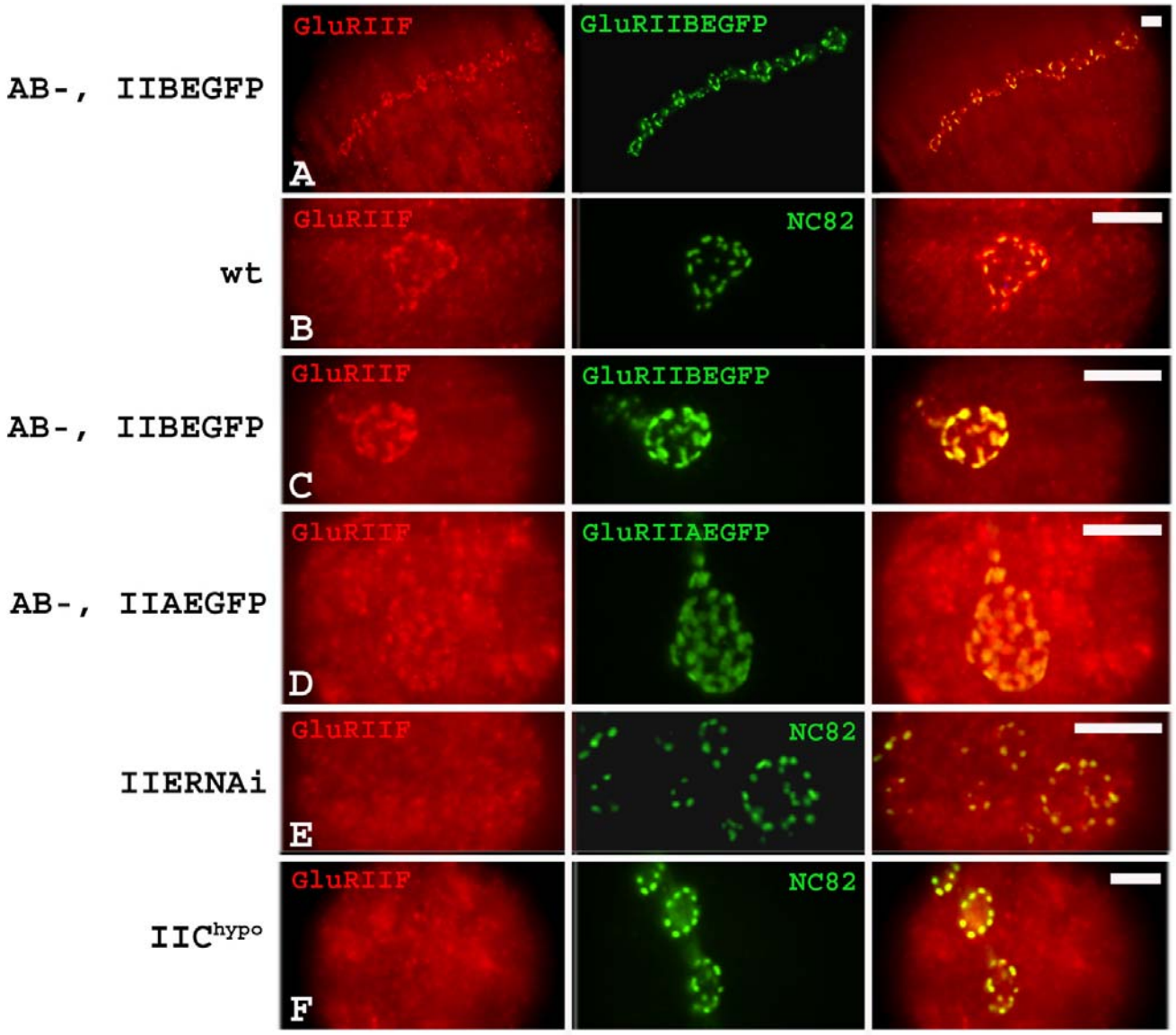

Figure 29 Presence of GluRIIF at the PSDs in dependence of the genetic background
Shown are epifluorescence pictures of GluRIIF (**A)-F)** red channel) together with either the presynaptic active zone marker NC82 (**B)**,**E)**,**F)** green channel) or GluRIIB-EGFP (**A)**,**C)** green channel) or GluRIIA-EGFP (**D)** green channel) both of them visualised via the GFP antibody. GluRIIF receptor levels are well detectable when GluRIIA is missing (AB-, IIBEGFP, **A)** and **C)**), reduced when GluRIIB is missing (AB-, IIAEGFP, **D)**) and almost completely absent when GluRIIE and GluRIIC levels are reduced (IIERNAi, **E)** and IIC^{hypo} **F)**). All larvae were reared at 25°C except for the IIERNAi larvae which were hatched at 29°C.

3.9.3 Exploring the effect of a decrease in GluRIIF levels on the glutamatergic transmission at the *Drosophila* NMJ

RNA interference (RNAi), a process in which doublestranded RNAs silence gene expression through specific degradation of their related mRNAs (Fire et al., 1998), was shown to be a direct and efficient way of producing loss-of-function mutant phenotypes of predicted genes in a multitude of organisms (Fraser et al., 2000; Gonczy et al., 2000).

Transgene mediated RNAi was shown to be a powerful tool for decreasing the expression levels of a single glutamate receptor subunit at the *Drosophila* NMJ as was shown for GluRIIE (Qin et al., 2005). Muscle specific RNAi against GluRIIE diminished the levels of GluRIIE RNA to 20% in comparison to wild type levels. Furthermore, RNAi against GluRIIE resulted in a massive reduction of the subunit levels of GluRIIC and GluRIID (Qin et al., 2005) as well as of GluRIIA (data not shown) *Drosophila* NMJ.

In order to reduce GluRIIF levels *in vivo* a hairpin construct directed against a 300bp long stretch at the N-terminal domain of GluRIIF was generated for GluRIIF RNAi.

GluRIIA and GluRIIC hypomorphs displayed a decreased postsynaptic responsiveness to glutamate (Marrus et al., 2004; Qin et al., 2005). The amplitude of miniature excitatory junctional currents (mEJCs), the postsynaptic response to the release of single quanta of neurotransmitter at the presynaptic site, are believed to represent the postsynaptic answer to a single vesicle fusion event. Additionally, through external short interval stimulation via a stimulation electrode at the presynaptic nerve, action potentials can be generated propagating to the presynaptic site and resulting in vesicle fusion and neurotransmitter release into the synaptic cleft. The resulting postsynaptic currents measured by the voltage clamp are termed evoked excitatory junctional currents (eEJCs). IIA^{hypo} and hypomorphic GluRIIC larvae showed no detectable mEJCs. In addition eEJCs were decreased in IIA^{hypo} larvae when compared to wild type animals (Marrus et al., 2004; Qin et al., 2005).

In order to examine a similar influence of reduced GluRIIF levels on the

postsynaptic glutamatergic transmission at the *Drosophila* NMJ, muscle specific GluRIIF RNAi (IIFRNAi) (for details on genetics of this genotype compare chapter 2.7.3) in 3rd instar larvae was examined by TEVC.

mEJC amplitude size recorded from 3rd instar larval body wall preparations of IIFRNAi animals (0,80 ±0,02nA) was significantly reduced when compared to wt animals (0,64 ±0,03nA) (Figure 30 A and B).

In comparison animals experiencing RNAi against GluRIIE (IIERNAi) showed no measureable mEJCs at all, which is consistent with the strong reduction of the anti GluRIIC, anti GluRIID (Qin et al., 2005) and anti GluRIIF staining (compare Figure 29 E) in this genotype.

eEJCs measured at a frequency of 0,2Hz showed a significant reduction for IIF RNAi larvae (52,9 ±2,7nA) of more than 25% and an even stronger reduction for IIE RNAi larvae (19,5±1,5nA) when compared to wt animals (72,8 ±4,5nA) (compare Figure 30 C and D).

The quotient of eEJCs and mEJCs termed quantal content represents the number of released vesicles per action potential. The quantal content of IIF RNAi animals (78,9 ±3,4nA) is not significantly changed compared to wt animals (89,8 ±6,4nA) (Figure 30 E).

In paired-pulse measurements two stimuli in a 20ms interval were presynaptically applied. Such closely spaced stimuli result in an increase of residual Ca^{2+} in the surrounding of presynaptic Ca^{2+} channels, whereby the probability of a vesicle to fuse within this region after the second stimulation pulse is increased (Katz and Miledi, 1968). For this reason the amplitude of the eEJC of the second pulse is slightly larger in size compared to the eEJC of the first pulse and the quotient of second pulse eEJC and first pulse eEJC called paired-pulse ratio is larger than 1. Paired-pulse ratios of wt larvae and IIF RNAi larvae showed no difference (wt: 1,04 ±0,03; IIF RNAi: 1,09 ±0,04) but for IIE RNAi larvae a paired-pulse ratio smaller than 1 (0,70±0,02) was obtained (compare Figure 30 F and G).

The electrophysiological data profile presented here is consistent with the idea, that IIFRNAi has reduced postsynaptic glutamate receptor numbers. Both effects, a reduction in mEJC and eEJC amplitudes as observed for IIF RNAi animals, can

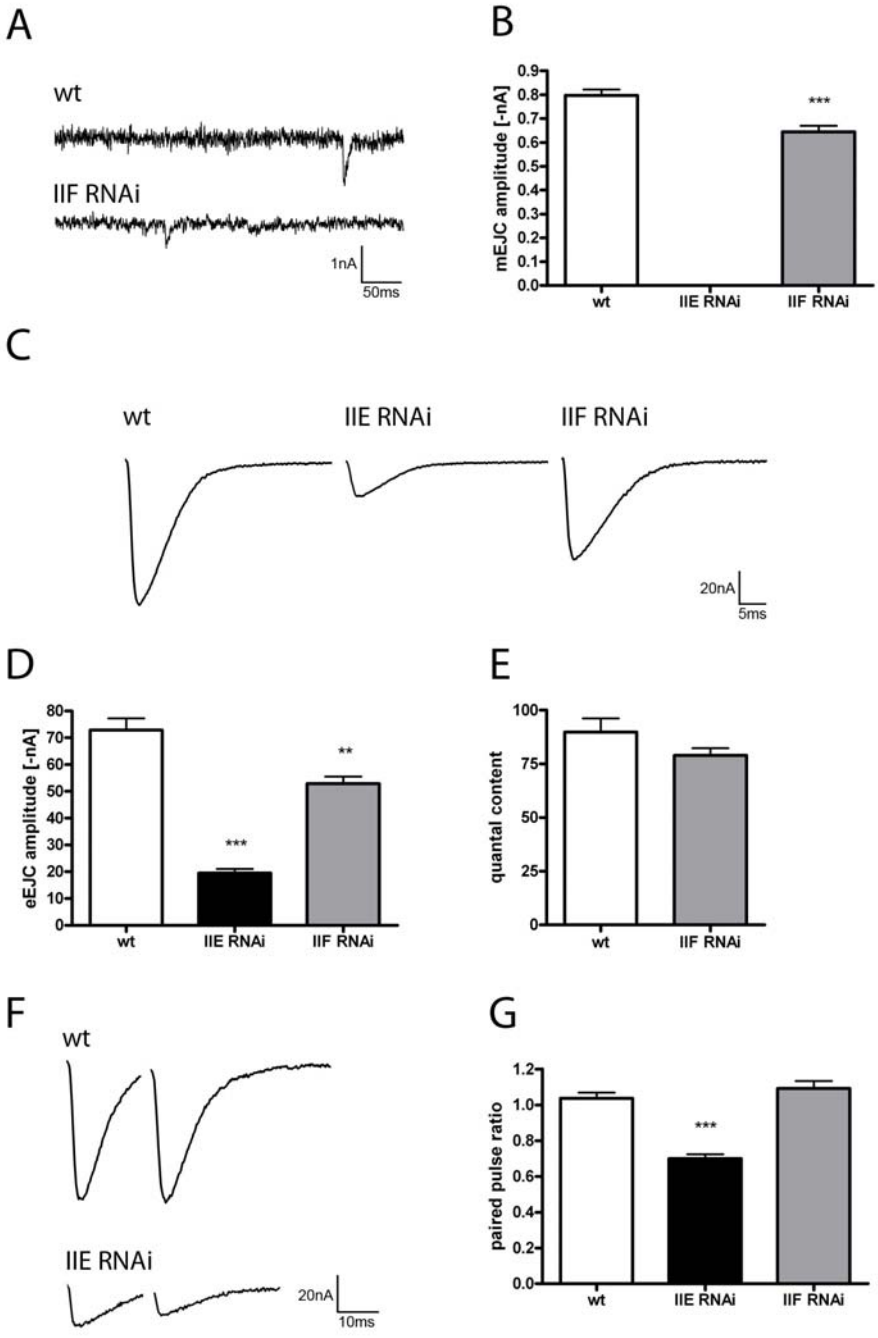

Figure 30 Electrophysiological characterisation of GluRIIF RNAi and GluRIIE RNAi constructs expressed in larval muscles

All electrophysiological data were obtained from muscle 6 of 3rd instar larval body wall preparations

A) Miniature excitatory junctional current (mEJC) from larvae resulting from crossing wild type flies to *24B-Gal4* flies (wt) and *UASgluRIIF RNAi* flies to *24B-Gal4* flies (IIF RNAi). **B)** mEJCs are significantly decreased for IIF RNAi larvae compared to wt animals (wt: 0,80 ±0,02nA [mean value±SEM] n=9; IIF RNAi: 0,64 ±0,03nA n=9 ***p=0,0002). Larvae obtained by crossing *UASgluRIIE RNAi* flies to the *24B-Gal4* strain (IIERNAi) do not exhibit any measurable mEJCs. **C)** Representative traces of evoked excitatory junctional currents (eEJCs) after 0,2Hz stimulation from wt animals, IIE RNAi animals and IIF RNAi animals. **D)** eEJCs after 0,2Hz stimulation. eEJCs are significantly decreased for IIFRNAi larvae (wt: 72,8 ±4,5nA n=10; IIF

RNAi 52,9 ±2,7nA n=11 **p=0,0017) and even more striking for IIE RNAi larvae (IIE RNAi: 19,5±1,5nA n=6 ***p=0,0002) compared to wt animals. **E)** Quantal content (eEJCs/mEJCs) is not significantly altered in IIF RNAi larvae compared to wt animals (wt: 89,8 ±6,4nA n=9; IIF RNAi: 78,93 ±3,4nA n=9 p=0,3401) **F)** Representative traces of paired pulse experiments for wt and IIE RNAi animals. Two eEJCs (0,2Hz stimulation) were recorded with an interpuls interval of 20ms. The second eEJC amplitude value was divided through the first eEJC amplitude value to obtain the paired pulse ratio. **G)** IIF RNAi larvae display no changed paired pulse ratio compared to wt animals (wt: 1,04 ±0,03 n=9; IIF RNAi: 1,09 ±0,04 n=11 p=0,536) while paired pulse ratio for IIE RNAi larvae is reduced (IIE RNAi: 0,70±0,02 n=5 ***p=0,001). Electrophysiological measurements were performed by Andreas Fröhlich. n: number of measured body wall preparations; p: P value of a nonparametric Mann-Whitney rank sum test.

be explained either by a reduction of postsynaptic receptor numbers or a reduction of presynaptic vesicles or neurotransmitter molecules per vesicle. However, the quantal content as a means of vesicle content is unchanged making a presynaptic effect unlikely. In the case of IIE RNAi animals the reduction of mEJC and eEJC amplitudes is even more severe; no mEJC amplitudes can be measured at all. Moreover, the paired-pulse ratio is smaller than 1. This result would be expected for a situation in which the presynapse compensates for a postsynaptic loss in sensitivity by increasing its vesicle release probability and in fact the IIE RNAi receptor number at the *Drosophila* NMJ is intensely decreased (Qin et al., 2005).

Despite displaying an electrophysiological phenotype IIFRNAi larvae did not display a massive reduction of GluRIIF RNA levels in real-time PCR experiments. Moreover, GluRIIF fluorescence intensities at the *Drosophila* NMJ were not significantly changed for IIFRNAi when compared to wild type animals as was shown in immunohistochemistry experiments performed at 3rd instar larval body wall preparations stained with the GluRIIF antibody (data not shown).

These findings are consistent with the milder reduction of mEJCs and eEJCs as well as a lack of presynaptic compensatory effects in IIFRNAi animals when compared to the IIE RNAi situation. It appears possible, that a more potent RNA interference for GluRIIF might cause a by far stronger reduction of postsynaptic currents and even a presynaptic compensation as observed for IIE RNAi.

4 Discussion

4.1 Expressing functional complexes of Drosophila muscle glutamate receptors

The functionnality of glutamate receptors, which mediate the main part of excitatory transmission in the vertebrate CNS, depends on the receptor complex composition. In vertebrates the expression of homomeric non-NMDA receptors in heterologous expression systems was sufficient for the obtainment of functional receptor complexes (Bettler et al., 1990; Boulter et al., 1990; Egebjerg et al., 1991). Furthermore, members of the TARP family were shown to participate among other things in the regulation of AMPA receptor ion channel properties (Priel et al., 2005; Tomita et al., 2005b).

In contrast, heterologous expression of functional *Drosophila* NMJ glutamate receptors was not successful so far. However, electrophysiological examination of *Drosophila* NMJ glutamate receptors were performed *in vivo* at the NMJ of embryos and larvae. Through electrophysiological characterisation of null mutants for either GluRIIA or GluRIIB differences in the physiological properties of GluRIIA and GluRIIB containing receptors were identified. GluRIIB receptor complexes displayed an about 10fold faster desensitisation time constant than GluRIIA complexes (DiAntonio et al., 1999). Although the single channel amplitude of GluRIIA and GluRIIB containing receptor complexes was not significantly different, null mutants for GluRIIA displayed a strong decrease in quantal size compared to wild type animals (Petersen et al., 1997; DiAntonio et al., 1999). This decrease in quantal size was accompanied by an increase in quantal content, displaying a retrograde presynaptic compensatory effect on the reduction of postsynaptic activity in order to maintain postsynaptic excitation (Petersen et al., 1997; Davis et al., 1998). Moreover, *in vivo* TEVC experiments on GluRII mutants demonstrated that subunits GluRIIC and GluRIID and the GluRIIA&GluRIIB subunit pair were indispensable for the formation of functional receptors at the NMJ (Marrus et al., 2004; Featherstone et al., 2005; Qin et al.,

2005). Moreover, null mutants for GluRIIC, GluRIID or GluRIIE or the double mutant for GluRIIA and GluRIIB caused the loss of glutamate receptors at the *Drosophila* NMJ in embryos (Qin et al., 2005).
Consequently, glutamate receptors at the *Drosophila* NMJ are suggested to form as complexes consisting of either subunits GluRIIA,C,D,E or GluRIIB,C,D,E. However, although differences of GluRIIA and GluRIIB containing receptors were shown by electrophysiological *in vivo* experiments so far, receptor complexes composed of subunits GluRIIA,C,D,E or GluRIIB,C,D,E could not be reconstructed in heterologous expression systems.

This work presents the first functional GluRIIB containing glutamate receptor from the *Drosophila* NMJ expressed in a heterologous expression system, the *Xenopus* oocyte (compare 3.7). Oocytes injected with the cRNA combination for subunits GluRIIB,C,D,E responded to glutamate application (Figure 19) with receptor currents, whereas oocytes injected with the cRNA combination for subunits GluRIIA,C,D,E did not respond. The current amplitudes obtained for GluRIIB containing receptor complexes were small in size but significant.
Actually, Schuster et al. (1991) reported on glutamate evoked currents observed in oocytes solely expressing the GluRIIA subunit. However, the source of these currents doubtfully represents a functionally homomeric GluRIIA receptor for the following reasons. First of all, the finding of a homomeric GluRIIA glutamate receptor contradicts the necessity for essential subunits to form a functional glutamate receptor at the *Drosophila* NMJ. In the absence of either GluRIIC, GluRIID or GluRIIE no GluRIIA signal was found at the *Drosophila* NMJ (Marrus et al., 2004; Qin et al., 2005). Moreover, overexpression of GluRIIA in GluRIID null mutants did not rescue mutant lethality (Featherstone et al., 2005). Second of all, no glutamate evoked currents could be detected in oocytes injected with the GluRIIA,C,D,E cRNA combination. Moreover, patch clamp recordings from Sf9 cells expressing GluRIIA or the combination of GluRIIA and GluRIIC displayed no glutamate evoked currents (data not shown). Third of all, although the *Drosophila* haemolymph displays glutamate levels of about 0,9mM in size

(Chen et al., 1968), the application of 30mM and 80mM glutamate, used for the displayed current traces in Schuster et al. (1991), must be doubted to represent at least rudimental physiological glutamate concentrations at the *Drosophila* NMJ.

Furthermore, this work shows the requirement of *Drosophila* SOL-1 for proper GluRIIB,C,D,E complex functionality (compare chapter 3.7.3). SOL-1 is suggested to regulate glutamate receptor desensitisation properties in *C. elegans*. A collaboration of SOL-1 and Con-A was shown to slow glutamate receptor desensitisation (Walker et al., 2006a). In fact, *Drosophila* SOL-1 in combination with Con-A was required for the resolution of a glutamate evoked current in *Xenopus* oocytes expressing a GluRIIB containing receptor complex (compare Figure 19). These findings are consistent with the fast desensitisation kinetics observed for GluRIIB containing receptor complexes (DiAntonio et al., 1999). Fast desensitisation kinetics reduce the receptor's single channel opening time. Consequently, the number of simultaneously opened ion channels is reduced, too. TEVC in *Xenopus* oocytes requires a simultaneous opening of many ion channels in order to measure a resolvable current signal. Since agonist cannot be applied to all receptor channels simultaneously, fast current components cannot be temporally resolved by TEVC in *Xenopus* oocytes, (Goldin, 1991). Consequently, no glutamate-evoked currents were measured for the GluRIIB containing receptor in the absence of *Drosophila* SOL-1. In the presence of SOL-1 the single channel opening time is prolongued and the probability for simultaneous channel openings is increased, resulting in a significant current response for oocytes expressing a GluRIIB containing receptor in *Xenopus* oocytes.

The observation that oocytes display a glutamate evoked current only in the presence of cRNA encoding subunits GluRIIB-E but not in the presence of cRNA encoding subunits GluRIIA, GluRIIC, GluRIID and GluRIIE does not neccessarily mean that a potential GluRIIA,C,D,E receptor complex does not exist. The

absence of a glutamate evoked current for a GluRIIA containing receptor in *Xenopus* oocytes can be explained by the following arguements.

First of all, the GluRIIA subunit or a subunit, which regulates GluRIIA trafficking, might not be properly expressed in oocytes. The finding of a glutamate evoked current for oocytes injected with cRNA of subunits GluRIIB-E does not necessarily mean, that all four receptor subunits are expressed. Indeed, there is evidence that the subunit expression rates in oocytes are low. Within a single oocyte batch, in which all oocytes were injected with the functional GluRIIB,C,D,E and *Drosophila* SOL-1 combination, just about 25% of the oocytes displayed a significant current signal. This observation indicates a wide spreading of protein expression levels within one oocyte batch. Despite the apparent low expression rates for GluRII subunits the expression of at least two proteins was confirmed. First of all, GluRIIB expression was ensured because replacement of GluRIIB with GluRIIA did not result in a current signal at all. Second of all, the expression of *Drosophila* SOL-1 was ensured, since the addition of *Drosophila* SOL-1 was a crucial factor to obtain measureable glutamate evoked currents. Consequently, since two injected cRNAs out of five are properly translated, it is rather unlikely, that all other glutamate receptor subunits, including the GluRIIA subunit, are not expressed in *Xenopus* oocytes with an approximately comparable efficiency.

As a second possibility, the inability to record current signals from ooyctes expressing GluRIIA containing receptor complexes can be due to the absence of a GluRIIA specific accessory protein. Since GluRIIB containing receptors required coexpression with SOL-1 for proper functionality and since GluRIIA containing receptors failed to display visuable current signals in the presence of SOL-1, the existence of an accessory protein for GluRIIA containing receptor complexes can be suggested. One potential candidate, which was not tested in *Xenopus* oocytes so far, is *Drosophila* stargazin. In this work *Apis* stargazin was shown neither to be crucial for the occurrence of GluRIIB containing glutamate evoked receptor currents nor to influence GluRIIA containing receptor properties in order to obtain a current response on glutamate application. Stargazin

homologues from different species were shown to be able to partially substitute for one another. However, a replacement of *C. elegans* stargazin with a stargazin homologue from *Apis* or *Drosophila* resulted in a decrease of the glutamate evoked current amplitude for GLR-1 by the factor of 2 (Walker et al., 2006b). Consequently *Drosophila* stargazin might be the required key molecule in order to increase the amplitude of glutamate evoked currents of GluRIIA and maybe GluRIIB receptor complexes as well.

4.2 Influence of accessory proteins on glutamate receptor presentation and function at the Drosophila NMJ

The two accessory proteins, stargazin and SOL-1 have been shown to regulate the functionality of AMPA receptors. Stargazin was demonstrated to both mediate receptor trafficking and regulate the biophysical ion channel properties in vertebrates (Chen et al., 2000b; Schnell et al., 2002; Tomita et al., 2003; Priel et al., 2005; Tomita et al., 2005b). The combination of *C. elegans* stargazin and SOL-1 is required for GLR-1 functionality. However, GLR-1 surface expression does not depend on the presence of either *C. elegans* stargazin or SOL-1 (Walker et al., 2006a).

This work suggests a regulatory role in the functionality of non-NMDA receptors at the NMJ for both *Drosophila* SOL-1 and *Drosophila* stargazin. *Drosophila* SOL-1 was shown to be an essential factor in order to obtain glutamate evoked currents for a GluRIIB containing receptor complex in *Xenopus* oocytes (compare chapter 3.7.3). *Drosophila* stargazin mutants were demonstrated to increase synaptic glutamate receptor levels at the *Drosophila* NMJ, indicating a role for stargazin in receptor functionality rather than in surface trafficking (compare chapter 3.8.4).

4.2.1 Drosophila SOL-1

This thesis suggests that the function of *Drosophila* SOL-1 mainly corresponds to SOL-1 function in *C. elegans*. *C. elegans* SOL-1 is supposed to regulate GLR-1 desensitisation. In the absence of SOL-1 GLR-1 exhibited a fast and complete GLR-1 desesensitisation and a prolonged desensitisation recovery as was shown in cultured *C. elegans* muscle cells (Walker et al., 2006a). Con-A, a plant lectin, was shown to slow AMPA receptor desensitisation (Partin et al., 1993). The Con-A mediated slowdown of GLR-1 desensitisation was demonstrated to depend on the presence of SOL-1 (Walker et al., 2006a). In analogy to these observations in *C. elegans*, a Con-A mediated slowdown of *Drosophila* glutamate receptor desensitisation required the presence of *Drosophila* SOL-1 (compare Figure 19). Con-A pretreatment of *Xenopus* oocytes injected with cRNA of subunits GluRIIB, GluRIIC, GluRIID and GluRIIE displayed a glutamate evoked current response only when *Drosophila* SOL-1 was expressed, too. Nevertheless, an all or nothing dependency for SOL-1 on Con-A is arguable since glutamate evoked currents were measured for one singular oocyte coinjected with cRNA of receptor subunits GluRIIB-E but lacking SOL-1 cRNA (data not shown). However, first of all, the observed current response was smaller than the observed mean of the current responses in the presence of SOL-1. Second of all the occurrence probability for a current response was just 7% (1 out of 14) in the absence of SOL-1 compared to 23% (5 out of 22) in the presence of SOL-1. By all means, this result still has to be reproduced in order to undoubtly display receptor currents for a GluRIIB containing receptor even in the absence of SOL-1.

Furthermore, *Drosophila* SOL-1 was shown to functionally substitute for its *C. elegans* homologue. However, no matter if *C. elegans* SOL-1 or its *Drosophila* homologue were coexpressed with GLR-1 in *Xenopus* oocytes, glutamate evoked currents were only detectable in the presence of stargazin (Walker et al., 2006a). In fact, replacement of *Drosophila* SOL-1 with *C. elegans* SOL-1 displayed the same effect (data not shown). A Con-A pretreated oocyte coinjected with the GluRIIB,C,D,E combination plus *C. elegans* SOL-1 responded with a glutamate evoked receptor current which, however, had a smaller

amplitude compared to oocytes expressing GluRIIB,C,D,E and *Drosophila* SOL-1. Likewise, the GLR-1 current response on the application of glutamate is reduced when *C. elegans* SOL-1 is replaced by *Drosophila* SOL-1 (Walker et al., 2006b). Thus SOL-1 functionality is likely to be conserved within the two species. However, the *Drosophila* NMJ glutamate receptors differ from *C. elgans* GLR-1 regarding their dependence on accessory proteins for surface expression. While homomeric GLR-1 receptors were shown to require both SOL-1 and stargazin expression in order to obtain a measureable current response on glutamate application, GluRIIB containing glutamate receptors required only *Drosophila* SOL-1 for proper functionality (compare Figure 19).

Finally, *Drosophila* SOL-1 displayed a potential preferation for GluRIIB containing receptors over GluRIIA containing receptors. While coinjection of subunits GluRIIB-E and SOL-1 produced glutamate evoked currents, no current response was observed when the GluRIIB subunit was replaced by the GluRIIA subunit (compare Figure 19). A GluRIIB preference for SOL-1 is not unlikely for the following reason. At *C. elegans* AVA interneurons the two subunits GLR-1 and GLR-2 mediate rapidly activating and inactivating glutamate-gated currents. Coexpression of GLR-1 and GLR-2 in oocytes additionally expressing SOL-1 and stargazin did not change the current amplitude of receptor currents compared to oocytes solely expressing GLR-1 plus SOL-1 and stargazin (Walker et al., 2006a). These results indicate a SOL-1 preference for GLR-1. However, it has to be noticed, that Walker et al. did not display TEVC data displaying the measurement of oocytes expressing GLR-2 plus SOL-1 and stargazin to confirm this indication.

4.2.2 Drosophila Stargazin

This thesis indicates that the presence of a TARP protein is not essential for the formation of a functional GluRIIB containing receptor in *Xenopus* oocytes (compare chapter 3.7.3). However, this work shows a connection between glutamate receptor levels at the *Drosophila* NMJ and the presence of *Drosophila*

stargazin. 1st exon deletion mutants as well as a 1st intron deletion mutant of *Drosophila* stargazin increase the synaptic glutamate receptor levels as was visualised through subunits GluRIIC and GluRIID (compare Figure 24, Figure 25). Two different functions of stargazin on glutamate receptors, one concerning receptor trafficking, the other concerning ion channel properties, could in principle mediate these changes in receptor levels. In vertebrates stargazin was suggested to exercise both of these functions. Vertebrate stargazin was shown to act as chaperone through AMPA receptor ER processing, increasing the AMPA receptor surface expression (Vandenberghe et al., 2005b) and furthermore to stabilise AMPA receptors on the cell surface (Tomita et al., 2004). Moreover, vertebrate stargazin was shown to mediate AMPA synapse targeting through interaction with PSD-95 and nPIST (Chen et al., 2000a; Cuadra et al., 2004). In addition to its importance for receptor trafficking vertebrate stargazin was shown to modulate the biophysical properties of AMPA receptors. Stargazin was displayed to mediate a reduction of AMPA receptor desensitisation (Priel et al., 2005; Tomita et al., 2005b; Turetsky et al., 2005), an enhanced recovery from desensitisation (Priel et al., 2005; Turetsky et al., 2005) and slowed deactivation rates (Priel et al., 2005; Tomita et al., 2005b). However, a comparison of vertebrate stargazin to its homologous proteins in *C. elegans* and *Drosophila* indicates, that just stargazin's role concerning the regulation of the ion channel properties is conserved.

First of all, heterologous expression of the *C. elegans* glutamate receptor GLR-1 was observed in *C. elegans* muscle cells in the absence of stargazin (Walker et al., 2006a). However, in *Xenopus* oocytes significant GLR-1 responses to glutamate could only be detected in the presence of stargazin and the obligatory SOL-1 (Walker et al., 2006b), thus indicating an important role for stargazin concerning receptor functionality in *C. elegans*.

Second of all, unlike its vertebrate homologue, *Drosophila* stargazin apparently does not influence glutamate receptor trafficking, since the loss of a functional stargazin protein did not result in a decrease of glutamate receptors numbers, as would be estimated for a protein crucial for receptor surface delivery. Quite the

contrary, the observed effect was an increase in receptor levels instead (compare Figure 24, Figure 25), which is consistent with a compensation for the loss of a protein involved in the regulation of receptor ion channel properties, in order to maintain a functional glutamate evoked postsynaptic transmission.
Third of all, in vertebrates glutamate receptor delivery into synapses was shown to be mediated by stargazin through binding to PSD-95 via the C-terminal putative PDZ binding motif –TTPV (Chen et al., 2000b; Schnell et al., 2002). Furthermore, vertebrate stargazin was displayed to bind to all AMPA receptor subunits (Tomita et al., 2003; Tomita et al., 2004; Fukata et al., 2005). The –TTPV motif, however, though conserved in the stargazin homologue in *Apis*, is absent in the *C. elegans* as well as in the *Drosophila* stargazin homologue (compare Figure 20 A). Furthermore, a protein, displaying functions similar to PSD-95 for all GluRII subunits, has not been described so far. The only member of the family of membrane associated guanylate kinases (MAGUK) and consequently the only known PSD-95 relative in *Drosophila* is DLG. So far, a direct interaction between DLG and GluRII subunits could not be shown. However, in DLG mutants anti-GluRIIB staining displayed reduced GluRIIB levels, whereas anti-GluRIIA staining showed unchanged GluRIIA levels (Chen and Featherstone, 2005). These findings indicate a selective DLG interaction with GluRIIB containing receptor complexes. The inverse effect was observed for mutants of choracle, a *Drosophila* homologue to the mammalian 4.1 proteins, which bind to the actin cytoskeleton. Immunostaining against GluRIIA showed a reduction of GluRIIA receptor levels, whereas anti-GluRIIB staining displayed no changes in the GluRIIB receptor levels (Chen et al., 2005), indicating a specific choracle-mediated stabilisation of GluRIIA receptor complexes at the PSD. Consequently, synaptic stabilisation seems to be glutamate receptor complex specifically mediated by different proteins at the *Drosophila* NMJ.

To sum it up, an essential stargazin-mediated mechanism for surface trafficking and synapse delivery as shown in vertebrates is not conserved in *Drosophila*. However, data from *C. elegans* and *Drosophila* indicate a conserved stargazin

function regarding the regulation of glutamate receptor channel properties.

4.3 GluRIIF is a novel glutamate receptor subunit at the Drosophila NMJ

Five different non-NMDA receptor subunits, GluRIIA-E, have been identified at the *Drosophila* NMJ so far (Schuster et al., 1991; Petersen et al., 1997; DiAntonio et al., 1999; Marrus et al., 2004; Featherstone et al., 2005; Qin et al., 2005).

This thesis introduces a sixth subunit, termed GluRIIF. The presence of this subunit at the neuromuscular junction was demonstrated through immunohistochemistry and electrophysiological data (compare Figure 28, Figure 29, Figure 30). GluRIIF colocalised with the other glutamate receptor subunits at the PSDs of the *Drosophila* NMJ (Figure 29). Moreover, reduction of GluRIIF decreased mEJC and eEJC amplitudes (Figure 30), most likely, as was shown for other receptor subunits (Marrus et al., 2004; Featherstone et al., 2005; Qin et al., 2005), through the reduction of the total synaptic glutamate receptor numbers. Interestingly, GluRIIF appears to favour GluRIIB containing receptor complexes over GluRIIA containing receptor complexes, since the GluRIIF fluorescence signal in the absence of GluRIIB was considerably weaker than in the absence of GluRIIA (compare Figure 29). However, GluRIIF appears not to be an essential subunit for basal glutamate receptor functionality, as was indicated by the finding of a functional receptor in the absence of the GluRIIF subunit (Figure 19). However, the influence of a GluRIIF null mutation on the glutamate receptor levels at the *Drosophila* NMJ has to be tested in order to finally judge if GluRIIF is an essential receptor subunit or not. In any case, GluRIIF displays some special characteristics in comparison to the other GluRII subunits.

First of all, GluRIIF is encoded on the fourth chromosome. The fourth chromosome in *Drosophila* differs from the other three chromosomes. On the one hand a high abundance of HP1, a heterochromatin protein, as well as selective methylation of histone 3 was found at the 4^{th} chromosome (Eissenberg

et al., 1992). On the other hand, reporter genes inserted in the 4th chromosome displayed a partially silenced expression (Wallrath and Elgin, 1995; Wallrath et al., 1996). These results indicate that the 4th chromosome shares properties typical for heterochromatin. Thus gene expression for the 4th chromosome requires chromosome specific proteins, which are supposed to be involved in a balancing mechanism that helps maintaining appropriate levels of gene expression on the 4th chromosome (Johansson et al., 2007).

Second of all, two GluRIIF transcripts were shown to be present both at the somatic muscles and in the CNS of *Drosophila* 3rd instar larvae (Figure 26 B). The only other *Drosophila* glutamate receptor subunit, which was shown to be expressed both in muscles as well as in the CNS is GluRIID (Featherstone et al., 2005). Alternative splicing has been reported for *Drosophila* NMDA receptor subunits dNR1 and dNR2. Two splice isoforms of dNR1 and 8 splice isoforms of dNR2 were identified (Xia et al., 2005).

The second GluRIIF transcript lacks the fourth transmembrane domain (TM4), forming a truncated receptor subunit (compare Figure 26 A). The functional role of TM4 has just been primarly described. A conserved methionine in TM4 was shown to be involved in receptor desensitisation and ion channel gating (Ren et al., 2003a). Truncation mutants lacking TM4 in NMDA receptors probably are still capable of forming heteromeric receptors with non-truncated subunits. The heterologous expression of a tandem construct, in which a truncated NR2A subunit was merged with a complete NR1 subunit, in HEK cells responded on coapplication of glutamate and glycine with a current response (Schorge and Colquhoun, 2003). Moreover, a truncated NR1A subunit lacking TM4 was reported to co-assemble with NR2A and form a complex, which was found at the cell surface in HEK cells (Meddows et al., 2001). However, this receptor complex appeared to be non-functional.

The expression of truncated receptor subunits has been reported for various other receptor types. In each case, alternative splicing generated a frameshift, which was responsible for the premature termination of the protein. In the metabotrope rat glutamate receptor mGluR6, a member of the GPCR family, an

additional exon was shown to cause a truncated receptor, which exhibits the glutamate binding pocket but lacks the complete transmembrane and intracellular region (Valerio et al., 2001), thus losing its ability to bind GTP-binding proteins. A similar mGluR splice variant was found for the receptor GRM2 in the human brain (Sartorius et al., 2006). Although missing all seven transmembrane domains this truncated receptor was shown to be still membrane bound. Another example for truncated receptors was identified for the α7 subunit of nicotinic acetylcholine receptors in the mouse. The truncated subunit was shown to lack the fourth transmembrane domain and the intracellular tail (Saragoza et al., 2003). Furthermore, this subunit was displayed to act as a dominant-negative effector for the function of the non-truncated α7 subunit. In another example, a splice variant of the tridecapeptide neurotensin receptor NTS2 formed a 5-transmembrane domain version of the otherwise 7-transmembrane receptor (Perron et al., 2005). Despite this truncation the receptor remained functional. Thus the finding of a truncated receptor isoform of the GluRIIF subunit is no singular case among receptors, although it is a novel feature for ionotropic glutamate receptors. One possible function of a glutamate receptor containing the truncated GluRIIF subunit could be to act as a so-called decoy receptor (Colotta et al., 1993), by simply reducing the glutamate concentration at the postsynaptic site. Since the absence of the last transmembrane domain as well as the C-terminal domain does not necessarily result in the loss but just in a modulation of the GluRIIF subunit function, the incorporation of the first or the second GluRIIF isoform might result in two receptors with different properties.

Third of all, a functional role for GluRIIF is supported by the presence of a positive amino acid in its pore forming region, the so-called Q/R editing site. The presence of an arginine (R) instead of a glutamine (Q) at this site was shown to alter ion permeability for mammalian AMPA and kainate receptors. More than 99% of the GluR2 subunits were found to consist of the arginine containing version in the brain of adult mice (Seeburg et al., 2001). In contrast, subunits GluR5 and GluR6 were shown to contain both versions in the adult brain of rats (Sommer et al., 1991; Kohler et al., 1993). The presence of the R containing

subunit version was demonstrated to cause a low Ca^{2+} permeability and a low single channel conductance for both AMPA and kainate receptors (Hume et al., 1991; Swanson et al., 1996). Interestingly exogenously expressed GluR2(R) subunits were displayed to be ER retained, where most of them were found as unassembled monomers, while GluR2(Q) subunits formed receptors which trafficked to the cell surface (Greger et al., 2002; Greger et al., 2003). Consequently, the single amino acid change from Q to R prevents surface trafficking of the homomeric AMPA receptor. However, this effect seems rather AMPA receptor specific, since homomeric receptors consisting of the R- form of kainate receptor subunits GluR5 and GluR6 displayed current responses when exogenously expressed (Burnashev et al., 1996; Wilding et al., 2005).

These findings suggest a potential regulatory role for GluRIIF regarding receptor channel ion selectivity and channel conductance. In fact, glutamate evoked currents change depending on the GluRIIF levels at the *Drosophila* NMJ (compare Figure 30). However, the reduction in mEJCs and eEJCs observed for the GluRIIF RNAi construct could be either due to a reduction in total glutamate receptor levels resulting in decreased synaptic receptor trafficking, or due to the decrease of single channel conductance caused by the reduction of GluRIIF containing receptors. Since the RNAi construct, which was used so far, caused just a mild reduction on GluRIIF receptor levels, as was suggested by immunohistochemical and real-time PCR data, the application of a more potent RNAi construct is required for the further characterisation of GluRIIF function.

4.4 Glutamate receptor subunit stoichiometry at the Drosophila NMJ

With the discovery of GluRIIF at the *Drosophila* NMJ the number of glutamate receptors colocalising in PSDs was increased from five to six. So far GluRIIC, GluRIID and GluRIIE were shown to be essential subunits. Null mutants for GluRIIC, GluRIID or GluRIIE or a double mutant for GluRIIA and GluRIIB

resulted in the abolishment of glutamate receptor complexes at the NMJ in embryos (Qin et al., 2005). In addition, a genetical reduction of the subunit levels of GluRIIC, GluRIID, GluRIIE or GluRIIA in the absence of GluRIIB resulted in a massive reduction of the remaining glutamate receptor subunits in the whole muscle (compare Figure 16) and more dramatically at the PSDs of the *Drosophila* NMJ (Marrus et al., 2004; Featherstone et al., 2005; Qin et al., 2005). Consequently, glutamate receptors at the *Drosophila* NMJ were suggested to form tetrameric complexes with a GluRIIA,C,D,E and GluRIIB,C,D,E subunit composition or a pentameric receptor assembly with a receptor composition such as $GluRIIA_2$,C,D,E and $GluRIIB_2$,C,D,E (Qin et al., 2005). With the addition of the GluRIIF subunit the existence of one single tetrameric receptor complex consisting of the three essential subunits GluRIIC-E and either GluRIIA or GluRIIB is questionable, since there is no space for an additional fifth subunit in a tetrameric receptor complex. Although there is a preference to believe in glutamate receptors as tetrameric assembled complexes the question if glutamate receptors really form tetrameric or rather pentameric complexes has not been answered explicitly by the hithero performed experiments. Biochemical data based on cross-linking experiments with glutamate receptors containing subunits GluR1-4 from the rat and native PAGE with rat GluR1 containing receptors favour a pentameric receptor assembly (Blackstone et al., 1992; Wenthold et al., 1992). These data are supported by electrophysiological experiments performed with homomeric GluR1 receptor complexes consisting of the wild type GluR1 subunit and a GluR1 mutant, which was shown to exhibit an increased sensitivity to the channel blocker PCP in *Xenopus* oocytes (Ferrer-Montiel and Montal, 1996). In addition electrophysiological single-channel current pattern analysis from mouse NR1 and NR2B subunits expressed in *Xenopus* oocytes (Premkumar and Auerbach, 1997) as well as biochemical cross-linking data from synaptic membrane fractions of rat cerebral cortex (Brose et al., 1993) favour a pentameric over a tetrameric receptor stoichiometry for NMDA receptors.

In contrast, the electrophysiological analysis of single channel conductance

states of a non-desensitising homomeric GluR3 receptor expressed in HEK cells (Rosenmund et al., 1998) as well as electrophysiological results from voltage clamp measurements in *Xenopus* oocytes, expressing the combination of wild type GluR1 and a GluR1 desensitisation mutant (Mano and Teichberg, 1998), indicate a tetrameric structure for non-NMDA receptors. In addition experimental data derived from density gradient centrifugation and electron microscopical analysis of GluR2 agree with a tetrameric receptor structure (Safferling et al., 2001). Furthermore, analysis of the agonist response properties through voltage clamp measurements in *Xenopus* oocytes, expressing combinations of a wild type as well as a low agonist affinity mutant version of the NR1 and NR2 subunits, suggests a tetrameric receptor stoichiometry (Laube et al., 1998). Similar experiments taking advantage of two different kinds of the same receptor subunit differing in their agonist affinity or sensitivity were used to predict a pentameric structure for GABA receptors (Chang et al., 1996) and glycine receptors (Kuhse et al., 1993). A further support for tetrameric glutamate receptor stoichiometry was recently given by fluorescence bleaching experiments through total internal reflection fluorescence microscopy. Photobleaching analysis of single fluorescent protein complexes, containing either GFP tagged NR1,NR2B or NR1,NR3B combinations, showed a maximum of four different bleaching steps in *Xenopus* oocytes (Ulbrich and Isacoff, 2007). Furthermore, the “dimer of dimers” model for receptor formation, which is supported by TEVC measurements in oocytes and coimmunoprecipitation experiments performed with chimeric GluR3,GluR6 subunits (Ayalon and Stern-Bach, 2001), proposes a tetrameric rather than a pentameric receptor assembly. Last but not least the significant amino acid homology ionotropic glutamate receptors share with K^+ channels, which were shown to assemble as a tetramer (Doyle et al., 1998), indicates a similar structure for both types of ion channel (Mayer and Armstrong, 2004).

In the end, a pentameric glutamate receptor consisting of GluRIIA,C,D,E,F or GluRIIB,C,D,E,F certainly is one possible solution in order to combine all six subunits in two functionally different receptors. However, this pentamer formation

would assume a direct interaction between all five subunits in this complex, which is worth discussing for two reasons. First of all, GluRIIF shares a low sequence homology with the five other GluRII subunits but is more closely related to human kainate receptors (compare Figure 27 B). Especially GluRIIB and GluRIIC share less than 30% amino acid identity with GluRIIF. Second of all, a functional receptor combination was found in the absence of GluRIIF (compare chapter 3.7), indicating that GluRIIF has no crucial role for surface receptor complex formation and basal receptor functionality. Nevertheless, the decrease of GluRIIF levels resulted in a reduced glutamatergic neurotransmission at the *Drosophila* NMJ, which was demonstrated by decreased mEJC and eEJC amplitudes in IIFRNAi larvae (Figure 30).

Thus, considering that the experimental data on glutamate receptors so far favour a tetrameric subunit assembly, a tetrameric receptor containing the GluRIIF subunit besides an GluRIIA,C,D,E and an GluRIIB,C,D,E combination can be suggested.
In this case GluRIIF might replace one of the other four subunits. However, since GluRIIA and GluRIIB containing receptors differ in receptor properties, subunits GluRIIC-E are most likely to be replaced. However, those three subunits were shown to be essential for receptor formation at the NMJ and considered to establish the receptor platform, whereas incorporation of either GluRIIA or GluRIIB determines the specific receptor functions (Qin et al., 2005). The absence of one of them results in the synaptic loss of all receptor subunits at the *Drosophila* NMJ. Consequently, five different subunits cannot be combined in a single tetrameric receptor complex. However, they can be distributed in two interacting complexes, each of which is a tetramer. Consequently, a dimerisation between two tetrameric receptor complexes is suggested.

Dimerisation processes have been described for G-protein coupled receptors (GPCRs), where they affect G-protein selectivity, receptor internalisation rates as well as receptor pharmacology (Maggio et al., 2005). Heterodimerisation of the

two opiod receptors κ and δ were shown to result in a new receptor with ligand binding and functional properties which differ from those of κ as well as δ receptors (Jordan and Devi, 1999). Even members of different GPCR families were shown to interact via heterooligomerisation. The oligomerisation of the dopamine receptor D2R and the somatostatin receptor SSTR5 were shown to create a new receptor with enhanced functional activity (Rocheville et al., 2000). In a third example heterooligomerisation was shown to be crucial for receptor surface expression. The GABA receptor $GABA_BR2$ was demonstrated to be functionally inactive when expressed alone. Coexpression of $GABA_BR2$ with $GABA_BR1$ resulted in a 10-fold increase in agonist potency compared to homomeric $GABA_BR1$ (Jones et al., 1998; Kaupmann et al., 1998).

Although G-protein coupled receptors are not ion channels but mediate cell signalling through G-proteins, a dimerisation process among glutamate receptors, though not descibed so far, must be taken in consideration.

The dimerisation could be either mediated directly by the interaction of subunits belonging to different receptor complexes or indirectly through additional interactions via non-glutamate receptor proteins.

4.5 Proteins interacting with GluRII subunits

The C-termini of ionotropic glutamate receptors are the predominant cytoplasmic regions of the whole receptor molecule. In vertebrates non-NMDA receptors have been shown to interact with other PSD proteins through their C-termini (compare chapters 1.6.3.1 and 1.6.4.1). Proteins interacting with the glutamate receptor C-termini were shown to be involved in receptor trafficking and membrane anchorage processes (Henley, 2003).

Prominent interactors involved in the membrane stabilsation of AMPA receptors are SAP97 for GluR1, protein 4.1 for GluR1 and GluR4 as well as PICK1, GRIP and NSF for GluR2 and GluR3.

SAP97, a member of the MAGUK family, which binds GluR1 complexes after receptor synthesis in the ER, was demonstrated to release the receptor complex

upon arrival at the synapse (Sans et al., 2001). Furthermore, SAP97 displays a linkage to protein kinases through its interaction with the kinase anchoring protein AKAP79/150 (Colledge et al., 2000).

Protein 4.1 is presumed to mediate the linkage of AMPA receptors to the cytoskeleton (Shen et al., 2000). The disruption of the interaction between AMPA receptor and protein 4.1 decreases surface expression of the receptor (Shen et al., 2000; Coleman et al., 2003).

Vertebrate GRIP, a seven PDZ domain protein, was shown to bind to GluR2 and GluR3 through PDZ interaction (Dong et al., 1997; Srivastava and Ziff, 1999). GRIP was further shown to support synaptic GluR2 accumulation via PDZ interaction. A GluR2 mutant lacking the PDZ binding site displayed a reduction in synaptic receptor accumulation (Osten et al., 2000). Interestingly, the highest GRIP concentrations were found not at glutamatergic excitatory synapses but in GABAergic nerve terminals (Wyszynski et al., 1999).

PICK1, a postsynaptic scaffolding protein binding to protein kinase Cα (Xia et al., 1999; Daw et al., 2000) was shown to reduce the plasma membrane levels of GluR2 and to form endosome like clusters with GluR2 (Perez et al., 2001). Thus GRIP and PICK1 are both suggested to affect synaptic AMPA receptor stabilisation. Mechanistically, GRIP interaction with GluR2 depends on the phosphorylation of Ser880. Upon phosphorylation of Ser880 the GluR2 binding affinity for GRIP but not for PICK1 was massively decreased (Chung et al., 2000).

The third participant in this mechanism is NSF. The coassembly of NSF and SNAPs to GluR2 was shown to dissociate the GluR2-PICK1 complex (Hanley et al., 2002). Thus NSF is supposed to be a regulator in PICK1-dependent GluR2 endocytosis (Barry and Ziff, 2002). Although kainate receptors display PDZ-domain mediated interaction with proteins like PSD-95, SAP97, SAP102 as well as PICK1 and GRIP, ER exit does not depend on PDZ interaction as was shown for GluR5 and GluR6 (Ren et al., 2003b; Jaskolski et al., 2004). However, PDZ interaction influences kainate receptor mediated synaptic transmission. The interactions with both GRIP and PICK1 were shown to be required for the

maintenance of kainate receptor mediated synaptic transmission (Hirbec et al., 2003).

In *Drosophila* several homologues of the above described vertebrate glutamate receptor interacting proteins have been identified. As previously described, DLG is the only MAGUK member found in Drosophila. DLG mediates a selective interaction with GluRIIB (Chen and Featherstone, 2005), however, a direct interaction between DLG and GluRII subunits could not be shown. In fact, DLG does not specify the localisation of GluRIIB containing receptors, since DLG was displayed to be present both synaptically and extrasynaptically (Chen and Featherstone, 2005). Thus DLG interaction with GluRII receptors is most likely mediated by an additional interaction partner, which has not been identified yet.
A GRIP homologue, termed DGRIP, was identified in *Drosophila*, specifically interacting with the C-terminal -EARV motif of GluRIIC (unpublished data from Laura Swan). However, DGRIP was no shown to be involved in the regulation of glutamate receptor membrane trafficking and stabilisation. In fact, DGRIP was shown to be a key factor in the regulation of embryonic muscle guidance (Swan et al., 2004; Swan et al., 2006). Moreover, DGRIP was displayed to be an important interactor in the internalisation process of Frizzled-2 (DFz2), the postsynaptic receptor for the presynaptically secreted protein Wingless (Wg) (Ataman et al., 2006). Wingless secretion is suggested to be required for synaptic bouton development. It was shown to be involved in the differentiation of active zones and postsynaptic specialisations (Packard et al., 2002; Packard et al., 2003). In the end, DGRIP, although interacting with GluRIIC, does not seem to be a key player in the regulation and stabilisation of GluRII receptor complexes at the *Drosophila* NMJ.
Two NSF homologues as well as one PICK1 homologue were identified in *Drosophila* (Ordway et al., 1994; Boulianne and Trimble, 1995; Takeya et al., 2000). However, an involvement of *Drosophila* NSF and PICK1 in postsynaptic processes involving glutamate receptors has not been reported yet.
One potential candidate, linking different receptor complexes together, is the

Drosophila 4.1 protein homologue choracle. Choracle displays a strong interaction with the GluRIIA C-terminus and weaker interactions with the C-termini of GluRIIC and GluRIID, as was shown by yeast two-hybird analysis (Chen et al., 2005).

Besides interaction via their C-termini AMPA receptors were shown to interact with accessory proteins like stargazin and SOL-1. Bedoukian et al. (2006) proposed an interaction of vertebrate stargazin with the S2 domain of the ligand binding site, the transmembrane domains as well as cytoplasmic parts of GluR1 and GluR2, but no interaction with the C-termini of the receptor subunits.

As previously discussed *Drosophila* SOL-1 and *Drosophila* stargazin affect GluRII receptor complexes by a modulation of the channel properties rather than a crucial role in receptor trafficking. However, although *Drosophila* SOL-1 was shown to be an essential factor for receptor desensitisation (compare chapter 3.7.3), an additional function as a stabilising interactor through receptor proliferation and synaptic localisation cannot be excluded. Alike, although the absence of a functional stargazin protein increases the glutamate receptor numbers at the *Drosophila* NMJ (compare chapter 3.8.4), it cannot be ruled out that stargazin might in addition to other proteins mediate a stabilising interaction on the glutamate receptor complexes.

To sum it up, several proteins, homologues of which were shown to be involved in glutamate receptor trafficking and surface stabilisation, are present in *Drosophila*. Whereas DGRIP, NSF and PICK1 do not mirror their vertebrate homologues' influence on non-NMDA receptor trafficking and membrane stabilisation in *Drosophila*, proteins like choracle, DLG, *Drosophila* SOL-1 and *Drosophila* stargazin were shown to be relevant GluRII interactors, affecting GluRII receptor trafficking or channel properties. Thus a subset of these proteins could be involved in a receptor dimerisation process suggested in chapter 4.4.

4.6 GluRII receptor subunit interactions and functions

In AMPA and kainate receptors functional assays for heteromer formation are compatible with a model where tetrameric glutamate receptors form in two sequential steps. In the first step of this model two subunits form dimers via interaction mediated by their N-termini. In the second step tetramers form a "dimer of dimers" via interactions medidated by the transmembrane domains as well as the C-terminal part of the S2 region (Ayalon and Stern-Bach, 2001) (compare Figure 6). The presence of six different glutamate receptor subunits at the *Drosophila* NMJ gives rise to the question which of these subunits directly interact with each other at the initial dimerisation step.

Moreover, the interdependence between the single subunits resulted in the identification of three essential receptor subunits (GluRIIC-E), one essential subunit pair (GluRIIA&GluRIIB) and in this thesis the identification of GluRIIF, which was shown to effect the glutamatergic transmission at the *Drosophila* NMJ (compare chapter 3.9.3). This subunit interdependency gives rise to the question, what functions the single receptor subunits execute within the receptor complex.

In this thesis, coimmunoprecipitation studies in Sf9 cells delivered no satisfying answer to the first question (compare chapter 3.4). The baculovirus system was shown to efficiently overexpress receptor proteins for biochemical studies in Sf9 cells (Mouillac et al., 1992; Ponimaskin et al., 1998; Ponimaskin et al., 2001; Ponimaskin et al., 2002). However, a massive overexpression of *Drosophila* glutamate receptor subunits, as occurring in Sf9 cells, displayed a non-neglectabel amount of unspecific protein-protein interaction (compare chapter 3.4). Thus subunit preferations on the level of dimer interaction could not be highlighted in this heterologous expression system.

Nevertheless, biochemical and immunohistochemical data from *Drosophila* 3rd instar larvae suggest specific subunit interactions. However the specific effects one subunit exercises on another, as described in the following, cannot be attributed to a direct contact between both subunits.

First of all, residual levels of GluRIIA in the absence of GluRIIB were sufficient to

preserve wild type GluRIIC levels in the muscle, as was shown in western blot analysis of 3rd instar larvae in this thesis (compare Figure 16 B). However, since larvae, in which residual levels of GluRIIB are expressed in the absence of GluRIIA, were not tested so far it cannot be ruled out that both GluRIIA and GluRIIB display the same stabilising effect on GluRIIC.

Second of all, GluRIID mutants, displaying either a mutation in the S2 domain of the glutamate binding site, an arginine instead of a glutamine at the Q/R editing site in the pore region or a replacement of its C-terminal region with the one of GluRIIC, showed decreased GluRIIB receptor levels in immunohistochemical studies, whereas GluRIIA receptor levels were unchanged (personal communication with Andreas Schmid and Stephan Sigrist). A suggested interaction of subunits GluRIIB and GluRIID is convenient with the finding of a functional GluRIIB containing complex in *Xenopus* oocytes, which required the coinjection of cRNA encoding for subunits GluRIIB, GluRIIC, GluRIID and GluRIIE (compare chapter 3.7.3).

These findings indicate specific interactions between GluRIIB and GluRIID as well as GluRIIA and GluRIIC. However, in order to investigate whether the observed interactions occurs on the level of a, according to Ayalon and Stern-Bach (2001), first dimerisation step, further coimmunoprecipitation experiments, ideally performed with physiological receptor subunit concentrations, are required.

Preffered subunit interactions indicate different roles for single subunits in a receptor complex. In vertebrate AMPA receptors different properties for GluR1 and GluR2 containing receptors were demonstrated. First of all, GluR2 was shown to influence the Ca^{2+} condunctance of the receptor ion channel via its arginine at the Q/R editing site (Hume et al., 1991; Swanson et al., 1996). However, in contrast to the unedited GluR2(Q), GluR2(R) was displayed to be ER retained (Greger et al., 2002). Second of all, GluR1 and GluR2 containing receptor complexes displayed different trafficking behaviours. After the induction of LTP, GluR1/2 complexes inserted de novo into the postsynaptic membrane in

an activity-dependent manner. GluR2/3 complexes, on the other hand, cycled continuously in and out of the synapse in a non-activity dependent manner (Shi et al., 2001; Barry and Ziff, 2002). The GluR1 function was dominant in receptor heteromers which also contained GluR2.

In *Drosophila* the roles GluRIIA and GluRIIB execute in the receptor complex have been intensely studied. GluRIIA containing receptors were demonstrated to mediate the dominant portion of synaptic transmission at the *Drosophila* NMJ (Petersen et al., 1997; DiAntonio et al., 1999; Reiff et al., 2002; Haghighi et al., 2003). Through overexpression of the GluRIIA subunit or an augmentation in larval locomotion the numbers of active zones as well as of synaptic boutons were increased, whereas perisynaptic FasII levels were decreased (Sigrist et al., 2000; Sigrist et al., 2002; Sigrist et al., 2003). This synaptic strengthening was suppressed by either the downregulation of GluRIIA or the upregulation of the GluRIIB receptor levels. Consequently, GluRIIA and GluRIIB were suggested to play antagonistic roles at the *Drosophila* NMJ. GluRIIB containing receptors displayed a 10-fold faster desensitisation rate compared to GluRIIA containing receptors (DiAntonio et al., 1999). Synaptic GluRIIA and GluRIIB receptor complexes were shown to be regulated by different interactors. Choracle, a protein 4.1 homologue, was shown to be involved in the synaptic clustering and stabilisation of GluRIIA (Chen et al., 2005), whereas DLG was displayed to regulate synaptic GluRIIB levels (Chen and Featherstone, 2005). *In vivo* imaging data displayed a direct correlation between synapse outgrowth and synaptic GluRIIA insertion (Rasse et al., 2005). Additionally, fuorescence recovery after photobleaching (FRAP) experimental data indicated a preferred incorporation of GluRIIA in growing PSDs, whereas GluRIIB was incorporated equally into all PSDs (personal communication with Andreas Schmid und Stephan Sigrist).

The role of GluRIIF as a potential regulator of receptor channel ion selectivity and channel conductance has already been discussed in chapter 4.3.

As already mentioned subunits GluRIIC, GluRIID and GluRIIE are essential subunits. Each of them is required for viability and synaptic transmission (Marrus et al., 2004; Featherstone et al., 2005; Qin et al., 2005). Null mutants for GluRIIC, GluRIID or GluRIIE cause a loss of synaptic glutamate receptor complexes at the NMJ in embryos (Qin et al., 2005). GluRIIC, GluRIID and GluRIIE are thought to form a platform, in which either GluRIIA or GluRIIB are inserted for the fine-tuning adjustements of the receptor physiology (Qin et al., 2005).
The requirement of three individual essential receptor subunits can be referred to physiological roles as well as roles during receptor trafficking.
First of all, the formation of a functional *Drosophila* GluRII receptor in *Xenopus* oocytes required besides GluRIIB cRNA the combination of GluRIIC, GluRIID and GluRIIE cRNA (compare chapter 3.7.3). Thus the essential subunits ensure proper receptor trafficking and help defining the ion channel properties as well, since every subunit in a receptor tetramer contributes to the shape of the ion channel pore.
Second of all, despite the loss of one essential subunit or subunit composition, the protein levels of GluRIIC were reduced in late stage *Drosophila* embryos (Figure 16), however, not to zero, which would reflect a complete degradation of this subunit. This result indicates the presence of a stabilised intracellular receptor pool. In the absence of an essential subunit, *Drosophila* glutamate receptors are trafficked incompletely and remain in an intracellular compartment, unable to continue to the synapse, since the essential subunit mediating the interaction, which is required for further processing, is missing.

Several crucial steps during the formation, proper surface trafficking and synaptic insertion of glutamate receptors have been identified. An early regulatory step in receptor trafficking regards the ER exit of the glutamate receptor. Short specific motifs, mostly located at the C-terminal part of the subunit, were shown to determine, whether a subunit is transported to the trans Golgi network (TGN) or whether it is ER retained (Ellgaard and Helenius, 2003). Subunits GluRIID, GluRIIE and GluRIIF all hold a potential RXR retention motif in their C-terminal

tail, where X represents any non-acidic amino acid. The RXR motif was first described in the C-terminal domain of subunits of the ATP-sensitive potassium channel and the $GABA_B$ receptor (Ma and Jan, 2002). Vertebrate glutamate receptor subunits NR2 and KA2, which both carry an ER retention signal, failed to exit the ER in the absence of another receptor subunit (Fukaya et al., 2003; Ren et al., 2003c). Through interaction with another receptor subunit, which did not possess a retention signal, NR2 and KA2 were further processed in heteromeric receptors. Besides retention signals, so-called ER export signals have been characterised, which enhance the rate of a protein's ER exit. The DXE motif was among others identified in the Kir2.1 potassium channel (Ma et al., 2001). A DXE motif is present at the C-terminal tail of GluRIID. Thus, GluRIID exhibits both a putative ER retention as well as a potential ER export motif. Actually, the introduction of the DXE signal into the α subunit of the T cell receptor, which itself harbours a retention signal, failed to mediate ER exit. Thus GluRIID most likely mediates an enhanced ER export rate in heteromeric receptor complexes, in which its retention signal is silenced through subunit interaction.

Proper protein folding is mediated by a subset of chaperones including BiP, calnexin and calreticulin. Correctly folded proteins are exported to the Golgi complex for further processing, while incorrectly folded proteins are targeted to the ER-associated degradation (ERAD). The promotion of glycoproteins was shown to be mediated by the lectins calreticulin and calnexin and regulated through glucosylation (Ellgaard and Helenius, 2003). In vertebrates the absence of stargazin was displayed to increase the BiP concentration in the ER, suggesting a chaperone like role for stargazin concerning AMPA receptors (Vandenberghe et al., 2005b). This finding is consistent with the identification of proteins, which alongside BiP, calnexin and calreticulin are required for the ER processing of secretory proteins. The proteins found were categorised into three groups. "Outfitters" are required for the folding and assembly of proteins, "escorts" accompany proteins out of the ER and "guides" are involved in the intracellular protein transport (Herrmann et al., 1999). Proteins destined for ER

export were shown to be packed into vesicles coated with the coatomer protein COPII and transported to the trans Golgi network (Ellgaard and Helenius, 2003). Since ER exit does not simply rely on the correct folding of a protein but on intramolecular signals and the interaction with other proteins, it is likely that one or several GluRII subunits serve as “outfitters”, “escorts” and “guides” for their receptor complex. The presence of a potential ER retention signal in GluRIID, GluRIIE and GluRIIF indicates a required interaction with subunits GluRIIA, GluRIIB or GluRIIC. The latter subunits may serve as “outfitter” and “escort”. The DXE motif in GluRIID suggests a “guide” role in glutamate receptor trafficking.

Receptor proteins are further processed in the TGN and targeted to the plasma membrane into PSDs. Furthermore, receptors at the plasma membrane can be internalised and through cycling processes between plasma membrane and endosomal compartiments either reinserted into the plasma membrane or targeted to lysosomal compartments for receptor degradation (Barry and Ziff, 2002). Transport processes to different intracellular compartments were demonstrated to be mediated by transport vesicles. Furthermore, the regulation of those vesicle mediated transport, involving targeting, tethering and fusion of transport vesicles, was shown to be mediated by Rab GTPases (Martinez and Goud, 1998). Members of the Rab family were displayed to be specifically targeted to intracellular vesicles and cell organelles, thus defining the intracellular process they are involved in. For GPCR receptors Rab4 and Rab11 were shown to mainly mediate the transport of internalised receptors from the endosomes back to the plasma membrane, whereas Rab5 was shown to regulate GPCR internalisation from the plasma membrane to the endosomal compartment (Dong et al., 2007). Interestingly, direct interaction between the angiotensin receptor AT1R and Rab5 was identified, indicating a possible control mechanism of receptor trafficking mediated by the physical contact between a receptor component and a Rab GTPase (Seachrist et al., 2002). Glutamate receptor trafficking relies on interaction with Rab proteins, too. Rab8 was shown to regulate synaptic cycling as well as synaptic delivery of AMPA receptor

heteromers GluR2/3 and GluR1/2 (Gerges et al., 2004). Furthermore, Rab11 was displayed to be involved in AMPA receptor cycling between recycling endosomes and the plasma membrane (Park et al., 2004). The abundance of Rab proteins in *Drosophila* was recently shown, when a set of 31 Rab proteins was identified (Zhang et al., 2007). Consequently, GluRII trafficking can be suggested to depend on the contact with Rab proteins through either direct interaction, as was shown for angiotensin receptors (Seachrist et al., 2002), or indirect interaction mediated by proteins binding to GluRII subunits.

To sum it up, three essential glutamate receptor subunits are opposed by a multiple number of proteins involved in the regulation of protein trafficking. Consequently, one possible explanation for the requirement of three essential subunits at the *Drosophila* NMJ is, that specific interactions between these receptor subunits and regulatory proteins like ER chaperones or Rab GTPases are essential at different steps of receptor complex trafficking and cycling.

5 Supplementary

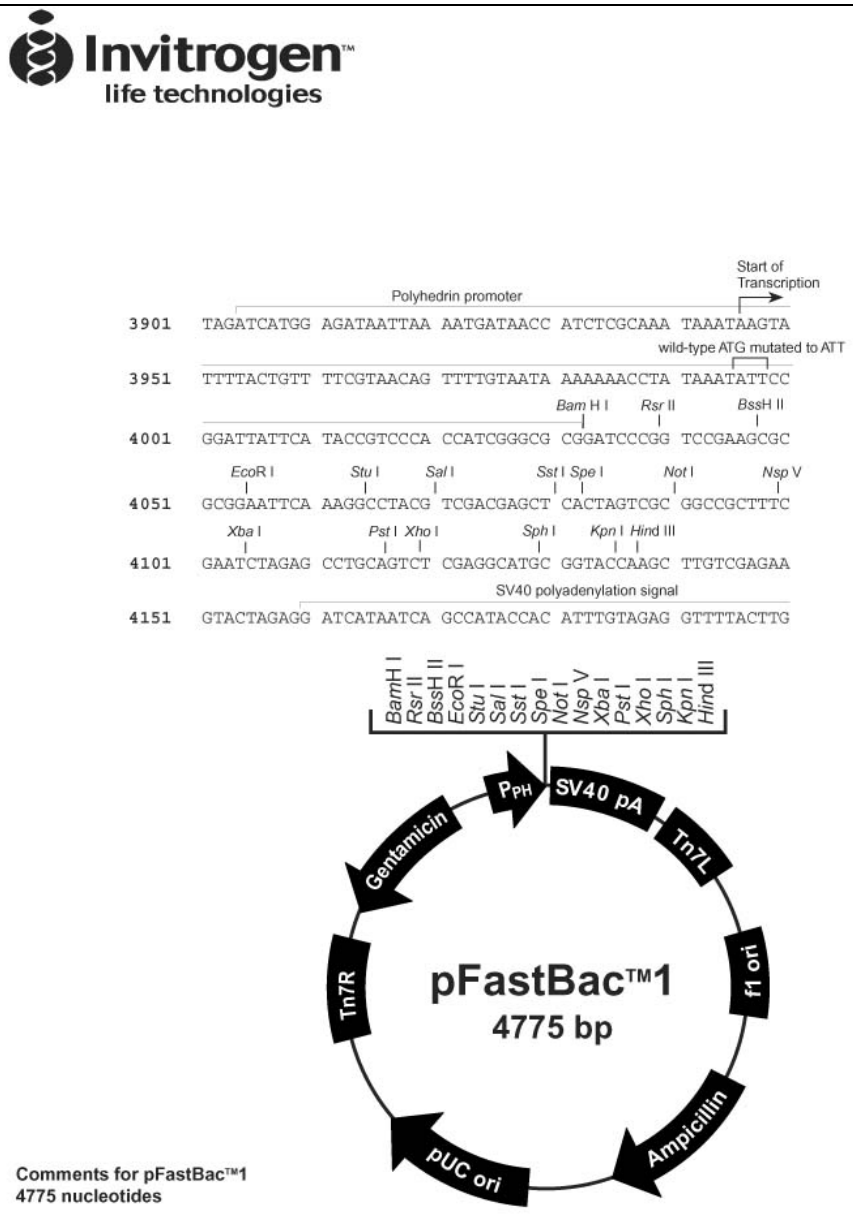

Figure 31 pFastbac1 (Invitrogen, Karlsruhe, Germany)

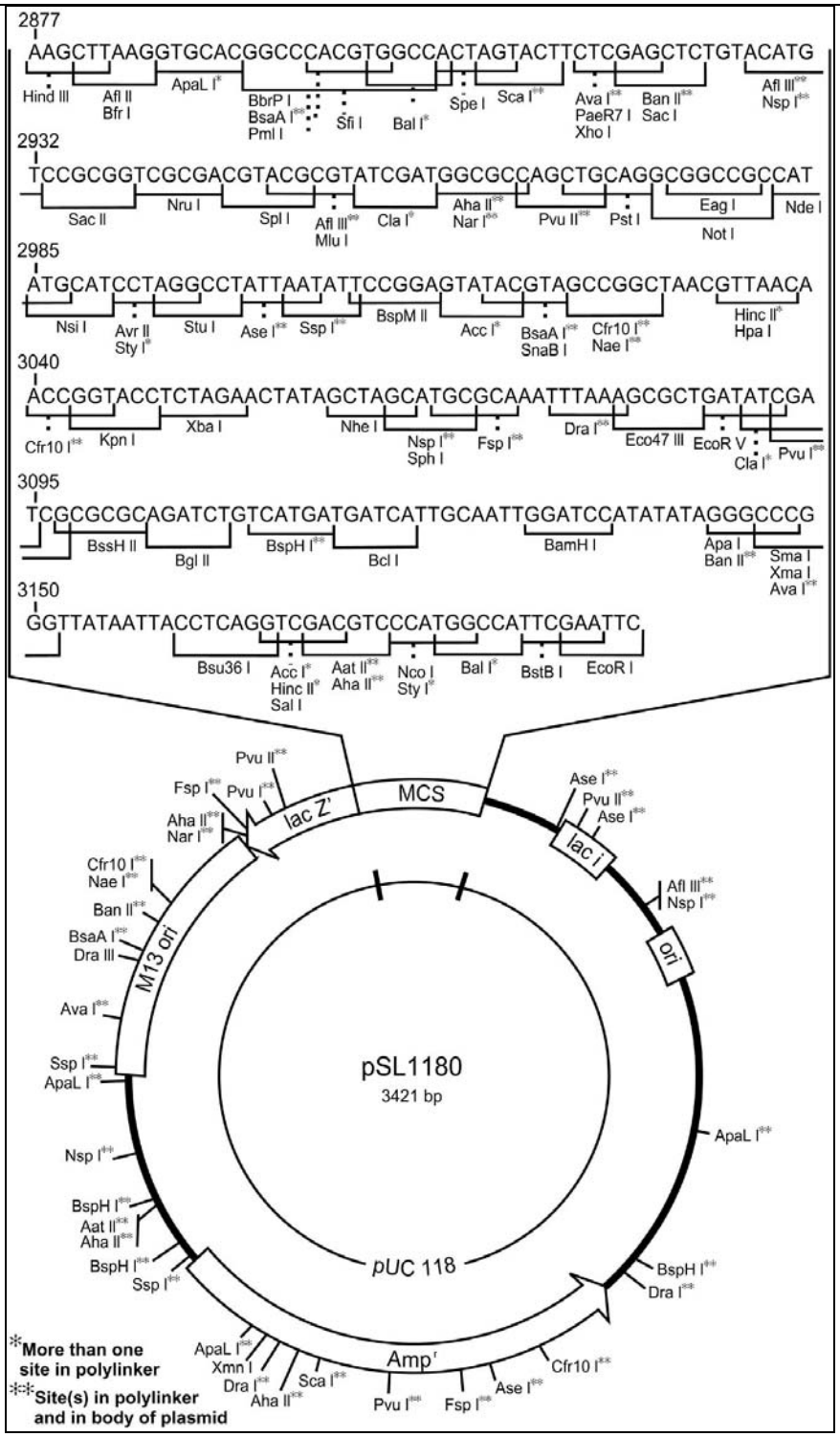

Figure 32 pSL1180 (Amersham Pharmacia Biotech, Buckinghamshire, England)

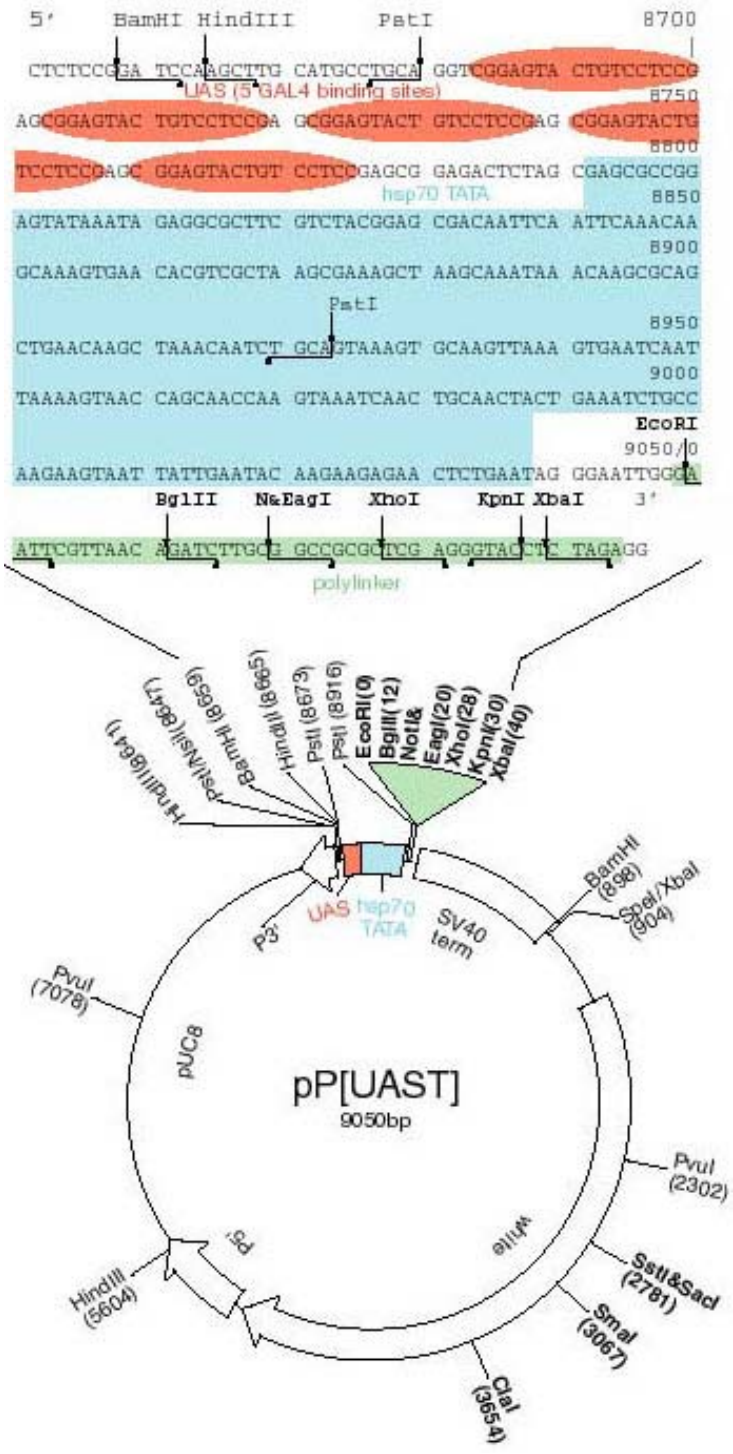

Figure 33 pUAST (adapted from (Brand and Perrimon, 1993))

pUAST XL+:

pUAST XL+ is a modified version of the pUAST vector.

Multiple cloning site:

5’ GAATTCGTTTAAACTAGTGGCCGGCCTTAATTAAGGCGCGCCATTTAA

ATGAATTCGTTAACGATCTGCGGCCGCGGCTCGAGGGTACCTCTAGA 3’

Bac-toBac® Expression System

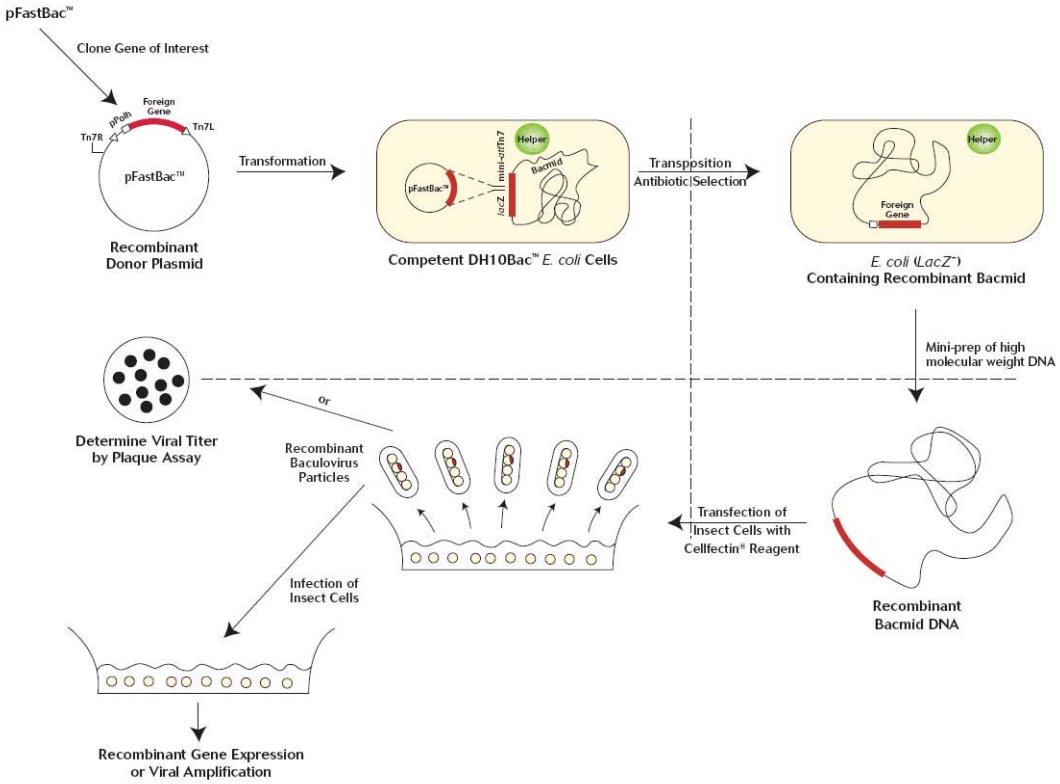

Figure 34 Generation of recombinant baculovirus and gene expression with the Bac-toBac® Expression System (taken from the Bac-toBac® Expression System brochure (Invitrogen, Karlsruhe, Germany)

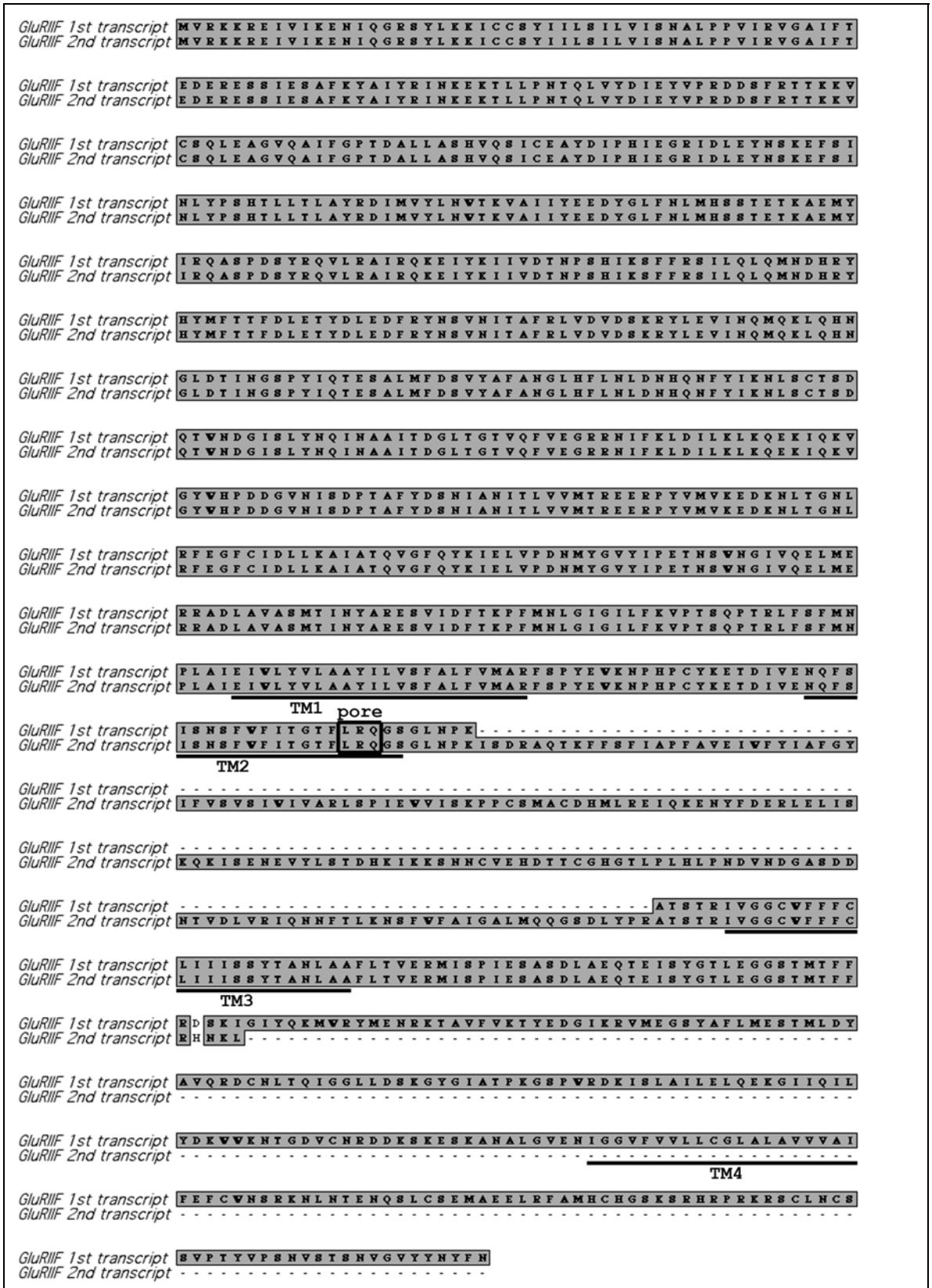

Figure 35 GluRIIF transcript amino acid sequence alignment

6 Abbrevations

AA	amino acid
AB	antibody
AEL	after egg laying
ABP	AMPA receptor binding protein
AChE	acetylcholinesterase
AChR	acetylcholine receptor
AEL	after egg laying
AMPA	alpha-amino-3-hydroxy-5-methyl-4-isoxazole-propionic acid
bp	base pairs
BRP	Bruchpilot protein
CAM	cell adhesion molecule
CaMKII	calmodulin-dependent kinase II
CAZ	cytomatrix at the active zone
CNS	central nervous system
Con-A	concanavalin-A
CTD	C-terminal domain
Dlg	Discs large
eEJC	evoked excitatory junctional current
EGFP	enhanced green fluorescent protein
EMS	ethyl methanesulfonate
EPP	endplate potential
EphR	ephrin receptor
ER	endoplasmatic reticulum
ERAD	ER-associated degradation
FasII	FasciclinII
FCS	foetal calf serum
FRAP	fluorescence recovery after photobleaching
GABA	γ-aminobutyric acid
GAL4	galactosidase 4 protein

GFP	green fluorescent protein
GKAP	guanylate kinase-associated protein
GluR	glutamate receptor
GRIP	glutamate receptor interacting protein
HRP	horse radish peroxidase
IP	immunoprecipitation
iGluR	ionotropic glutamate receptor
kDa	Kilodalton
LIVBP	leucine-isoleucine-valine-binding protein
LTD	long-term depression
LTP	long-term potentiation
MAGUK	membrane-associated guanylate kinase
mEJC	miniature excitatory junctional current
mGluR	metabotropic glutamate receptor
Mhc	myosin heavy chain
MuSK	muscle-specific kinase
NCAM	neural cell adhesion molecule
NFR	normal frog ringer
NGS	natural goat serum
nPIST	neuronal isoform of protein-interacting specificially with TC10
NSF	N-ethylmaleimide-sensitive factor
NMDA	*N*-methyl-D-aspartate
NMJ	neuromuscular junction
PAGE	polyacrylamide gele electrophoresis
PAK	p21-activated kinase
PBS	phosphate-buffered saline
PFA	paraformaldehyde
PICK1	protein interacting with C-kinase 1
PIX	PAK-interacting exchange factor
PKA	protein kinase A
PKC	protein kinase C

PMP	peripheral myelin protein
PS	penicillin/streptomycin
PSD	postsynaptic density
PSD-95	postsynaptic density protein 95
PTV	piccolo/bassoon transport vesicle
RNAi	RNA interference
SAP97	synapse-associated protein 97
SER	smooth endoplasmic reticulum
SNAP	soluble *N*-ethylmaleimide-sensitive factor attachment protein
SNARE	SNAP receptor
SOL-1	suppressor of lurcher
SSR	subsynaptic reticulum
TARP	transmembrane AMPA receptor regulatory protein
tbp-1	TaT binding protein-1
TEVC	two-electrode voltage clamp
TGN	trans Golgi network
TM	transmembrane domain
UAS	upstream activating sequence
UTR	untranslated region
V_{cmd}	command potential
VDCC	voltage-dependent calcium channel
V_m	membrane potential
WB	western blot
wt	wild type

7 Table of figures

8 References

Adams MD, Celniker SE, Holt RA, Evans CA, Gocayne JD, Amanatides PG, Scherer SE, Li PW, Hoskins RA, Galle RF, George RA, Lewis SE, Richards S, Ashburner M, Henderson SN, Sutton GG, Wortman JR, Yandell MD, Zhang Q, Chen LX, Brandon RC, Rogers YH, Blazej RG, Champe M, Pfeiffer BD, Wan KH, Doyle C, Baxter EG, Helt G, Nelson CR, Gabor GL, Abril JF, Agbayani A, An HJ, Andrews-Pfannkoch C, Baldwin D, Ballew RM, Basu A, Baxendale J, Bayraktaroglu L, Beasley EM, Beeson KY, Benos PV, Berman BP, Bhandari D, Bolshakov S, Borkova D, Botchan MR, Bouck J, Brokstein P, Brottier P, Burtis KC, Busam DA, Butler H, Cadieu E, Center A, Chandra I, Cherry JM, Cawley S, Dahlke C, Davenport LB, Davies P, de Pablos B, Delcher A, Deng Z, Mays AD, Dew I, Dietz SM, Dodson K, Doup LE, Downes M, Dugan-Rocha S, Dunkov BC, Dunn P, Durbin KJ, Evangelista CC, Ferraz C, Ferriera S, Fleischmann W, Fosler C, Gabrielian AE, Garg NS, Gelbart WM, Glasser K, Glodek A, Gong F, Gorrell JH, Gu Z, Guan P, Harris M, Harris NL, Harvey D, Heiman TJ, Hernandez JR, Houck J, Hostin D, Houston KA, Howland TJ, Wei MH, Ibegwam C, et al. (2000) The genome sequence of Drosophila melanogaster. Science 287:2185-2195.

Ahmari SE, Buchanan J, Smith SJ (2000) Assembly of presynaptic active zones from cytoplasmic transport packets. Nat Neurosci 3:445-451.

Albin SD, Davis GW (2004) Coordinating structural and functional synapse development: postsynaptic p21-activated kinase independently specifies glutamate receptor abundance and postsynaptic morphology. J Neurosci 24:6871-6879.

Anderson D, Harris R, Polayes D, Ciccarone V, Donahue R, Gerard G, Jessee J (1996) Rapid Generation of Recombinant Baculoviruses and Expression of Foreign Genes Using the Bac-To-Bac® Baculovirus Expression System. Focus 17:53-58.

Apel ED, Glass DJ, Moscoso LM, Yancopoulos GD, Sanes JR (1997) Rapsyn is required for MuSK signaling and recruits synaptic components to a MuSK-containing scaffold. Neuron 18:623-635.

Armstrong N, Sun Y, Chen GQ, Gouaux E (1998) Structure of a glutamate-receptor ligand-binding core in complex with kainate. Nature 395:913-917.

Ataman B, Ashley J, Gorczyca D, Gorczyca M, Mathew D, Wichmann C, Sigrist SJ, Budnik V (2006) Nuclear trafficking of Drosophila Frizzled-2 during synapse development requires the PDZ protein dGRIP. Proc Natl Acad Sci U S A 103:7841-7846.

Atwood HL, Govind CK, Wu CF (1993) Differential ultrastructure of synaptic terminals on ventral longitudinal abdominal muscles in Drosophila larvae. J Neurobiol 24:1008-1024.

Ayalon G, Stern-Bach Y (2001) Functional assembly of AMPA and kainate receptors is mediated by several discrete protein-protein interactions. Neuron 31:103-113.

Barbon A, Vallini I, Barlati S (2001) Genomic organization of the human GRIK2 gene and evidence for multiple splicing variants. Gene 274:187-197.
Barnard EA, Bilbe G, Houamed K, Moss SJ, Van Renterghem C, Smart TG (1987) Functional expression in the Xenopus oocyte of messenger ribonucleic acids encoding brain neurotransmitter receptors: further characterisation of the implanted GABA receptor. Neuropharmacology 26:837-844.
Barry MF, Ziff EB (2002) Receptor trafficking and the plasticity of excitatory synapses. Curr Opin Neurobiol 12:279-286.
Bate M, Landgraf M, Ruiz Gomez Bate M (1999) Development of larval body wall muscles. Int Rev Neurobiol 43:25-44.
Beattie EC, Carroll RC, Yu X, Morishita W, Yasuda H, von Zastrow M, Malenka RC (2000) Regulation of AMPA receptor endocytosis by a signaling mechanism shared with LTD. Nat Neurosci 3:1291-1300.
Bedoukian MA, Weeks AM, Partin KM (2006) Different domains of the AMPA receptor direct stargazin-mediated trafficking and stargazin-mediated modulation of kinetics. J Biol Chem 281:23908-23921.
Bellen HJ, Levis RW, Liao G, He Y, Carlson JW, Tsang G, Evans-Holm M, Hiesinger PR, Schulze KL, Rubin GM, Hoskins RA, Spradling AC (2004) The BDGP gene disruption project: single transposon insertions associated with 40% of Drosophila genes. Genetics 167:761-781.
Bettler B, Boulter J, Hermans-Borgmeyer I, O'Shea-Greenfield A, Deneris ES, Moll C, Borgmeyer U, Hollmann M, Heinemann S (1990) Cloning of a novel glutamate receptor subunit, GluR5: expression in the nervous system during development. Neuron 5:583-595.
Blackstone CD, Moss SJ, Martin LJ, Levey AI, Price DL, Huganir RL (1992) Biochemical characterization and localization of a non-N-methyl-D-aspartate glutamate receptor in rat brain. J Neurochem 58:1118-1126.
Borgdorff AJ, Choquet D (2002) Regulation of AMPA receptor lateral movements. Nature 417:649-653.
Boulianne GL, Trimble WS (1995) Identification of a second homolog of N-ethylmaleimide-sensitive fusion protein that is expressed in the nervous system and secretory tissues of Drosophila. Proc Natl Acad Sci U S A 92:7095-7099.
Boulter J, Hollmann M, O'Shea-Greenfield A, Hartley M, Deneris E, Maron C, Heinemann S (1990) Molecular cloning and functional expression of glutamate receptor subunit genes. Science 249:1033-1037.
Brand AH, Perrimon N (1993) Targeted gene expression as a means of altering cell fates and generating dominant phenotypes. Development 118:401-415.
Broadie K, Bate M (1993a) Innervation directs receptor synthesis and localization in Drosophila embryo synaptogenesis. Nature 361:350-353.
Broadie K, Sink H, Van Vactor D, Fambrough D, Whitington PM, Bate M, Goodman CS (1993) From growth cone to synapse: the life history of the RP3 motor neuron. Dev Suppl:227-238.
Broadie KS, Bate M (1993b) Development of the embryonic neuromuscular

synapse of Drosophila melanogaster. J Neurosci 13:144-166.
Broadie KS, Bate M (1993c) Development of larval muscle properties in the embryonic myotubes of Drosophila melanogaster. J Neurosci 13:167-180.
Brose N, Gasic GP, Vetter DE, Sullivan JM, Heinemann SF (1993) Protein chemical characterization and immunocytochemical localization of the NMDA receptor subunit NMDA R1. J Biol Chem 268:22663-22671.
Burette A, Khatri L, Wyszynski M, Sheng M, Ziff EB, Weinberg RJ (2001) Differential cellular and subcellular localization of ampa receptor-binding protein and glutamate receptor-interacting protein. J Neurosci 21:495-503.
Burgess DL, Gefrides LA, Foreman PJ, Noebels JL (2001) A cluster of three novel Ca2+ channel gamma subunit genes on chromosome 19q13.4: evolution and expression profile of the gamma subunit gene family. Genomics 71:339-350.
Burnashev N, Villarroel A, Sakmann B (1996) Dimensions and ion selectivity of recombinant AMPA and kainate receptor channels and their dependence on Q/R site residues. J Physiol 496 (Pt 1):165-173.
Capani F, Martone ME, Deerinck TJ, Ellisman MH (2001) Selective localization of high concentrations of F-actin in subpopulations of dendritic spines in rat central nervous system: a three-dimensional electron microscopic study. J Comp Neurol 435:156-170.
Carroll RC, Beattie EC, Xia H, Luscher C, Altschuler Y, Nicoll RA, Malenka RC, von Zastrow M (1999) Dynamin-dependent endocytosis of ionotropic glutamate receptors. Proc Natl Acad Sci U S A 96:14112-14117.
Castiglioni MC (1951) [Distribution of pigments in the eye of alleles of white and their compounds in Drosophila melanogaster.]. Sci Genet 4:57-60.
Chang Y, Wang R, Barot S, Weiss DS (1996) Stoichiometry of a recombinant GABAA receptor. J Neurosci 16:5415-5424.
Chen BE, Lendvai B, Nimchinsky EA, Burbach B, Fox K, Svoboda K (2000a) Imaging high-resolution structure of GFP-expressing neurons in neocortex in vivo. Learn Mem 7:433-441.
Chen K, Featherstone DE (2005) Discs-large (DLG) is clustered by presynaptic innervation and regulates postsynaptic glutamate receptor subunit composition in Drosophila. BMC Biol 3:1.
Chen K, Merino C, Sigrist SJ, Featherstone DE (2005) The 4.1 protein coracle mediates subunit-selective anchoring of Drosophila glutamate receptors to the postsynaptic actin cytoskeleton. J Neurosci 25:6667-6675.
Chen L, Bao S, Qiao X, Thompson RF (1999) Impaired cerebellar synapse maturation in waggler, a mutant mouse with a disrupted neuronal calcium channel gamma subunit. Proc Natl Acad Sci U S A 96:12132-12137.
Chen L, Chetkovich DM, Petralia RS, Sweeney NT, Kawasaki Y, Wenthold RJ, Bredt DS, Nicoll RA (2000b) Stargazin regulates synaptic targeting of AMPA receptors by two distinct mechanisms. Nature 408:936-943.
Chen PS, Kubli E, Hanimann F (1968) [Separation of the free ninhydrin-positive substances in Phormia and Drosophila, using two-dimensional high-voltage electrophoresis]. Rev Suisse Zool 75:509-523.
Cho KO, Hunt CA, Kennedy MB (1992) The rat brain postsynaptic density

fraction contains a homolog of the Drosophila discs-large tumor suppressor protein. Neuron 9:929-942.
Chu PJ, Robertson HM, Best PM (2001) Calcium channel gamma subunits provide insights into the evolution of this gene family. Gene 280:37-48.
Chung HJ, Steinberg JP, Huganir RL, Linden DJ (2003) Requirement of AMPA receptor GluR2 phosphorylation for cerebellar long-term depression. Science 300:1751-1755.
Chung HJ, Xia J, Scannevin RH, Zhang X, Huganir RL (2000) Phosphorylation of the AMPA receptor subunit GluR2 differentially regulates its interaction with PDZ domain-containing proteins. J Neurosci 20:7258-7267.
Ciabarra AM, Sullivan JM, Gahn LG, Pecht G, Heinemann S, Sevarino KA (1995) Cloning and characterization of chi-1: a developmentally regulated member of a novel class of the ionotropic glutamate receptor family. J Neurosci 15:6498-6508.
Coleman A (1984) Translation of eucaryotic messenger RNA in Xenopus oocytes. Transcription and translation: a practical approach, IRL Press, Washington, D C, USA:271–301.
Coleman SK, Cai C, Mottershead DG, Haapalahti JP, Keinanen K (2003) Surface expression of GluR-D AMPA receptor is dependent on an interaction between its C-terminal domain and a 4.1 protein. J Neurosci 23:798-806.
Colledge M, Dean RA, Scott GK, Langeberg LK, Huganir RL, Scott JD (2000) Targeting of PKA to glutamate receptors through a MAGUK-AKAP complex. Neuron 27:107-119.
Collins MO, Husi H, Yu L, Brandon JM, Anderson CN, Blackstock WP, Choudhary JS, Grant SG (2006) Molecular characterization and comparison of the components and multiprotein complexes in the postsynaptic proteome. J Neurochem 97 Suppl 1:16-23.
Colotta F, Re F, Muzio M, Bertini R, Polentarutti N, Sironi M, Giri JG, Dower SK, Sims JE, Mantovani A (1993) Interleukin-1 type II receptor: a decoy target for IL-1 that is regulated by IL-4. Science 261:472-475.
Cuadra AE, Kuo SH, Kawasaki Y, Bredt DS, Chetkovich DM (2004) AMPA receptor synaptic targeting regulated by stargazin interactions with the Golgi-resident PDZ protein nPIST. J Neurosci 24:7491-7502.
Dascal N (1987) The use of Xenopus oocytes for the study of ion channels. CRC Crit Rev Biochem 22:317-387.
Davis GW, DiAntonio A, Petersen SA, Goodman CS (1998) Postsynaptic PKA controls quantal size and reveals a retrograde signal that regulates presynaptic transmitter release in Drosophila. Neuron 20:305-315.
Daw MI, Chittajallu R, Bortolotto ZA, Dev KK, Duprat F, Henley JM, Collingridge GL, Isaac JT (2000) PDZ proteins interacting with C-terminal GluR2/3 are involved in a PKC-dependent regulation of AMPA receptors at hippocampal synapses. Neuron 28:873-886.
Dean C, Dresbach T (2006) Neuroligins and neurexins: linking cell adhesion, synapse formation and cognitive function. Trends Neurosci 29:21-29.
DiAntonio A, Petersen SA, Heckmann M, Goodman CS (1999) Glutamate receptor expression regulates quantal size and quantal content at the

Drosophila neuromuscular junction. J Neurosci 19:3023-3032.
Dingledine R, Borges K, Bowie D, Traynelis SF (1999) The glutamate receptor ion channels. Pharmacol Rev 51:7-61.
Dong C, Filipeanu CM, Duvernay MT, Wu G (2007) Regulation of G protein-coupled receptor export trafficking. Biochim Biophys Acta 1768:853-870.
Dong H, O'Brien RJ, Fung ET, Lanahan AA, Worley PF, Huganir RL (1997) GRIP: a synaptic PDZ domain-containing protein that interacts with AMPA receptors. Nature 386:279-284.
Dong H, Zhang P, Song I, Petralia RS, Liao D, Huganir RL (1999) Characterization of the glutamate receptor-interacting proteins GRIP1 and GRIP2. J Neurosci 19:6930-6941.
Doyle DA, Morais Cabral J, Pfuetzner RA, Kuo A, Gulbis JM, Cohen SL, Chait BT, MacKinnon R (1998) The structure of the potassium channel: molecular basis of K+ conduction and selectivity. Science 280:69-77.
Dunaevsky A, Mason CA (2003) Spine motility: a means towards an end? Trends Neurosci 26:155-160.
Egebjerg J, Bettler B, Hermans-Borgmeyer I, Heinemann S (1991) Cloning of a cDNA for a glutamate receptor subunit activated by kainate but not AMPA. Nature 351:745-748.
Ehlers MD (2000) Reinsertion or degradation of AMPA receptors determined by activity-dependent endocytic sorting. Neuron 28:511-525.
Eissenberg JC, Morris GD, Reuter G, Hartnett T (1992) The heterochromatin-associated protein HP-1 is an essential protein in Drosophila with dosage-dependent effects on position-effect variegation. Genetics 131:345-352.
El-Husseini Ael D, Schnell E, Dakoji S, Sweeney N, Zhou Q, Prange O, Gauthier-Campbell C, Aguilera-Moreno A, Nicoll RA, Bredt DS (2002) Synaptic strength regulated by palmitate cycling on PSD-95. Cell 108:849-863.
Ellgaard L, Helenius A (2003) Quality control in the endoplasmic reticulum. Nat Rev Mol Cell Biol 4:181-191.
Featherstone DE, Rushton E, Broadie K (2002) Developmental regulation of glutamate receptor field size by nonvesicular glutamate release. Nat Neurosci 5:141-146.
Featherstone DE, Rushton E, Rohrbough J, Liebl F, Karr J, Sheng Q, Rodesch CK, Broadie K (2005) An essential Drosophila glutamate receptor subunit that functions in both central neuropil and neuromuscular junction. J Neurosci 25:3199-3208.
Ferrer-Montiel AV, Montal M (1996) Pentameric subunit stoichiometry of a neuronal glutamate receptor. Proc Natl Acad Sci U S A 93:2741-2744.
Fifkova E, Delay RJ (1982) Cytoplasmic actin in neuronal processes as a possible mediator of synaptic plasticity. J Cell Biol 95:345-350.
Fire A, Xu S, Montgomery MK, Kostas SA, Driver SE, Mello CC (1998) Potent and specific genetic interference by double-stranded RNA in Caenorhabditis elegans. Nature 391:806-811.
Fischer M, Kaech S, Wagner U, Brinkhaus H, Matus A (2000) Glutamate receptors regulate actin-based plasticity in dendritic spines. Nat Neurosci 3:887-894.

Fraser AG, Kamath RS, Zipperlen P, Martinez-Campos M, Sohrmann M, Ahringer J (2000) Functional genomic analysis of C. elegans chromosome I by systematic RNA interference. Nature 408:325-330.

Fukata Y, Tzingounis AV, Trinidad JC, Fukata M, Burlingame AL, Nicoll RA, Bredt DS (2005) Molecular constituents of neuronal AMPA receptors. J Cell Biol 169:399-404.

Fukaya M, Kato A, Lovett C, Tonegawa S, Watanabe M (2003) Retention of NMDA receptor NR2 subunits in the lumen of endoplasmic reticulum in targeted NR1 knockout mice. Proc Natl Acad Sci U S A 100:4855-4860.

Garcia EP, Mehta S, Blair LA, Wells DG, Shang J, Fukushima T, Fallon JR, Garner CC, Marshall J (1998) SAP90 binds and clusters kainate receptors causing incomplete desensitization. Neuron 21:727-739.

Gautam M, Noakes PG, Mudd J, Nichol M, Chu GC, Sanes JR, Merlie JP (1995) Failure of postsynaptic specialization to develop at neuromuscular junctions of rapsyn-deficient mice. Nature 377:232-236.

Gerges NZ, Backos DS, Esteban JA (2004) Local control of AMPA receptor trafficking at the postsynaptic terminal by a small GTPase of the Rab family. J Biol Chem 279:43870-43878.

Gloor GB, Preston CR, Johnson-Schlitz DM, Nassif NA, Phillis RW, Benz WK, Robertson HM, Engels WR (1993) Type I repressors of P element mobility. Genetics 135:81-95.

Goldin AL (1991) Expression of ion channels by injection of mRNA into Xenopus oocytes. Methods Cell Biol 36:487-509.

Gonczy P, Echeverri C, Oegema K, Coulson A, Jones SJ, Copley RR, Duperon J, Oegema J, Brehm M, Cassin E, Hannak E, Kirkham M, Pichler S, Flohrs K, Goessen A, Leidel S, Alleaume AM, Martin C, Ozlu N, Bork P, Hyman AA (2000) Functional genomic analysis of cell division in C. elegans using RNAi of genes on chromosome III. Nature 408:331-336.

Gorczyca M, Augart C, Budnik V (1993) Insulin-like receptor and insulin-like peptide are localized at neuromuscular junctions in Drosophila. J Neurosci 13:3692-3704.

Gramates LS, Budnik V (1999) Assembly and maturation of the Drosophila larval neuromuscular junction. Int Rev Neurobiol 43:93-117.

Gray EG (1959) Electron microscopy of synaptic contacts on dendrite spines of the cerebral cortex. Nature 183:1592-1593.

Gray EG (1963) Electron microscopy of presynaptic organelles of the spinal cord. J Anat 97:101-106.

Greger IH, Khatri L, Ziff EB (2002) RNA editing at arg607 controls AMPA receptor exit from the endoplasmic reticulum. Neuron 34:759-772.

Greger IH, Khatri L, Kong X, Ziff EB (2003) AMPA receptor tetramerization is mediated by Q/R editing. Neuron 40:763-774.

Gregor P, O'Hara BF, Yang X, Uhl GR (1993) Expression and novel subunit isoforms of glutamate receptor genes GluR5 and GluR6. Neuroreport 4:1343-1346.

Guan Z, Saraswati S, Adolfsen B, Littleton JT (2005) Genome-wide transcriptional changes associated with enhanced activity in the

Drosophila nervous system. Neuron 48:91-107.
Gundersen CB, Miledi R, Parker I (1983) Voltage-operated channels induced by foreign messenger RNA in Xenopus oocytes. Proc R Soc Lond B Biol Sci 220:131-140.
Gurdon JB, Lane CD, Woodland HR, Marbaix G (1971) Use of frog eggs and oocytes for the study of messenger RNA and its translation in living cells. Nature 233:177-182.
Haghighi AP, McCabe BD, Fetter RD, Palmer JE, Hom S, Goodman CS (2003) Retrograde control of synaptic transmission by postsynaptic CaMKII at the Drosophila neuromuscular junction. Neuron 39:255-267.
Hanley JG, Khatri L, Hanson PI, Ziff EB (2002) NSF ATPase and alpha-/beta-SNAPs disassemble the AMPA receptor-PICK1 complex. Neuron 34:53-67.
Hashimoto K, Fukaya M, Qiao X, Sakimura K, Watanabe M, Kano M (1999) Impairment of AMPA receptor function in cerebellar granule cells of ataxic mutant mouse stargazer. J Neurosci 19:6027-6036.
Hayashi Y, Shi SH, Esteban JA, Piccini A, Poncer JC, Malinow R (2000) Driving AMPA receptors into synapses by LTP and CaMKII: requirement for GluR1 and PDZ domain interaction. Science 287:2262-2267.
Heimbeck G, Bugnon V, Gendre N, Haberlin C, Stocker RF (1999) Smell and taste perception in Drosophila melanogaster larva: toxin expression studies in chemosensory neurons. J Neurosci 19:6599-6609.
Henley JM (2003) Proteins interactions implicated in AMPA receptor trafficking: a clear destination and an improving route map. Neurosci Res 45:243-254.
Hermans E, Challiss RA (2001) Structural, signalling and regulatory properties of the group I metabotropic glutamate receptors: prototypic family C G-protein-coupled receptors. Biochem J 359:465-484.
Herrmann JM, Malkus P, Schekman R (1999) Out of the ER--outfitters, escorts and guides. Trends Cell Biol 9:5-7.
Hirbec H, Francis JC, Lauri SE, Braithwaite SP, Coussen F, Mulle C, Dev KK, Coutinho V, Meyer G, Isaac JT, Collingridge GL, Henley JM (2003) Rapid and differential regulation of AMPA and kainate receptors at hippocampal mossy fibre synapses by PICK1 and GRIP. Neuron 37:625-638.
Hollmann M, Heinemann S (1994) Cloned glutamate receptors. Annu Rev Neurosci 17:31-108.
Hughes BW, Kusner LL, Kaminski HJ (2006) Molecular architecture of the neuromuscular junction. Muscle Nerve 33:445-461.
Hughes TE (1994) Transmembrane topology of the glutamate receptors. A tale of novel twists and turns. J Mol Neurosci 5:211-217.
Hume RI, Dingledine R, Heinemann SF (1991) Identification of a site in glutamate receptor subunits that controls calcium permeability. Science 253:1028-1031.
Hung AY, Sheng M (2002) PDZ domains: structural modules for protein complex assembly. J Biol Chem 277:5699-5702.
Ishii T, Moriyoshi K, Sugihara H, Sakurada K, Kadotani H, Yokoi M, Akazawa C, Shigemoto R, Mizuno N, Masu M, et al. (1993) Molecular characterization

of the family of the N-methyl-D-aspartate receptor subunits. J Biol Chem 268:2836-2843.
Jahn R, Sudhof TC (1999) Membrane fusion and exocytosis. Annu Rev Biochem 68:863-911.
Jan LY, Jan YN (1976) L-glutamate as an excitatory transmitter at the Drosophila larval neuromuscular junction. J Physiol 262:215-236.
Jaskolski F, Normand E, Mulle C, Coussen F (2005) Differential trafficking of GluR7 kainate receptor subunit splice variants. J Biol Chem 280:22968-22976.
Jaskolski F, Coussen F, Nagarajan N, Normand E, Rosenmund C, Mulle C (2004) Subunit composition and alternative splicing regulate membrane delivery of kainate receptors. J Neurosci 24:2506-2515.
Johansen J, Halpern ME, Johansen KM, Keshishian H (1989) Stereotypic morphology of glutamatergic synapses on identified muscle cells of Drosophila larvae. J Neurosci 9:710-725.
Johansson AM, Stenberg P, Bernhardsson C, Larsson J (2007) Painting of fourth and chromosome-wide regulation of the 4th chromosome in Drosophila melanogaster. Embo J 26:2307-2316.
Johnson JW, Ascher P (1987) Glycine potentiates the NMDA response in cultured mouse brain neurons. Nature 325:529-531.
Jones KA, Borowsky B, Tamm JA, Craig DA, Durkin MM, Dai M, Yao WJ, Johnson M, Gunwaldsen C, Huang LY, Tang C, Shen Q, Salon JA, Morse K, Laz T, Smith KE, Nagarathnam D, Noble SA, Branchek TA, Gerald C (1998) GABA(B) receptors function as a heteromeric assembly of the subunits GABA(B)R1 and GABA(B)R2. Nature 396:674-679.
Jontes JD, Smith SJ (2000) Filopodia, spines, and the generation of synaptic diversity. Neuron 27:11-14.
Jordan BA, Devi LA (1999) G-protein-coupled receptor heterodimerization modulates receptor function. Nature 399:697-700.
Karess RE, Rubin GM (1984) Analysis of P transposable element functions in Drosophila. Cell 38:135-146.
Katz B, Miledi R (1968) The role of calcium in neuromuscular facilitation. J Physiol 195:481-492.
Kaupmann K, Malitschek B, Schuler V, Heid J, Froestl W, Beck P, Mosbacher J, Bischoff S, Kulik A, Shigemoto R, Karschin A, Bettler B (1998) GABA(B)-receptor subtypes assemble into functional heteromeric complexes. Nature 396:683-687.
Kennedy MB (2000) Signal-processing machines at the postsynaptic density. Science 290:750-754.
Kim E, Sheng M (2004) PDZ domain proteins of synapses. Nat Rev Neurosci 5:771-781.
Kim E, Niethammer M, Rothschild A, Jan YN, Sheng M (1995a) Clustering of Shaker-type K+ channels by interaction with a family of membrane-associated guanylate kinases. Nature 378:85-88.
Kim S, Ko J, Shin H, Lee JR, Lim C, Han JH, Altrock WD, Garner CC, Gundelfinger ED, Premont RT, Kaang BK, Kim E (2003) The GIT family of

proteins forms multimers and associates with the presynaptic cytomatrix protein Piccolo. J Biol Chem 278:6291-6300.
Kim TW, Wu K, Xu JL, McAuliffe G, Tanzi RE, Wasco W, Black IB (1995b) Selective localization of amyloid precursor-like protein 1 in the cerebral cortex postsynaptic density. Brain Res Mol Brain Res 32:36-44.
Kirov SA, Harris KM (1999) Dendrites are more spiny on mature hippocampal neurons when synapses are inactivated. Nat Neurosci 2:878-883.
Kistner U, Wenzel BM, Veh RW, Cases-Langhoff C, Garner AM, Appeltauer U, Voss B, Gundelfinger ED, Garner CC (1993) SAP90, a rat presynaptic protein related to the product of the Drosophila tumor suppressor gene dlg-A. J Biol Chem 268:4580-4583.
Kittel RJ, Wichmann C, Rasse TM, Fouquet W, Schmidt M, Schmid A, Wagh DA, Pawlu C, Kellner RR, Willig KI, Hell SW, Buchner E, Heckmann M, Sigrist SJ (2006) Bruchpilot promotes active zone assembly, Ca2+ channel clustering, and vesicle release. Science 312:1051-1054.
Klauck TM, Scott JD (1995) The postsynaptic density: a subcellular anchor for signal transduction enzymes. Cell Signal 7:747-757.
Klugbauer N, Dai S, Specht V, Lacinova L, Marais E, Bohn G, Hofmann F (2000) A family of gamma-like calcium channel subunits. FEBS Lett 470:189-197.
Koh YH, Popova E, Thomas U, Griffith LC, Budnik V (1999) Regulation of DLG localization at synapses by CaMKII-dependent phosphorylation. Cell 98:353-363.
Kohda K, Wang Y, Yuzaki M (2000) Mutation of a glutamate receptor motif reveals its role in gating and delta2 receptor channel properties. Nat Neurosci 3:315-322.
Kohler M, Burnashev N, Sakmann B, Seeburg PH (1993) Determinants of Ca2+ permeability in both TM1 and TM2 of high affinity kainate receptor channels: diversity by RNA editing. Neuron 10:491-500.
Kong XC, Barzaghi P, Ruegg MA (2004) Inhibition of synapse assembly in mammalian muscle in vivo by RNA interference. EMBO Rep 5:183-188.
Kornau HC, Schenker LT, Kennedy MB, Seeburg PH (1995) Domain interaction between NMDA receptor subunits and the postsynaptic density protein PSD-95. Science 269:1737-1740.
Krejci E, Thomine S, Boschetti N, Legay C, Sketelj J, Massoulie J (1997) The mammalian gene of acetylcholinesterase-associated collagen. J Biol Chem 272:22840-22847.
Krejci E, Coussen F, Duval N, Chatel JM, Legay C, Puype M, Vandekerckhove J, Cartaud J, Bon S, Massoulie J (1991) Primary structure of a collagenic tail peptide of Torpedo acetylcholinesterase: co-expression with catalytic subunit induces the production of collagen-tailed forms in transfected cells. Embo J 10:1285-1293.
Kuhse J, Laube B, Magalei D, Betz H (1993) Assembly of the inhibitory glycine receptor: identification of amino acid sequence motifs governing subunit stoichiometry. Neuron 11:1049-1056.
Kutsuwada T, Kashiwabuchi N, Mori H, Sakimura K, Kushiya E, Araki K, Meguro H, Masaki H, Kumanishi T, Arakawa M, et al. (1992) Molecular diversity of

the NMDA receptor channel. Nature 358:36-41.
Kuusinen A, Arvola M, Keinanen K (1995) Molecular dissection of the agonist binding site of an AMPA receptor. Embo J 14:6327-6332.
Kuusinen A, Abele R, Madden DR, Keinanen K (1999) Oligomerization and ligand-binding properties of the ectodomain of the alpha-amino-3-hydroxy-5-methyl-4-isoxazole propionic acid receptor subunit GluRD. J Biol Chem 274:28937-28943.
Landgraf M, Thor S (2006) Development of Drosophila motoneurons: specification and morphology. Semin Cell Dev Biol 17:3-11.
Laube B, Kuhse J, Betz H (1998) Evidence for a tetrameric structure of recombinant NMDA receptors. J Neurosci 18:2954-2961.
Lee HK, Barbarosie M, Kameyama K, Bear MF, Huganir RL (2000) Regulation of distinct AMPA receptor phosphorylation sites during bidirectional synaptic plasticity. Nature 405:955-959.
Lee HK, Takamiya K, Han JS, Man H, Kim CH, Rumbaugh G, Yu S, Ding L, He C, Petralia RS, Wenthold RJ, Gallagher M, Huganir RL (2003) Phosphorylation of the AMPA receptor GluR1 subunit is required for synaptic plasticity and retention of spatial memory. Cell 112:631-643.
Lerma J (2006) Kainate receptor physiology. Curr Opin Pharmacol 6:89-97.
Letts VA, Felix R, Biddlecome GH, Arikkath J, Mahaffey CL, Valenzuela A, Bartlett FS, 2nd, Mori Y, Campbell KP, Frankel WN (1998) The mouse stargazer gene encodes a neuronal Ca2+-channel gamma subunit. Nat Genet 19:340-347.
Lin Y, Skeberdis VA, Francesconi A, Bennett MV, Zukin RS (2004) Postsynaptic density protein-95 regulates NMDA channel gating and surface expression. J Neurosci 24:10138-10148.
Lissin DV, Gomperts SN, Carroll RC, Christine CW, Kalman D, Kitamura M, Hardy S, Nicoll RA, Malenka RC, von Zastrow M (1998) Activity differentially regulates the surface expression of synaptic AMPA and NMDA glutamate receptors. Proc Natl Acad Sci U S A 95:7097-7102.
Littleton JT, Ganetzky B (2000) Ion channels and synaptic organization: analysis of the Drosophila genome. Neuron 26:35-43.
Lu W, Man H, Ju W, Trimble WS, MacDonald JF, Wang YT (2001) Activation of synaptic NMDA receptors induces membrane insertion of new AMPA receptors and LTP in cultured hippocampal neurons. Neuron 29:243-254.
Ma D, Jan LY (2002) ER transport signals and trafficking of potassium channels and receptors. Curr Opin Neurobiol 12:287-292.
Ma D, Zerangue N, Lin YF, Collins A, Yu M, Jan YN, Jan LY (2001) Role of ER export signals in controlling surface potassium channel numbers. Science 291:316-319.
Madden DR (2002) The structure and function of glutamate receptor ion channels. Nat Rev Neurosci 3:91-101.
Madhavan R, Zhao XT, Ruegg MA, Peng HB (2005) Tyrosine phosphatase regulation of MuSK-dependent acetylcholine receptor clustering. Mol Cell Neurosci 28:403-416.
Maggio R, Novi F, Scarselli M, Corsini GU (2005) The impact of G-protein-

coupled receptor hetero-oligomerization on function and pharmacology. Febs J 272:2939-2946.
Malenka RC (1994) Synaptic plasticity. Mucking up movements. Nature 372:218-219.
Malenka RC (2003) Synaptic plasticity and AMPA receptor trafficking. Ann N Y Acad Sci 1003:1-11.
Malenka RC, Nicoll RA (1993) NMDA-receptor-dependent synaptic plasticity: multiple forms and mechanisms. Trends Neurosci 16:521-527.
Malinow R, Malenka RC (2002) AMPA receptor trafficking and synaptic plasticity. Annu Rev Neurosci 25:103-126.
Mano I, Teichberg VI (1998) A tetrameric subunit stoichiometry for a glutamate receptor-channel complex. Neuroreport 9:327-331.
Marrus SB, Portman SL, Allen MJ, Moffat KG, DiAntonio A (2004) Differential localization of glutamate receptor subunits at the Drosophila neuromuscular junction. J Neurosci 24:1406-1415.
Martinez O, Goud B (1998) Rab proteins. Biochim Biophys Acta 1404:101-112.
Matus A (2000) Actin-based plasticity in dendritic spines. Science 290:754-758.
Matus A (2005) Growth of dendritic spines: a continuing story. Curr Opin Neurobiol 15:67-72.
Matus A, Ackermann M, Pehling G, Byers HR, Fujiwara K (1982) High actin concentrations in brain dendritic spines and postsynaptic densities. Proc Natl Acad Sci U S A 79:7590-7594.
Mayer ML (2005) Glutamate receptor ion channels. Curr Opin Neurobiol 15:282-288.
Mayer ML, Armstrong N (2004) Structure and function of glutamate receptor ion channels. Annu Rev Physiol 66:161-181.
Mayer ML, Westbrook GL, Guthrie PB (1984) Voltage-dependent block by Mg2+ of NMDA responses in spinal cord neurones. Nature 309:261-263.
Mayer ML, Olson R, Gouaux E (2001) Mechanisms for ligand binding to GluR0 ion channels: crystal structures of the glutamate and serine complexes and a closed apo state. J Mol Biol 311:815-836.
McKinney RA, Capogna M, Durr R, Gahwiler BH, Thompson SM (1999) Miniature synaptic events maintain dendritic spines via AMPA receptor activation. Nat Neurosci 2:44-49.
Meddows E, Le Bourdelles B, Grimwood S, Wafford K, Sandhu S, Whiting P, McIlhinney RA (2001) Identification of molecular determinants that are important in the assembly of N-methyl-D-aspartate receptors. J Biol Chem 276:18795-18803.
Meguro H, Mori H, Araki K, Kushiya E, Kutsuwada T, Yamazaki M, Kumanishi T, Arakawa M, Sakimura K, Mishina M (1992) Functional characterization of a heteromeric NMDA receptor channel expressed from cloned cDNAs. Nature 357:70-74.
Miledi R, Sumikawa K (1982) Synthesis of cat muscle acetylcholine receptors by Xenopus oocytes. Biomed Res 3:390–399.
Monastirioti M, Gorczyca M, Rapus J, Eckert M, White K, Budnik V (1995) Octopamine immunoreactivity in the fruit fly Drosophila melanogaster. J

Comp Neurol 356:275-287.
Monyer H, Sprengel R, Schoepfer R, Herb A, Higuchi M, Lomeli H, Burnashev N, Sakmann B, Seeburg PH (1992) Heteromeric NMDA receptors: molecular and functional distinction of subtypes. Science 256:1217-1221.
Moriyoshi K, Masu M, Ishii T, Shigemoto R, Mizuno N, Nakanishi S (1991) Molecular cloning and characterization of the rat NMDA receptor. Nature 354:31-37.
Mosbacher J, Schoepfer R, Monyer H, Burnashev N, Seeburg PH, Ruppersberg JP (1994) A molecular determinant for submillisecond desensitization in glutamate receptors. Science 266:1059-1062.
Mouillac B, Caron M, Bonin H, Dennis M, Bouvier M (1992) Agonist-modulated palmitoylation of beta 2-adrenergic receptor in Sf9 cells. J Biol Chem 267:21733-21737.
Nakanishi S, Nakajima Y, Masu M, Ueda Y, Nakahara K, Watanabe D, Yamaguchi S, Kawabata S, Okada M (1998) Glutamate receptors: brain function and signal transduction. Brain Res Brain Res Rev 26:230-235.
Niethammer M, Kim E, Sheng M (1996) Interaction between the C terminus of NMDA receptor subunits and multiple members of the PSD-95 family of membrane-associated guanylate kinases. J Neurosci 16:2157-2163.
Nimchinsky EA, Sabatini BL, Svoboda K (2002) Structure and function of dendritic spines. Annu Rev Physiol 64:313-353.
Nishi M, Hinds H, Lu HP, Kawata M, Hayashi Y (2001) Motoneuron-specific expression of NR3B, a novel NMDA-type glutamate receptor subunit that works in a dominant-negative manner. J Neurosci 21:RC185.
Nowak L, Bregestovski P, Ascher P, Herbet A, Prochiantz A (1984) Magnesium gates glutamate-activated channels in mouse central neurones. Nature 307:462-465.
O'Hara PJ, Sheppard PO, Thogersen H, Venezia D, Haldeman BA, McGrane V, Houamed KM, Thomsen C, Gilbert TL, Mulvihill ER (1993) The ligand-binding domain in metabotropic glutamate receptors is related to bacterial periplasmic binding proteins. Neuron 11:41-52.
Ohtsuka T, Takao-Rikitsu E, Inoue E, Inoue M, Takeuchi M, Matsubara K, Deguchi-Tawarada M, Satoh K, Morimoto K, Nakanishi H, Takai Y (2002) Cast: a novel protein of the cytomatrix at the active zone of synapses that forms a ternary complex with RIM1 and munc13-1. J Cell Biol 158:577-590.
Ordway RW, Pallanck L, Ganetzky B (1994) Neurally expressed Drosophila genes encoding homologs of the NSF and SNAP secretory proteins. Proc Natl Acad Sci U S A 91:5715-5719.
Osten P, Khatri L, Perez JL, Kohr G, Giese G, Daly C, Schulz TW, Wensky A, Lee LM, Ziff EB (2000) Mutagenesis reveals a role for ABP/GRIP binding to GluR2 in synaptic surface accumulation of the AMPA receptor. Neuron 27:313-325.
Packard M, Mathew D, Budnik V (2003) Wnts and TGF beta in synaptogenesis: old friends signalling at new places. Nat Rev Neurosci 4:113-120.
Packard M, Koo ES, Gorczyca M, Sharpe J, Cumberledge S, Budnik V (2002)

The Drosophila Wnt, wingless, provides an essential signal for pre- and postsynaptic differentiation. Cell 111:319-330.
Palay SL (1956) Synapses in the central nervous system. J Biophys Biochem Cytol 2:193-202.
Park M, Penick EC, Edwards JG, Kauer JA, Ehlers MD (2004) Recycling endosomes supply AMPA receptors for LTP. Science 305:1972-1975.
Partin KM, Patneau DK, Winters CA, Mayer ML, Buonanno A (1993) Selective modulation of desensitization at AMPA versus kainate receptors by cyclothiazide and concanavalin A. Neuron 11:1069-1082.
Passafaro M, Piech V, Sheng M (2001) Subunit-specific temporal and spatial patterns of AMPA receptor exocytosis in hippocampal neurons. Nat Neurosci 4:917-926.
Perez JL, Khatri L, Chang C, Srivastava S, Osten P, Ziff EB (2001) PICK1 targets activated protein kinase Calpha to AMPA receptor clusters in spines of hippocampal neurons and reduces surface levels of the AMPA-type glutamate receptor subunit 2. J Neurosci 21:5417-5428.
Perron A, Sarret P, Gendron L, Stroh T, Beaudet A (2005) Identification and functional characterization of a 5-transmembrane domain variant isoform of the NTS2 neurotensin receptor in rat central nervous system. J Biol Chem 280:10219-10227.
Petersen SA, Fetter RD, Noordermeer JN, Goodman CS, DiAntonio A (1997) Genetic analysis of glutamate receptors in Drosophila reveals a retrograde signal regulating presynaptic transmitter release. Neuron 19:1237-1248.
Pickard L, Noel J, Duckworth JK, Fitzjohn SM, Henley JM, Collingridge GL, Molnar E (2001) Transient synaptic activation of NMDA receptors leads to the insertion of native AMPA receptors at hippocampal neuronal plasma membranes. Neuropharmacology 41:700-713.
Pinheiro P, Mulle C (2006) Kainate receptors. Cell Tissue Res 326:457-482.
Ponimaskin E, Harteneck C, Schultz G, Schmidt MF (1998) A cysteine-11 to serine mutant of G alpha12 impairs activation through the thrombin receptor. FEBS Lett 429:370-374.
Ponimaskin EG, Schmidt MF, Heine M, Bickmeyer U, Richter DW (2001) 5-Hydroxytryptamine 4(a) receptor expressed in Sf9 cells is palmitoylated in an agonist-dependent manner. Biochem J 353:627-634.
Ponimaskin EG, Heine M, Joubert L, Sebben M, Bickmeyer U, Richter DW, Dumuis A (2002) The 5-hydroxytryptamine(4a) receptor is palmitoylated at two different sites, and acylation is critically involved in regulation of receptor constitutive activity. J Biol Chem 277:2534-2546.
Premkumar LS, Auerbach A (1997) Stoichiometry of recombinant N-methyl-D-aspartate receptor channels inferred from single-channel current patterns. J Gen Physiol 110:485-502.
Priel A, Kolleker A, Ayalon G, Gillor M, Osten P, Stern-Bach Y (2005) Stargazin reduces desensitization and slows deactivation of the AMPA-type glutamate receptors. J Neurosci 25:2682-2686.
Prokop A (1999) Integrating bits and pieces: synapse structure and formation in Drosophila embryos. Cell Tissue Res 297:169-186.

Prokop A, Meinertzhagen IA (2006) Development and structure of synaptic contacts in Drosophila. Semin Cell Dev Biol 17:20-30.

Prokop A, Landgraf M, Rushton E, Broadie K, Bate M (1996) Presynaptic development at the Drosophila neuromuscular junction: assembly and localization of presynaptic active zones. Neuron 17:617-626.

Qin G, Schwarz T, Kittel RJ, Schmid A, Rasse TM, Kappei D, Ponimaskin E, Heckmann M, Sigrist SJ (2005) Four different subunits are essential for expressing the synaptic glutamate receptor at neuromuscular junctions of Drosophila. J Neurosci 25:3209-3218.

Rasse TM, Fouquet W, Schmid A, Kittel RJ, Mertel S, Sigrist CB, Schmidt M, Guzman A, Merino C, Qin G, Quentin C, Madeo FF, Heckmann M, Sigrist SJ (2005) Glutamate receptor dynamics organizing synapse formation in vivo. Nat Neurosci 8:898-905.

Reiff DF, Thiel PR, Schuster CM (2002) Differential regulation of active zone density during long-term strengthening of Drosophila neuromuscular junctions. J Neurosci 22:9399-9409.

Ren H, Honse Y, Karp BJ, Lipsky RH, Peoples RW (2003a) A site in the fourth membrane-associated domain of the N-methyl-D-aspartate receptor regulates desensitization and ion channel gating. J Biol Chem 278:276-283.

Ren Z, Riley NJ, Needleman LA, Sanders JM, Swanson GT, Marshall J (2003b) Cell surface expression of GluR5 kainate receptors is regulated by an endoplasmic reticulum retention signal. J Biol Chem 278:52700-52709.

Ren Z, Riley NJ, Garcia EP, Sanders JM, Swanson GT, Marshall J (2003c) Multiple trafficking signals regulate kainate receptor KA2 subunit surface expression. J Neurosci 23:6608-6616.

Rheuben MB, Yoshihara M, Kidokoro Y (1999) Ultrastructural correlates of neuromuscular junction development. Int Rev Neurobiol 43:69-92.

Ritzenthaler S, Chiba A (2001) Multiple personalities: synaptic target cells as introverts and extroverts. Dev Growth Differ 43:503-508.

Rivlin PK, St Clair RM, Vilinsky I, Deitcher DL (2004) Morphology and molecular organization of the adult neuromuscular junction of Drosophila. J Comp Neurol 468:596-613.

Rocheville M, Lange DC, Kumar U, Patel SC, Patel RC, Patel YC (2000) Receptors for dopamine and somatostatin: formation of hetero-oligomers with enhanced functional activity. Science 288:154-157.

Rosenmund C, Stern-Bach Y, Stevens CF (1998) The tetrameric structure of a glutamate receptor channel. Science 280:1596-1599.

Rothman JE (1994) Mechanisms of intracellular protein transport. Nature 372:55-63.

Rubin GM, Spradling AC (1982) Genetic transformation of Drosophila with transposable element vectors. Science 218:348-353.

Safferling M, Tichelaar W, Kummerle G, Jouppila A, Kuusinen A, Keinanen K, Madden DR (2001) First images of a glutamate receptor ion channel: oligomeric state and molecular dimensions of GluRB homomers. Biochemistry 40:13948-13953.

Salinas PC, Price SR (2005) Cadherins and catenins in synapse development. Curr Opin Neurobiol 15:73-80.
Sambrook J, Fritsch E, Maniatis T (1989) Molecular cloning: A laboratory manual, 2nd Edition. Cold Spring Harbor, NY: Cold Spring Harbor Laboratory Press.
Sanes JR, Lichtman JW (1999) Development of the vertebrate neuromuscular junction. Annu Rev Neurosci 22:389-442.
Sans N, Racca C, Petralia RS, Wang YX, McCallum J, Wenthold RJ (2001) Synapse-associated protein 97 selectively associates with a subset of AMPA receptors early in their biosynthetic pathway. J Neurosci 21:7506-7516.
Saragoza PA, Modir JG, Goel N, French KL, Li L, Nowak MW, Stitzel JA (2003) Identification of an alternatively processed nicotinic receptor alpha7 subunit RNA in mouse brain. Brain Res Mol Brain Res 117:15-26.
Sartorius LJ, Nagappan G, Lipska BK, Lu B, Sei Y, Ren-Patterson R, Li Z, Weinberger DR, Harrison PJ (2006) Alternative splicing of human metabotropic glutamate receptor 3. J Neurochem 96:1139-1148.
Schiffer HH, Swanson GT, Heinemann SF (1997) Rat GluR7 and a carboxy-terminal splice variant, GluR7b, are functional kainate receptor subunits with a low sensitivity to glutamate. Neuron 19:1141-1146.
Schmid A, Qin G, Wichmann C, Kittel RJ, Mertel S, Fouquet W, Schmidt M, Heckmann M, Sigrist SJ (2006) Non-NMDA-type glutamate receptors are essential for maturation but not for initial assembly of synapses at Drosophila neuromuscular junctions. J Neurosci 26:11267-11277.
Schnell E, Sizemore M, Karimzadegan S, Chen L, Bredt DS, Nicoll RA (2002) Direct interactions between PSD-95 and stargazin control synaptic AMPA receptor number. Proc Natl Acad Sci U S A 99:13902-13907.
Schorge S, Colquhoun D (2003) Studies of NMDA receptor function and stoichiometry with truncated and tandem subunits. J Neurosci 23:1151-1158.
Schuster CM, Davis GW, Fetter RD, Goodman CS (1996a) Genetic dissection of structural and functional components of synaptic plasticity. II. Fasciclin II controls presynaptic structural plasticity. Neuron 17:655-667.
Schuster CM, Davis GW, Fetter RD, Goodman CS (1996b) Genetic dissection of structural and functional components of synaptic plasticity. I. Fasciclin II controls synaptic stabilization and growth. Neuron 17:641-654.
Schuster CM, Ultsch A, Schloss P, Cox JA, Schmitt B, Betz H (1991) Molecular cloning of an invertebrate glutamate receptor subunit expressed in Drosophila muscle. Science 254:112-114.
Scott BB, Losowsky MS (1976) Peroral small-intestinal biopsy: experience with the hydraulic multiple biopsy instrument in routine clinical practice. Gut 17:740-743.
Seachrist JL, Laporte SA, Dale LB, Babwah AV, Caron MG, Anborgh PH, Ferguson SS (2002) Rab5 association with the angiotensin II type 1A receptor promotes Rab5 GTP binding and vesicular fusion. J Biol Chem 277:679-685.

Seeburg PH (2002) A-to-I editing: new and old sites, functions and speculations. Neuron 35:17-20.
Seeburg PH, Single F, Kuner T, Higuchi M, Sprengel R (2001) Genetic manipulation of key determinants of ion flow in glutamate receptor channels in the mouse. Brain Res 907:233-243.
Serpinskaya AS, Feng G, Sanes JR, Craig AM (1999) Synapse formation by hippocampal neurons from agrin-deficient mice. Dev Biol 205:65-78.
Shapira M, Zhai RG, Dresbach T, Bresler T, Torres VI, Gundelfinger ED, Ziv NE, Garner CC (2003) Unitary assembly of presynaptic active zones from Piccolo-Bassoon transport vesicles. Neuron 38:237-252.
Shen L, Liang F, Walensky LD, Huganir RL (2000) Regulation of AMPA receptor GluR1 subunit surface expression by a 4. 1N-linked actin cytoskeletal association. J Neurosci 20:7932-7940.
Sheng M, Pak DT (2000) Ligand-gated ion channel interactions with cytoskeletal and signaling proteins. Annu Rev Physiol 62:755-778.
Sheng M, Sala C (2001) PDZ domains and the organization of supramolecular complexes. Annu Rev Neurosci 24:1-29.
Shi S, Hayashi Y, Esteban JA, Malinow R (2001) Subunit-specific rules governing AMPA receptor trafficking to synapses in hippocampal pyramidal neurons. Cell 105:331-343.
Shi SH, Hayashi Y, Petralia RS, Zaman SH, Wenthold RJ, Svoboda K, Malinow R (1999) Rapid spine delivery and redistribution of AMPA receptors after synaptic NMDA receptor activation. Science 284:1811-1816.
Sigrist SJ, Thiel PR, Reiff DF, Schuster CM (2002) The postsynaptic glutamate receptor subunit DGluR-IIA mediates long-term plasticity in Drosophila. J Neurosci 22:7362-7372.
Sigrist SJ, Reiff DF, Thiel PR, Steinert JR, Schuster CM (2003) Experience-dependent strengthening of Drosophila neuromuscular junctions. J Neurosci 23:6546-6556.
Sigrist SJ, Thiel PR, Reiff DF, Lachance PE, Lasko P, Schuster CM (2000) Postsynaptic translation affects the efficacy and morphology of neuromuscular junctions. Nature 405:1062-1065.
Smith GE, Ju G, Ericson BL, Moschera J, Lahm HW, Chizzonite R, Summers MD (1985) Modification and secretion of human interleukin 2 produced in insect cells by a baculovirus expression vector. Proc Natl Acad Sci U S A 82:8404-8408.
Sommer B, Kohler M, Sprengel R, Seeburg PH (1991) RNA editing in brain controls a determinant of ion flow in glutamate-gated channels. Cell 67:11-19.
Sommer B, Burnashev N, Verdoorn TA, Keinanen K, Sakmann B, Seeburg PH (1992) A glutamate receptor channel with high affinity for domoate and kainate. Embo J 11:1651-1656.
Sommer B, Keinanen K, Verdoorn TA, Wisden W, Burnashev N, Herb A, Kohler M, Takagi T, Sakmann B, Seeburg PH (1990) Flip and flop: a cell-specific functional switch in glutamate-operated channels of the CNS. Science 249:1580-1585.

Sone M, Suzuki E, Hoshino M, Hou D, Kuromi H, Fukata M, Kuroda S, Kaibuchi K, Nabeshima Y, Hama C (2000) Synaptic development is controlled in the periactive zones of Drosophila synapses. Development 127:4157-4168.

Song I, Huganir RL (2002) Regulation of AMPA receptors during synaptic plasticity. Trends Neurosci 25:578-588.

Spacek J, Harris KM (1997) Three-dimensional organization of smooth endoplasmic reticulum in hippocampal CA1 dendrites and dendritic spines of the immature and mature rat. J Neurosci 17:190-203.

Srivastava S, Ziff EB (1999) ABP: a novel AMPA receptor binding protein. Ann N Y Acad Sci 868:561-564.

Stern-Bach Y, Bettler B, Hartley M, Sheppard PO, O'Hara PJ, Heinemann SF (1994) Agonist selectivity of glutamate receptors is specified by two domains structurally related to bacterial amino acid-binding proteins. Neuron 13:1345-1357.

Stewart BA, Atwood HL, Renger JJ, Wang J, Wu CF (1994) Improved stability of Drosophila larval neuromuscular preparations in haemolymph-like physiological solutions. J Comp Physiol [A] 175:179-191.

Sucher NJ, Akbarian S, Chi CL, Leclerc CL, Awobuluyi M, Deitcher DL, Wu MK, Yuan JP, Jones EG, Lipton SA (1995) Developmental and regional expression pattern of a novel NMDA receptor-like subunit (NMDAR-L) in the rodent brain. J Neurosci 15:6509-6520.

Swan LE, Schmidt M, Schwarz T, Ponimaskin E, Prange U, Boeckers T, Thomas U, Sigrist SJ (2006) Complex interaction of Drosophila GRIP PDZ domains and Echinoid during muscle morphogenesis. Embo J 25:3640-3651.

Swan LE, Wichmann C, Prange U, Schmid A, Schmidt M, Schwarz T, Ponimaskin E, Madeo F, Vorbruggen G, Sigrist SJ (2004) A glutamate receptor-interacting protein homolog organizes muscle guidance in Drosophila. Genes Dev 18:223-237.

Swanson GT, Feldmeyer D, Kaneda M, Cull-Candy SG (1996) Effect of RNA editing and subunit co-assembly single-channel properties of recombinant kainate receptors. J Physiol 492 (Pt 1):129-142.

Takeya R, Takeshige K, Sumimoto H (2000) Interaction of the PDZ domain of human PICK1 with class I ADP-ribosylation factors. Biochem Biophys Res Commun 267:149-155.

Thomas U, Kim E, Kuhlendahl S, Koh YH, Gundelfinger ED, Sheng M, Garner CC, Budnik V (1997) Synaptic clustering of the cell adhesion molecule fasciclin II by discs-large and its role in the regulation of presynaptic structure. Neuron 19:787-799.

Tomita S, Fukata M, Nicoll RA, Bredt DS (2004) Dynamic interaction of stargazin-like TARPs with cycling AMPA receptors at synapses. Science 303:1508-1511.

Tomita S, Stein V, Stocker TJ, Nicoll RA, Bredt DS (2005a) Bidirectional synaptic plasticity regulated by phosphorylation of stargazin-like TARPs. Neuron 45:269-277.

Tomita S, Chen L, Kawasaki Y, Petralia RS, Wenthold RJ, Nicoll RA, Bredt DS (2003) Functional studies and distribution define a family of transmembrane AMPA receptor regulatory proteins. J Cell Biol 161:805-816.

Tomita S, Adesnik H, Sekiguchi M, Zhang W, Wada K, Howe JR, Nicoll RA, Bredt DS (2005b) Stargazin modulates AMPA receptor gating and trafficking by distinct domains. Nature 435:1052-1058.

Turetsky D, Garringer E, Patneau DK (2005) Stargazin modulates native AMPA receptor functional properties by two distinct mechanisms. J Neurosci 25:7438-7448.

Ulbrich MH, Isacoff EY (2007) Subunit counting in membrane-bound proteins. Nat Methods 4:319-321.

Valerio A, Ferraboli S, Paterlini M, Spano P, Barlati S (2001) Identification of novel alternatively-spliced mRNA isoforms of metabotropic glutamate receptor 6 gene in rat and human retina. Gene 262:99-106.

Vandenberghe W, Nicoll RA, Bredt DS (2005a) Stargazin is an AMPA receptor auxiliary subunit. Proc Natl Acad Sci U S A 102:485-490.

Vandenberghe W, Nicoll RA, Bredt DS (2005b) Interaction with the unfolded protein response reveals a role for stargazin in biosynthetic AMPA receptor transport. J Neurosci 25:1095-1102.

Verdoorn TA, Burnashev N, Monyer H, Seeburg PH, Sakmann B (1991) Structural determinants of ion flow through recombinant glutamate receptor channels. Science 252:1715-1718.

Walker CS, Francis MM, Brockie PJ, Madsen DM, Zheng Y, Maricq AV (2006a) Conserved SOL-1 proteins regulate ionotropic glutamate receptor desensitization. Proc Natl Acad Sci U S A 103:10787-10792.

Walker CS, Brockie PJ, Madsen DM, Francis MM, Zheng Y, Koduri S, Mellem JE, Strutz-Seebohm N, Maricq AV (2006b) Reconstitution of invertebrate glutamate receptor function depends on stargazin-like proteins. Proc Natl Acad Sci U S A 103:10781-10786.

Wallrath LL, Elgin SC (1995) Position effect variegation in Drosophila is associated with an altered chromatin structure. Genes Dev 9:1263-1277.

Wallrath LL, Guntur VP, Rosman LE, Elgin SC (1996) DNA representation of variegating heterochromatic P-element inserts in diploid and polytene tissues of Drosophila melanogaster. Chromosoma 104:519-527.

Weigmann K, Klapper R, Strasser T, Rickert C, Technau G, Jackle H, Janning W, Klambt C (2003) FlyMove--a new way to look at development of Drosophila. Trends Genet 19:310-311.

Wenthold RJ, Yokotani N, Doi K, Wada K (1992) Immunochemical characterization of the non-NMDA glutamate receptor using subunit-specific antibodies. Evidence for a hetero-oligomeric structure in rat brain. J Biol Chem 267:501-507.

Westrum LE, Jones DH, Gray EG, Barron J (1980) Microtubules, dendritic spines and spine appratuses. Cell Tissue Res 208:171-181.

Wilding TJ, Zhou Y, Huettner JE (2005) Q/R site editing controls kainate receptor inhibition by membrane fatty acids. J Neurosci 25:9470-9478.

Wilson MH, Deschenes MR (2005) The neuromuscular junction: anatomical features and adaptations to various forms of increased, or decreased neuromuscular activity. Int J Neurosci 115:803-828.
Wood SJ, Slater CR (1997) The contribution of postsynaptic folds to the safety factor for neuromuscular transmission in rat fast- and slow-twitch muscles. J Physiol 500 (Pt 1):165-176.
Wood SJ, Slater CR (2001) Safety factor at the neuromuscular junction. Prog Neurobiol 64:393-429.
Wucherpfennig T, Wilsch-Brauninger M, Gonzalez-Gaitan M (2003) Role of Drosophila Rab5 during endosomal trafficking at the synapse and evoked neurotransmitter release. J Cell Biol 161:609-624.
Wyszynski M, Valtschanoff JG, Naisbitt S, Dunah AW, Kim E, Standaert DG, Weinberg R, Sheng M (1999) Association of AMPA receptors with a subset of glutamate receptor-interacting protein in vivo. J Neurosci 19:6528-6537.
Xia J, Zhang X, Staudinger J, Huganir RL (1999) Clustering of AMPA receptors by the synaptic PDZ domain-containing protein PICK1. Neuron 22:179-187.
Xia S, Miyashita T, Fu TF, Lin WY, Wu CL, Pyzocha L, Lin IR, Saitoe M, Tully T, Chiang AS (2005) NMDA receptors mediate olfactory learning and memory in Drosophila. Curr Biol 15:603-615.
Yamazaki M, Ohno-Shosaku T, Fukaya M, Kano M, Watanabe M, Sakimura K (2004) A novel action of stargazin as an enhancer of AMPA receptor activity. Neurosci Res 50:369-374.
Yan S, Sanders JM, Xu J, Zhu Y, Contractor A, Swanson GT (2004) A C-terminal determinant of GluR6 kainate receptor trafficking. J Neurosci 24:679-691.
Yoshihara M, Adolfsen B, Galle KT, Littleton JT (2005) Retrograde signaling by Syt 4 induces presynaptic release and synapse-specific growth. Science 310:858-863.
Yuste R, Bonhoeffer T (2004) Genesis of dendritic spines: insights from ultrastructural and imaging studies. Nat Rev Neurosci 5:24-34.
Zamanillo D, Sprengel R, Hvalby O, Jensen V, Burnashev N, Rozov A, Kaiser KM, Koster HJ, Borchardt T, Worley P, Lubke J, Frotscher M, Kelly PH, Sommer B, Andersen P, Seeburg PH, Sakmann B (1999) Importance of AMPA receptors for hippocampal synaptic plasticity but not for spatial learning. Science 284:1805-1811.
Zhai RG, Bellen HJ (2004) The architecture of the active zone in the presynaptic nerve terminal. Physiology (Bethesda) 19:262-270.
Zhang J, Schulze KL, Hiesinger PR, Suyama K, Wang S, Fish M, Acar M, Hoskins RA, Bellen HJ, Scott MP (2007) 31 Flavors of Drosophila Rab Proteins. Genetics.
Zheng Y, Mellem JE, Brockie PJ, Madsen DM, Maricq AV (2004) SOL-1 is a CUB-domain protein required for GLR-1 glutamate receptor function in C. elegans. Nature 427:451-457.
Zheng Y, Brockie PJ, Mellem JE, Madsen DM, Walker CS, Francis MM, Maricq AV (2006) SOL-1 is an auxiliary subunit that modulates the gating of GLR-

1 glutamate receptors in Caenorhabditis elegans. Proc Natl Acad Sci U S A 103:1100-1105.
Ziff EB (1997) Enlightening the postsynaptic density. Neuron 19:1163-1174.
Zito K, Fetter RD, Goodman CS, Isacoff EY (1997) Synaptic clustering of Fascilin II and Shaker: essential targeting sequences and role of Dlg. Neuron 19:1007-1016.
Ziv NE, Smith SJ (1996) Evidence for a role of dendritic filopodia in synaptogenesis and spine formation. Neuron 17:91-102.
Ziv NE, Garner CC (2004) Cellular and molecular mechanisms of presynaptic assembly. Nat Rev Neurosci 5:385-399.
Zuo J, De Jager PL, Takahashi KA, Jiang W, Linden DJ, Heintz N (1997) Neurodegeneration in Lurcher mice caused by mutation in delta2 glutamate receptor gene. Nature 388:769-773.

9 Curiculum vitae

Personal details

Surname:	Schwarz
Forename:	Tobias
Date of birth:	28.04.1977
Place of birth:	Fulda
Nationality:	German
Marital status:	single
Work address:	ENI Grisebachstr. 5 37077 Göttingen, Germany Tel.: (+49)-(0)551-3912364 e-mail: tschwar3@gwdg.de

Scientific education

June1996	Abitur at the Freiherr-vom-Stein-Gymnasium Fulda
July 1996 - July1997	Civil service at Städtisches Klinikum Fulda
WS 1997 - Mai 2003	studies in Biochemistry at the University of Hannover Diploma thesis „Untersuchungen zur Umlagerung von Troponin durch Fluoreszenz-Resonanz-Energie-transfer-Messungen an einzelnen Skelettmuskel-fasern“ at the Institut für Molekular- und Zellphysiologie, MHH, Supervisor: Prof. Theresia Kraft, Prof. Bernhard Brenner
Mai 2003	graduation as Diplom-Biochemiker
Since Mai 2004	PHD student in the Neuroplasticity group, ENI Göttingen, Grisebachstr. 5, 37077 Göttingen

10 List of publications

Swan LE, Wichmann C, Prange U, Schmid A, Schmidt M, Schwarz T, Ponimaskin E, Madeo F, Vorbruggen G, Sigrist SJ (2004) A glutamate receptor-interacting protein homolog organizes muscle guidance in Drosophila. Genes Dev 18:223-237.

Qin G, Schwarz T, Kittel RJ, Schmid A, Rasse TM, Kappei D, Ponimaskin E, Heckmann M, Sigrist SJ (2005) Four different subunits are essential for expressing the synaptic glutamate receptor at neuromuscular junctions of Drosophila. J Neurosci 25:3209-3218.

Swan LE, Schmidt M, Schwarz T, Ponimaskin E, Prange U, Boeckers T, Thomas U, Sigrist SJ (2006) Complex interaction of Drosophila GRIP PDZ domains and Echinoid during muscle morphogenesis. Embo J 25:3640-3651.